



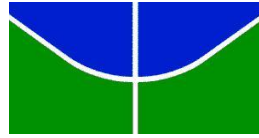
**UNIVERSIDADE DE BRASÍLIA
FACULDADE DE AGRONOMIA E MEDICINA VETERINÁRIA**

HISTOMORFOMETRIA DA CÓRNEA DE AVES

RAFAELA ALVES RIBON TOZETTI

TESE DE DOUTORADO EM CIÊNCIAS ANIMAIS

**BRASÍLIA/DF
JULHO DE 2023**



**UNIVERSIDADE DE BRASÍLIA
FACULDADE DE AGRONOMIA E MEDICINA VETERINÁRIA**

HISTOMORFOMETRIA DA CÓRNEA DE AVES

ALUNA: RAFAELA ALVES RIBON TOZETTI

ORIENTADORA: PROFESORA DR^a PAULA DINIZ GALERA

TESE DE DOUTORADO EM CIÊNCIAS ANIMAIS

PUBLICAÇÃO:

**BRASÍLIA/DF
JULHO DE 2023**

**UNIVERSIDADE DE BRASÍLIA
FACULDADE DE AGRONOMIA E MEDICINA VETERINÁRIA**

HISTOMORFOMETRIA DA CÓRNEA DE AVES

RAFAELA ALVES RIBON TOZETTI

**TESE DE DOUTORADO SUBMETIDA AO
PROGRAMA DE PÓS-GRADUAÇÃO EM
CIÊNCIAS ANIMAIS, COMO PARTE DOS
REQUISITOS NECESSÁRIOS À OBTENÇÃO
DO GRAU DE DOUTORA EM CIÊNCIAS
ANIMAIS.**

APROVADA POR:

**Paula Diniz Galera, Dra. (Universidade de Brasília).
(ORIENTADORA)**

**Márcio Botelho de Castro, Dr. (Universidade de Brasília).
(EXAMINADOR INTERNO)**

**Giane Regina Paludo, Dra. (Universidade de Brasília).
(EXAMINADOR INTERNO)**

**Angélica de Mendonça Vaz Safatle, Dra. (Universidade de São Paulo)
(EXAMINADOR EXTERNO)**

**Fabiano Montiani-Ferreira, Dr. (Universidade Federal do Paraná).
(EXAMINADOR EXTERNO)**

BRASÍLIA/DF, 31 de julho de 2023

REFERÊNCIA BIBLIOGRÁFICA E CATALOGAÇÃO

TOZETTI, R. A. R. **Histomorfometria da córnea de aves**. Brasília: Faculdade de Agronomia e Medicina Veterinária, Universidade de Brasília, 2023, (nº páginas- 95p.). Tese de Doutorado.

Documento formal, autorizando reprodução desta tese de doutorado para empréstimo ou comercialização, exclusivamente para fins acadêmicos, foi passado pelo autor à Universidade de Brasília e acha-se arquivado na Secretaria do Programa. O autor e seu orientador reservam para si os direitos autorais de publicação. Nenhuma parte desta dissertação pode ser reproduzida sem autorização por escrito do autor ou de seu orientador. Citações são estimuladas, desde que citada a fonte.

FICHA CATALOGRÁFICA

TOZETTI, Rafaela Alves Ribon. **Histomorfometria da córnea de aves**. Brasília: Faculdade de Agronomia e Medicina Veterinária da Universidade de Brasília, 2022. 95p. Tese de Doutorado –Faculdade de Agronomia e Medicina Veterinária da Universidade de Brasília, 2022.

1.Córnea. 2. Aves. 3. Histologia. 4. Microscopia eletrônica de varredura.

EPÍGRAFE

“Por vezes sentimos que aquilo que fazemos não é senão uma gota de água no mar. Mas o mar seria menor se lhe faltasse uma gota”.

Madre Teresa de Calcutá

DEDICATÓRIA

Dedico ao meu pai, Geraldo Tozetti, e à minha mãe, Sandra Darc Alves, que moldaram minha personalidade e poliram meu caráter, dentro dos ensinamentos de Deus.

Dedico também ao meu filho, Henrique, para que isso o inspire a seguir sempre pelo caminho do conhecimento, da ciência e do respeito à vida plural do nosso planeta.

AGRADECIMENTOS

Agradeço a equipe de animais silvestres do Hospital Veterinário da UnB, por me proporcionar os meios para que eu pudesse realizar essa pesquisa, em especial à Evelyn e à Professora Dr^a Líria Aquino.

Agradeço a Ana Carolina Rodarte, por seu auxílio com as amostras.

Agradeço a Rose, que esteve sempre comigo, instruindo e auxiliando diretamente nos processos para análise das amostras. Por ter me incentivado e me inspirado.

Agradeço ao Matheus Loes, por ser solícito e por seu trabalho impecável com as amostras histológicas.

Agradeço ao professor Dr. Moore, por se disponibilizar a ler e contribuir na escrita dos artigos científicos.

Agradeço aos Professores da banca, Dr.^a Angélica de Mendonça Vaz Safatle, Dr. Fabiano Montiani-Ferreira, Dr. Márcio Botelho e Dr.^a Giane Regina Paludo, que aceitaram o convite para avaliar e contribuir para o aprimoramento desse estudo, e assim torná-lo possível.

Agradeço a Professora Dr.^a Paula, por sua paciência, insistência e por ter acreditado em mim quando nem eu mais acreditava. Por sua tutoria e orientação.

Agradeço ao meu marido, Lucas, por ter pegado na minha mão e caminhado comigo até aqui. Me dando forças e ajudando em tudo que fosse necessário para que eu conseguisse desenvolver esse trabalho.

ÍNDICE

RESUMO	9
ABSTRACT	10
LISTA DE FIGURAS	10
LISTA DE TABELAS	12
CAPÍTULO I.....	13
INTRODUÇÃO	14
Contextualização	14
Problemática e relevância.....	14
Objetivo.....	14
REVISÃO BIBLIOGRÁFICA	16
A visão das aves	16
Estruturas Oculares	18
A córnea das aves.....	26
CAPÍTULO II.....	31
Corneal histomorphometry of birds from the Brazilian Midwest.....	32
CAPÍTULO III	60
Evaluation of the Common Pauraque (<i>Nyctidromus albicollis</i>) cornea using light and scanning electron microscopy.....	61
CAPÍTULO IV	83
CONSIDERAÇÕES FINAIS	84
REFERÊNCIAS BIBLIOGRÁFICAS	85

RESUMO

Cada estrutura ocular sofre variações, não só entre as classes de vertebrados, mas também entre as ordens aviárias, correlacionadas com seus diferentes hábitos e habitat, a exemplo da córnea. Este trabalho descreveu as estruturas histomorfométricas da córnea das seguintes aves: *Asio stygius*, *Crotophaga ani*, *Pitangus sulphuratus*, *Turdus rufiventris*, *Ramphastos toco*, *Rhea americana*, *Ara macao*, *Nyctidromus albicollis* e *Nyctibius griseus*; habitantes da região Centro-Oeste brasileiro. Adicionalmente, avaliaram-se as características do endotélio corneano do *Nyctidromus albicollis*, por meio da microscopia eletrônica de varredura. Os resultados nos permitiram observar que a composição da córnea é a mesma em todas as aves, mas diferem entre si na espessura das camadas corneanas, na espessura entre as regiões centrais e periféricas, e no número de camadas epiteliais. Estes resultados auxiliam na compreensão da fisiologia da visão e das exigências visuais destas espécies, favorecendo esforços em prol da sua conservação, bem como na interpretação de alterações patológicas da córnea das aves.

Palavras-chave: olho de aves, córnea, endotélio, histologia, morfologia, morfometria.

ABSTRACT

Each ocular structure undergoes variations not only among vertebrate classes, but also among avian orders, correlated with their different habits and habitats, such as the cornea. This work described the histomorphometric structures of the cornea of the following birds: *Asio stygius*, *Crotophaga ani*, *Pitangus sulphuratus*, *Turdus rufiventris*, *Ramphastos toco*, *Rhea americana*, *Ara macao*, *Nyctidromus albicollis* and *Nyctibius griseus*; all inhabitants of the Brazilian Midwest region. Additionally, it evaluated the characteristics of the corneal endothelium of *Nyctidromus albicollis*, through scanning electron microscopy. The results allowed us to observe that the composition of the cornea is the same in all birds, but they differ in the thickness of the corneal layers, in the thickness between the central and peripheral regions and in the number of epithelial layers. These results will help understanding the physiology of vision and visual requirements and contribute towards the conservation of different avian species, improving the interpretation of pathological changes in the cornea of birds.

Keywords: avian eye, cornea, endothelium, histology, morphology, morphometry

LISTA DE FIGURAS

CAPÍTULO II

Figure 1. Macroscopy of the ocular bulbs demonstrating the variation of the corneal curvature, of *Crotophaga ani* (A) with a low degree of curvature, and of *Nyctibius griseus* (B), with high convexity. 50

Figure 2. Cornea of the *Turdus rufiventris*. Columnar-shaped basal epithelial squamous cells (asterisk), polyhedral cells (arrowhead), and wing cells (arrows). The Bowman's membrane (BL) can be visualized in the image below. 400x. 50

Figure 3. Representation of the percentage of epithelium and stroma in relation to the total corneal thickness of the birds. 51

Figure 4. Measurement of total corneal thickness (L1) and its individual layers; Epithelium (L2), Bowman's membrane (L3), stroma (L4), Descemet's membrane (L5). A) Central region of the *Asio stygius* cornea; B) Central corneal region of *Rhea americana*. 100x..... 51

Figure 5. Peripheral region of the *Pitangus sulphuratus* cornea. Eosinophilic keratocyte nuclei (arrowhead) and artifacts (arrows) scattered throughout the stroma. Measurements referring to the thickness of the total cornea (L1), epithelium (L2), Bowman's membrane (BL), stroma (L3) and Descemet's membrane (L4). 100x. 52

CAPÍTULO III

Figure 1. Histology of Common Pauraque cornea. L1 - total corneal thickness; L2 - epithelium thickness; L3 - Bowman's layer thickness; L4- stroma thickness; L5 – Descemet's layer thickness. HE. 400x. 78

Figure 2. Scanning electron micrograph showing the corneal endothelium of the Common Pauraque (*Nyctidromus albicollis*). Note majority of cells are healthy, small, and hexagonal, compared to scant larger cells with variable shapes..... 79

Figure 3. Scanning electron micrograph of normal corneal endothelial cell of the Common Pauraque (*Nyctidromus albicollis*) showing microvilli (white structures). Note the highest density localized at the intercellular junctions. 79

LISTA DE TABELAS

CAPÍTULO II

Table 1. Order, family, and popular names of bird species. 53

Table 2. Measurement of the total cornea and its layers from avian species, in micrometers (μm). 54

Table 3. Number of layers and characteristics of the corneal epithelium from avian species. 55

Table 4. Total corneal thickness of previously studied bird species and of the birds studied here, including their sizes/weights, habits and feeding. 56

CAPÍTULO III

Table 1. Total corneal thickness of birds described in previous studies..... 80

CAPÍTULO I

INTRODUÇÃO

Contextualização

A classe das aves inclui 23 ordens e mais de 9.000 espécies com múltiplos modos de vida, sendo o clado de vertebrados com maior variedade de espécies. Ao longo dos últimos 20 anos as aves tornaram-se parte importante da clínica de oftalmologia veterinária, não só porque são frequentemente mantidas como animais de estimação, mas também porque há uma crescente consciência de conservação ambiental; e uma boa visão é essencial para aves de vida livre, já que tem influência direta no voo, alimentação e reprodução. Esses animais possuem um complexo sistema visual e cada estrutura ocular tem um papel específico e fundamental possibilitando a recepção de alta qualidade de informação visual (BAYÓN; ALMELA; TALAVERA, 2008; MOORE et al., 2022).

O sistema visual das aves e sua percepção do ambiente variam entre as espécies, de acordo com os diferentes nichos ecológicos habitados. Embora o olho assemelhe-se aos demais vertebrados, notadamente há diferenças estruturais e fisiológicas. Logo, a posição dos olhos no crânio, a amplitude de campo visual, o formato do bulbo ocular, a curvatura da córnea, a distribuição das células da retina e o espectro visual das cores, entre muitos outros exemplos, ajudam a interpretar a interação entre a visão das aves e o meio onde elas vivem, garantindo a sobrevivência das espécies (GARAMSZEGI; MØLLER; ERRITZØE, 2002; HALL; ROSS, 2007; CARVALHO et al., 2018; AUSPREY; NEWELL; ROBINSON, 2020).

Problemática e relevância

Buscando-se aprimorar o conhecimento das estruturas oculares e da capacidade visual das aves, faz-se necessário o registro de informações sobre diferentes espécies, obtidos com auxílio de métodos que se complementam. Dadas as diferenças oculares entre o grupo da classe aves, com grande distinção entre as ordens, famílias e espécies, a compreensão de suas particularidades será material para diagnósticos e terapêuticas mais precisas.

Objetivo

Objetivou-se descrever morfológicamente córneas saudáveis de aves. No primeiro trabalho, realizou-se a análise morfométrica da estrutura histológica da córnea de oito

espécies, por meio da microscopia de luz. No segundo estudo, objetivou-se analisar a córnea do bacurau, ave da espécie *Nyctidromus albicollis*, por microscopia de luz, e avaliar a morfologia e morfometria do endotélio pela da microscopia eletrônica de varredura.

REVISÃO BIBLIOGRÁFICA

A visão das aves

O sistema visual das aves e sua percepção do meio ambiente variam tanto quanto a quantidade de espécies. Compreender a interação das aves com seu meio auxilia na interpretação dos hábitos de caça, fuga e acasalamento desses animais (AUSPREY; NEWELL; ROBINSON, 2020). Apesar de possuírem outros sentidos para realizar suas atividades diárias - como campos magnéticos e sonoros, tato, olfato e audição - a visão parece ser de mais alta relevância na maioria das espécies aviárias (GRIGG et al., 2017; IWANIUK; WYLIE, 2020; POTIER; MITKUS; KELBER, 2020; WAGENER; NIEDER, 2020; PUSCH et al., 2023). Bacuraus e urutaus, da família caprimulgiformes, tem a tática de assentar e esperar que os insetos passem perto de suas cabeças para abocanhá-los, contando com suas fendas palpebrais, por onde essas aves podem enxergar mesmo de olhos fechados, e com a função tátil das vibrissas de seus bicos (DELAUNAY et al., 2020; SALAZAR et al., 2020). Águias, falcões, gaviões e urubus-pretos voam alto, onde suas capacidades olfativas e auditivas não alcançam; logo, acessam suas presas pela habilidade visual. Já o urubu-rei, se guia principalmente pelo olfato, para encontrar animais em decomposição (GRIGG et al., 2017; POTIER; MITKUS; KELBER, 2020).

Suas vantagens visuais compreendem até a retina, onde a variedade de fotorreceptores traz uma visão tetra cromática a esses animais (MEYER, 1977; GÜNTHER et al., 2021). O quarto tipo de cone, presente na retina das aves, confere a captação da luz no espectro ultravioleta, proporcionando melhor localização dos alimentos e de seus parceiros (KAMMERLING et al., 2018; ESPINHEIRA GOMES et al., 2020). Além de enxergar um maior espectro de cores, ainda há uma variação na predominância de fotorreceptores, sendo que as aves noturnas possuem mais bastonetes e as aves diurnas possuem maior densidade de cones em suas retinas (BORGES et al., 2019; ZUEVA et al., 2019; POTIER; MITKUS; KELBER, 2020). Isso porque as aves diurnas, mais coloridas, tem necessidade visual de identificar diferentes padrões e intensidades de cores, assim como maior detalhamento das imagens, funções que competem aos cones. Já as aves noturnas requerem maior habilidade de captação da pouca luz ambiente, função que compete aos bastonetes. Os quais, juntamente

com o formato tubular do bulbo ocular de corujas, bacuraus e urutaus permitem que a luz permaneça por mais tempo no interior ocular, intensificando sua captação pelos fotorreceptores (ROJAS et al., 2004^a; ROSS, 2007; BORGES et al., 2019; HALL; IWANIUK; WYLIE, 2020;).

Alguns exemplos de rapinantes diurnos ainda podem contar com duas fóveas em cada olho. A fóvea é a região da retina onde se localiza a maior densidade de cones, levando a uma alta resolução espacial que permite avistar as presas mesmo em longas distâncias (TYRRELL; FERNÁNDEZ-JURICIC, 2017a). A região da retina responsável pela resolução espacial difere com os hábitos de caça e o campo visual de cada espécie. Nos caprimulgiformes a fóvea se encontra na região ventrotemporal da retina, tendo seu campo visual binocular direcionado para a porção dorsal do seu bico (MARTIN et al., 2004; SALAZAR et al., 2020).

O campo visual varia conforme a posição das órbitas no crânio, e isso define a amplitude da visão monocular e binocular. A visão binocular é responsável pela visão estereoscópica, ou seja, a capacidade visual tridimensional (TYRRELL; FERNÁNDEZ-JURICIC, 2017b). Sabe-se que aves com os olhos posicionados frontalmente têm maior amplitude horizontal binocular, como as corujas. E quanto mais lateralizada for a posição das órbitas no crânio, mais estreito será o campo visual binocular frontal (MARTIN, 2007). Porém, diferente do que acontece em mamíferos, a visão estereoscópica não é essencial nas aves. A principal necessidade da visão binocular para as aves é observar o próprio bico, podendo controlar seus movimentos para apreensão das presas (MARTIN, 2009).

O comprimento do bico também influencia no campo visual, já que o mesmo causa um ponto cego logo a frente dele. Em aves com os olhos lateralizados, as que têm bicos curtos tem uma área cega rostral maior que as de bicos longos (TYRRELL; FERNÁNDEZ-JURICIC, 2017b), inclusive águias e urubus, tem uma extensa área cega acima de suas cabeças, o que os colocam em risco de colisão em pleno voo (TYRRELL; FERNÁNDEZ-JURICIC, 2017^a; POTIER; MITKUS; KELBER, 2020; MARTIN, 2022). Portanto, devido às limitações de campo visual, as aves desenvolveram mecanismos compensatórios de acordo com a necessidade das espécies. Seus olhos tem movimentos coordenados e em direções contrárias (mesmo tendo pouca movimentação dentro das órbitas); sua cabeça tem alta amplitude de moção e são movidas repetidamente e rapidamente para fixar o objeto de imagem; ainda contam com o movimento de “*head-bobbing*”, claramente visível em pombos, que acontece ao caminhar para estabilizar a imagem na retina (VOSS; BISCHOF, 2009;

GUNJI; FUJITA; HIGUCHI, 2013; BUTLER; TEMPLETON; FERNÁNDEZ-JURICIC, 2018; KAMMERLING et al., 2018; YORZINSKI, 2019).

Estruturas Oculares

Órbita

Ambas as cavidades orbitárias delimitam o espaço preenchido pelos bulbos oculares e alguns de seus anexos, tendo como objetivo abrigar e proteger esses órgãos. Os olhos das aves se acomodam estreitamente na órbita, sendo que em muitos casos os bulbos encaixam-se incompletamente na cavidade, pelo grande tamanho do segmento posterior desses olhos (MOORE et al., 2022a). Por esse mesmo motivo, as órbitas ocupam uma grande porção do crânio, levando a um deslocamento caudal do cérebro, e também a um septo ósseo interorbital estreito. Os ossos que formam essa estrutura são: o frontal, pré-frontal, esfenoide, etmoide (septo interorbital), palatino, quadrado e arco jugal (MCLELLAND, 1991; JONES; PIERCE; WARD, 2007).

A órbita é aberta ventralmente na maioria das espécies aviárias, sendo essa margem inferior delimitada pelo ligamento suborbital (WILLIAMS, 2012; CARVALHO et al., 2018), embora em alguns psittaciformes a encontramos fechada pelo arco suborbital (MACHADO; DOS SANTOS SCHMIDT; MONTIANI-FERREIRA, 2006). Na junção caudal do septo interorbital (paredes medial e ventral) encontra-se o forame óptico por onde passa o nervo óptico. Ventralmente a esse, três pequenos forames permitem a passagem dos nervos oculomotor, troclear e o ramo oftálmico do nervo trigêmeo. Os ossos envolvidos na composição da órbita são pneumáticos, por isso são mais frágeis e suscetíveis a fraturas (WILLIAMS, 2012).

A porção ventral da órbita faz fronteira com os seios paranasais e com o divertículo do seio infraorbitário (VELADIANO et al., 2016). Em muitas aves (psittaciformes, galloanserae e passeriformes insetívoros), os seios infraorbitais direito e esquerdo se comunicam, mas não em passeriformes não insetívoros (MOORE et al., 2022a). Devido à proximidade com o bulbo, a sinusite do seio paranasal e do divertículo infraorbitário podem levar a alterações oftálmicas atingindo órbita, periórbita e bulbo ocular, causando edema, compressão, exoftalmia, conjuntivite e uveíte (WILLIS; WILKIE, 1999; CARVALHO et al., 2018).

A vascularização da órbita é realizada pela artéria tèmpero-orbitária, que tem origem da artéria carótida interna. Essa se ramifica em artérias infraorbitária, oftalmotemporal e

supraorbitária, que fazem o suprimento de sangue arterial, enquanto a drenagem é realizada paralelamente por veias com os mesmos nomes, que direcionam o sangue venoso para a veia maxilar e cefálica rostral (PORTER; WITMER, 2016).

Anexos Oculares

Fazem parte dos anexos oculares, pálpebras, músculos, aparato lacrimal e glândulas. As pálpebras são três: superior, inferior e terceira pálpebra. A pálpebra inferior contém uma placa tarsal fibrosa, é sempre maior, mais móvel, mais transparente e delgada que a superior, sendo a principal responsável pela oclusão da comissura palpebral (CARVALHO et al., 2018; MOORE et al., 2022a). Essas características não se aplicam às corujas (RODARTE-ALMEIDA et al., 2013). A porção mais externa das pálpebras superior e inferior pode ser recoberta por filoplumas ou estarem com a pele à mostra, como é o caso das araras. A estrutura da plumagem peripalpebral é especializada e variável entre as espécies aviárias, dependendo das necessidades protetoras e sensoriais de cada uma. Na maioria das aves de rapina, por exemplo, há uma crista superciliar bem desenvolvida onde as penas dessa região se estendem a cima e a frente dos olhos, com o objetivo de diminuir a incidência ou reflexo da luz solar diminuindo o reflexo de ofuscamento (JONES; PIERCE; WARD, 2007). A porção média das pálpebras é composta por músculos, glândulas de Zeiss e de Moll, sebáceas e sudoríparas respectivamente. Aves não possuem glândulas de meibômio. Três músculos estriados permitem a movimentação, o elevador da pálpebra superior, o retrator da pálpebra inferior e o músculo orbicular presente em ambas as pálpebras. Esses são inervados respectivamente pelo oculomotor e pelo nervo mandibular. A camada interna é a conjuntiva palpebral, onde se localizam as células caliciformes e o tecido linfoide associado à conjuntiva (BAYÓN; ALMELA; TALAVERA, 2008; MONÇÃO-SILVA et al., 2016).

As pálpebras também caracterizam dois tipos de aves de acordo com sua eclosão. Quando as pálpebras estão bem desenvolvidas e a fissura palpebral está aberta no momento da eclosão, são chamadas aves precociais; galináceos e anatídeos são exemplos, pois são filhotes relativamente maduros e capazes de seguir a progenitora em busca de alimento. Enquanto que pálpebras seladas e incompletamente desenvolvidas são características de aves altriciais, espécies eclodidas sem plumagem, sem capacidade de andar e dependente dos indivíduos adultos. O tempo de abertura das pálpebras em aves altriciais é variável: no caso das cacatuas ocorre entre 10-17 dias após a eclosão e nas araras 17-26 dias. A separação palpebral inicia-se centralmente, progredindo medial e lateralmente (SCHEIBER et al., 2017; CHEN et al., 2019a, 2019b).

A terceira pálpebra é uma membrana delgada e muitas vezes transparente, altamente móvel, que cobre toda a córnea partindo da porção dorsonasal para a ventrotemporal, também chamada de membrana nictante. O músculo piramidal, que move a terceira pálpebra, origina-se na esclera posterior e circunda o nervo óptico por meio do ligamento do músculo quadrado (WILLIAMS, 2012). A membrana nictante é responsável por espalhar o filme lacrimal, remover debris e corpos estranhos, e principalmente proteger e evitar danos à córnea, permitindo o voo e/ou mergulho de olhos abertos, pois não interfere na refração da córnea quando a recobre (SIVAK; BOBIER; LEVY, 1978).

As glândulas das aves são de dois tipos: a lacrimal, que produz o fluido lacrimal aquoso, e a glândula de Harder, que produz secreção mista. A glândula lacrimal tem menor relevância nas aves que nos mamíferos, e algumas espécies como corujas nem a possuem. Já as aves semiaquáticas possuem uma grande glândula lacrimal, localizada ventrolateralmente ao bulbo, e seus micro ductos se abrem no saco conjuntival, na porção lateral da pálpebra inferior, por onde secretam a porção aquosa do filme lacrimal. A glândula de Harder é maior, mais desenvolvida e a principal fonte lacrimal nas aves (BAYÓN; ALMELA; TALAVERA, 2008; WILLIAMS, 2012). Ela está localizada medialmente ao bulbo, entre os músculos oblíquo ventral e reto medial. Seus ductos liberam substâncias lipídicas e seromucóides que compõe o filme lacrimal, depositado entre a membrana da terceira pálpebra e a córnea, nutrindo diretamente a córnea e desempenhando papel de defesa imunológica (MOORE et al., 2022a). Há ainda, em algumas aves marinhas, a glândula de sal, que faz a eliminação de eletrólitos absorvidos durante a imersão subaquática (MOORE et al., 2022a).

O sistema de drenagem lacrimal inclui dois óstios e canalículos lacrimais, assim como nos mamíferos e répteis, e estão posicionados próximos à comissura lacrimal medial das pálpebras superior e inferior. Os canalículos se unem ao ducto nasolacrimal que desemboca na cavidade oronasal dorsal, rostralmente às coanas (WILLIS; WILKIE, 1999; WILLIAMS, 2012).

Os músculos extraoculares são seis, sendo quatro retos – dorsal, ventral, medial e lateral – e dois oblíquos – ventral e dorsal. Nas aves, o músculo retrator do bulbo está ausente e os músculos extraoculares existentes são pouco desenvolvidos em relação aos mamíferos. Pois além de o bulbo ocupar quase toda órbita, ainda há a porção óssea da esclera que é aderida à margem orbitária, limitando a movimentação do olho. A inervação dos músculos é realizada pelo ramo dorsal do nervo oculomotor (reto dorsal), ramo ventral do oculomotor

(retos medial e ventral, e oblíquo ventral), nervo troclear (oblíquo dorsal) e nervo abducente (reto lateral) (MOORE et al., 2022a).

Bulbo ocular

O olho é dividido em três camadas: a externa, a média e a interna, também conhecidas como túnicas fibrosa, vascular e nervosa, respectivamente. O bulbo também é dividido em segmentos e câmaras. No segmento anterior está presente a córnea, câmara anterior e câmara posterior preenchidas por humor aquoso, íris, lente e corpo ciliar. O segmento posterior é maior que o anterior, e nas aves chega a ser 2 a 3 vezes maior. Nele estão presentes coróide, retina, vítreo, pecten ocular e nervo óptico (MOORE et al., 2022a).

O bulbo ocular nas aves é tão grande que, em algumas espécies, o equador do bulbo excede as margens da órbita, como nas corujas. O seu formato varia entre as espécies, podendo ser três: achatado, globoso e tubular (BAYÓN; ALMELA; TALAVERA, 2008). O olho achatado tem o eixo anteroposterior curto em relação aos outros formatos, assim como a região da câmara anterior e corpo ciliar, pois tanto a córnea (convexa) como a região média do bulbo (côncava) tem sua curvatura diminuída, próximo ao eixo plano. É o formato mais comum e presente na maioria das aves diurnas, como em psitacídeos, passeriformes e aves aquáticas. O comprimento anteroposterior intermediário é encontrado no formato globoso, onde a córnea é mais convexa e a região do corpo ciliar tem maior concavidade que o formato anterior. Esse formato é encontrado em aves diurnas com a cabeça mais larga, que tem uma necessidade visual mais exigente, como aves insetívoras, de rapina e avestruzes (MARTIN; ASHASH; KATZIR, 2001; BAYÓN; ALMELA; TALAVERA, 2008; CARVALHO et al., 2018; MOORE et al., 2022a). Em aves noturnas, nas quais é necessário maior aproveitamento da luz presente, o comprimento do bulbo se faz maior com o formato tubular. A região média dos bulbos tubulares é longa e côncava, formando um túnel para o segmento posterior. O equador do bulbo se encontra rostralmente à órbita, com córneas grandes e bem convexas, como no caso das corujas (BAYÓN; ALMELA; TALAVERA, 2008; RODARTE-ALMEIDA et al., 2013).

O suprimento vascular do bulbo das aves é dado pela artéria oftálmica externa, ramo da subdivisão interna da artéria carótida comum. Essa dá origem à artéria oftalmotemporal, e seus ramos são a principal irrigação do olho. Esse modelo vascular é o mesmo conhecido em mamíferos (HOSSLER; OLSON, 1984; PORTER; WITMER, 2016; DOWNIE et al., 2021). Para o suprimento do pecten, um ramo específico da artéria oftalmotemporal foi

desenvolvido, a artéria *pectinis oculi* (FERREIRA; GIANNICO; MONTIANI-FERREIRA, 2016).

A inervação do bulbo ocular é realizada pelo nervo oftálmico, ramo do nervo trigêmeo, e pelo nervo óptico. O nervo oftálmico se ramifica em nervos ciliares curtos e longos que adentram o equador da esclera, provendo controle voluntário da íris, e resposta sensorial a córnea e corpo ciliar. O nervo óptico é responsável por transmitir ao cérebro a informação de imagem. Já a inervação autônoma vem do gânglio cervical, projetando mais fibras simpáticas do que parassimpáticas (LACERDA et al., 2014; HE; PHAM; BAZAN, 2022; WU; ZHAO; ZHANG, 2022).

Esclera

A túnica fibrosa ou externa, é composta pela esclera e córnea. Elas formam um envoltório fibroso, como o nome sugere, que recobre todo o bulbo e tem como principal função a proteção das estruturas internas, também é a camada que confere formato e rigidez ao bulbo. A esclera é uma camada densa, branca, vascularizada e formada por fibras colágenas. Diferente de outros vertebrados, a esclera das aves possui um anel escleral formado por pequenos ossos pneumáticos que circundam o equador do bulbo, nomeados de ossículos esclerais. Essa é a região que se adere ao periósteo da órbita, e onde os músculos ciliares se conectam (FISCHER; SCHOENEMANN, 2019; ZEHTABVAR et al., 2022).

A córnea será amplamente discutida na secção *A córnea das aves*.

Lente

A lente é uma estrutura biconvexa, transparente, flexível e macia. Nas aves tem formato quase esférico em olhos tubulares, e alongado em olhos chatos e globosos, tendo a porção anterior mais aplanada e a posterior mais abaulada. Possui uma almofada anular fibrosa em seu equador que permite uma resistente conexão com o corpo ciliar e os músculos ciliares (GLASSER; HOWLAND, 1996; BEEBE; COATS, 2000; MONÇÃO-SILVA et al., 2016).

A principal função da lente é permitir a chegada da luz na retina, por meio da sua propriedade refrativa. Para que isso ocorra, além de transparência, é necessário o ajuste da distância focal, realizado pelo mecanismo de acomodação. Esse mecanismo é a capacidade de mudança da curvatura da lente e da córnea das aves, alterando o poder de refração da luz (MEYER, 1977; GLASSER; HOWLAND, 1996; SIVAK, 2004; POTIER; MITKUS;

KELBER, 2020). As aves aquáticas têm suas córneas quase planas e não flexíveis, então deixam a lente com toda a função de acomodação sub aquática (SIVAK, 2004; COLLIN; COLLIN, 2021). A acomodação é promovida por músculos ciliares estriados, denominados músculo de Crampton, músculo de Brucke e músculo de Müller, e o músculo esfíncter da íris. O primeiro tem ação na córnea, e os demais na lente. Em aves mergulhadoras, esfíncter pupilar potencializa a contração do músculo ciliar para acomodação da lente, encurtando-a até o formato próximo ao esférico, e possibilitando o ajuste do foco subaquático para caça e fuga (HOWLAND, 1983; HOWLAND, 1987; MURPHY; SIVAK, 2004; BAYÓN; ALMELA; TALAVERA, 2008; SCHAEFFEL; WILLIAMS, 2012).

Íris, corpo ciliar, coroide e pécten

A túnica vascular ou média é composta pelas estruturas responsáveis pelo suprimento vascular e função imunológica do olho. A íris e o corpo ciliar suprem a porção anterior do bulbo ocular, enquanto a coroide e o pécten são responsáveis pela retina (KIAMA et al., 2001; REESE; HORST; LIEBICH, 2005; JONES; PIERCE; WARD, 2007; ALBINI; DAVIS, 2015).

A íris é a estrutura responsável por controlar a incidência de luz na retina. Sua face anterior é o estroma, composto por vasos sanguíneos, músculos, pigmentos carotenoides, purinas, pteridinas, e melanócitos, que dão cor a íris. Essa pigmentação nas aves varia entre as espécies, e também entre a idade e sexo da mesma espécie. A face posterior é composta por mioepitélio colunar pigmentado (JONES; PIERCE; WARD, 2007; BAYÓN; ALMELA; TALAVERA, 2008; MONÇÃO-SILVA et al., 2016). Pode-se dividir a íris em duas regiões, a borda ciliar, porção mais externa que está ligada ao corpo ciliar, e a borda pupilar, região que forma a pupila. Na borda pupilar há o músculo esfíncter que contrai fazendo o fechamento da pupila, ou miose. Na borda ciliar está presente o músculo dilatador da pupila, responsável pela midríase. A pupila apresenta uma grande variedade de formatos nos vertebrados, e o que confere essa distinção é a disposição das fibras musculares na borda pupilar. O mecanismo de contração e dilatação da pupila se dá por músculos estriados, ou seja, nas aves o movimento da íris é voluntário. Isso permite alcançar maior profundidade de foco através da miose voluntária (SIVAK, 2004; WILLIAMS, 2012).

O corpo ciliar tem origem na base da íris e sua extensão vai até onde começa a retina. É formado por duas regiões, a *pars plicata*, onde estão os processos ciliares e ligamentos zonulares que fixam a lente, e a *pars plana* que segue para o segmento posterior e se encontra

com a retina. Assim como nos demais vertebrados, o corpo ciliar das aves tem a função de produzir humor aquoso, sustentar a lente e participar da defesa imune dos olhos (REESE; HORST; LIEBICH, 2005; JONES; PIERCE; WARD, 2007). A drenagem do humor aquoso ocorre pelo ângulo iridocorneano, que é bem desenvolvido nas aves, e seus ligamentos pectinados são claramente definidos, em algumas aves podem ser observados sem lente de gonioscopia (HARRIS et al., 2008; RODARTE-ALMEIDA et al., 2013; SOKOLENKO et al., 2021)

A coroide se inicia com o término do corpo ciliar, se encontra justaposta e externamente à retina, localizada no segmento posterior. É composta por 4 camadas, da mais externa para a mais interna: a lâmina supracoroide, que está em contato com a esclera; a camada vascular, que contém grandes vasos sanguíneos; a camada de coriocapilares, formada por uma rede de capilares oriundos da camada anterior, que tem papel essencial na nutrição da retina; e a lâmina basal sobre a qual repousa a retina (JONES; PIERCE; WARD, 2007; PLATZL et al., 2022). A lâmina supracoroide, ou membrana fusca, das aves é mais desenvolvida que em mamíferos, sendo mais espessa e flexível. Isso auxilia na adesão da coroide com a esclera, e na absorção de impactos no interior dos olhos de aves mergulhadoras e aves que atingem altas distâncias de voos (DE STEFANO; MUGNAINI, 1997). O fundo do olho das aves é normalmente descrito como atapetal, pois não é visualizado um *tapetum* verdadeiro no exame direto da retina ou histologicamente (ROJAS et al., 2004b; MARTIN et al., 2014; CARVALHO et al., 2018; MOORE et al., 2022b).

O pécten, peculiaridade das aves, é uma membrana pregueada, altamente vascularizada. Essa estrutura se origina da coroide e adere à retina. Sua base repousa sobre a papila óptica, recobrando-a, e seu corpo se projeta para o interior do vítreo direcionada para o centro do bulbo. É composto por capilares e células estromais pigmentadas extra vascularmente. É delimitado por uma fina lâmina basal contínua e a membrana limitante interna da retina (KIAMA et al., 2001; MONÇÃO-SILVA et al., 2016). O pécten é responsável por complementar o suporte nutricional da retina, assim como realizar sua barreira imune. Também produz humor aquoso e reduz o ofuscamento, diminuindo a incidência de luz direta na retina e papila óptica (FERREIRA; GIANNICO; MONTIANI-FERREIRA, 2016; FERREIRA et al., 2019). O pécten possui variações em seu formato e na quantidade de pregas de acordo com a espécie aviária. A quantidade de pregas demonstra estar relacionado às atividades noturnas (com menor número) ou diurnas (com maior número) das aves (ABUMANDOUR; BASSUONI; HANAFY, 2021). São descritos 3 formatos de

pécten: o cônico, presente em aves kiwis; em formato denominado “vanned”, descrito em avestruzes; e o plissado, pertencentes a maioria das aves (DAYAN; OZAYDN, 2013; YILMAZ et al., 2021).

Retina e nervo óptico

Ainda no segmento posterior, encontramos a túnica nervosa ou interna, que compreende a retina e o nervo óptico. Conectado a túnica nervosa está o vítreo, corpo denso de colágeno transparente que ocupa toda a câmara vítrea e aloja o pécten em seu interior (JONES; PIERCE; WARD, 2007).

A retina das aves é anangiótica, e recebe nutrientes e oxigênio através da coroide e do pécten. Assim como as demais estruturas oculares, a retina também tem especificidades nas aves. Porém suas camadas recebem a mesma nomenclatura e tem as mesmas constituições celulares básicas que a retina dos mamíferos (RUGGERI et al., 2010; POTIER; MITKUS; KELBER, 2020). A retina tem a função de captar a luz e converter os estímulos luminosos em sinais elétricos que serão transmitidos ao cérebro. A captação dos espectros luminosos é realizada pelos fotorreceptores, cones e bastonetes (EGBUNIWE; AYO, 2016; ZUEVA et al., 2019). As aves possuem um tipo de bastonete, um cone duplo, e quatro tipos de cones simples. Os cones duplos são predominantes em aves diurnas. Cada tipo de cone possui uma opsonina, que capta uma frequência luminosa diferente, e gotículas de óleo em seu interior. Essas gotículas de óleo filtram a luz e tornam o comprimento de onda mais longo, aumentando a sensibilidade espectral dos cones (MITKUS et al., 2018; GÜNTHER et al., 2021). A distribuição e a densidade dos fotorreceptores na retina variam de acordo com os hábitos de cada espécie aviária. Não só sobre visão escotópica (predominância de bastonetes) ou fotópica (predominância de cones), mas também variam a distribuição de acordo com o campo visual de suas necessidades para caça. A alta densidade de fotorreceptores leva a um espessamento da retina, sendo mais espessa no centro. Aves de rapina diurnas tem suas retinas consideravelmente mais espessa que outras espécies de aves (ROJAS et al., 2004b; EGBUNIWE; AYO, 2016; TYRRELL; FERNÁNDEZ-JURICIC, 2017a; MITKUS et al., 2018; POTIER; MITKUS; KELBER, 2020). Há, ainda na região central da retina, uma alta concentração de cones e células ganglionares. Quando há invaginação da retina essa região é denominada fóvea, sem a invaginação denomina-se área *centralis*. Em águias, gaviões e falcões, encontram-se duas fóveas, a segunda ocupa a região temporal da retina. Já urubus e condores, tem apenas a fóvea central, mas na região temporal eles possuem uma área *temporalis*, local com alta densidade de cones. Algumas aves têm apenas a área *centralis*.

Toda função que a fóvea exerce ainda é objeto de estudo, mas é sabido que essa estrutura é responsável por fixar a imagem no campo binocular e aumentar a resolução da mesma (TYRRELL; FERNÁNDEZ-JURICIC, 2017a; POTIER et al., 2020a, 2020b; POTIER; MITKUS; KELBER, 2020).

O nervo óptico é formado pelos axônios das células ganglionares da retina, que se tornam mielinizadas à medida que penetram a esclera. As fibras seguem caudalmente através do forame óptico e decussam quase completamente no quiasma óptico, para então seguir o caminho até o córtex visual. O diâmetro transversal do nervo óptico das aves é maior que o da medula espinhal cervical (OROSZ; BRADSHAW, 2007). O modelo de decussação do nervo óptico das aves levava a acreditar que esses animais não tinham reflexo pupilar consensual, e sim um reflexo pupilar direto devido a iluminação que atingia o olho contralateral através do septo interorbital, que é delgado a ponto de permitir a passagem da luz de uma órbita a outra. Porém foi demonstrado experimentalmente que o reflexo pupilar consensual realmente está presente em aves (LI; HOWLAND, 1999; MOORE et al., 2022a).

A córnea das aves

A córnea é a estrutura mais externa do bulbo ocular, responsável por prover proteção às estruturas internas e poder de refração da imagem. Para que isso seja possível, a córnea precisa ser transparente, convexa e ter uma relativa rigidez (ABDELFTAH et al., 2021; DOWNIE et al., 2021). Sua convexidade, ou curvatura, varia de acordo com o formato do bulbo ocular, sendo levemente aplanada em bulbos achatados, e próximas a uma semiesfera em bulbos tubulares. A curvatura associada à transparência desempenha a função de refração e convergência da luz, sendo a córnea a primeira superfície óptica que a luz ultrapassa para chegar à retina e possibilitar a formação da imagem (JONES; PIERCE; WARD, 2007; MARTIN, 2022). O poder refrativo da córnea chega a ser igual ao da lente em aves com olhos globosos ou tubulares; enquanto nas aves de bulbo ocular achatado, a lente exerce o maior poder de refração (MARTIN; ASHASH; KATZIR, 2001; LIU et al., 2016). Embora a córnea seja rígida, para proteção contra impactos externos e sustentação das estruturas internas, essa rigidez não é absoluta. A córnea tem propriedades reológicas, para que seja possível sua deformação (atenuação ou acentuação da curvatura) diante do mecanismo de acomodação para focalizar a imagem (LIU et al., 2016; ABDELFTAH et al., 2021; COLLIN; COLLIN, 2021).

A transparência da córnea é possível por ser avascular, por ter seu estroma com fibras de colágeno organizadas paralelamente - camada responsável pela maior parte de sua espessura-, e por fim, pela manutenção do estado de deturgescência, responsável pelo epitélio e endotélio (MATTHYSSEN et al., 2018; COYO et al., 2019; COLLIN; COLLIN, 2021). Como não há presença de vasos sanguíneo ou linfáticos na córnea, o fornecimento de oxigênio e nutrientes é proveniente do filme lacrimal, humor aquoso e vascularização perilímbica. A maior parte do suprimento de oxigênio é oriundo do ar atmosférico, transportado pela lágrima. Enquanto o humor aquoso é a principal fonte de glicose e aminoácidos essenciais (DOWNIE et al., 2021).

Assim como nos mamíferos, a inervação sensorial e autônoma da córnea é feita pelo ramo oftálmico do nervo trigêmeo, que se ramifica em nervos ciliares curtos e longos. Seus feixes nervosos adentram a esclera e a coróide, e alcançam a região periférica da córnea, onde se ramificam densamente por toda circunferência corneana e a penetram radialmente pelo estroma. Os feixes continuam se ramificando em direção ao centro e à superfície (epitélio) da córnea, ocupando-a de forma homogênea (LACERDA et al., 2014; DOWNIE et al., 2021; HE; PHAM; BAZAN, 2022; WU; ZHAO; ZHANG, 2022). Como particularidade das aves, a densidade de fibras nervosas na periferia da córnea é maior que em mamíferos. Essas fibras também não fazem anastomose no centro do estroma, sendo que em mamíferos há formação de uma malha nervosa estromal. Outra diferença é que nas aves os nervos não formam um formato centrípeto em direção ao centro corneano, e sim percorrem radialmente a córnea (HE; PHAM; BAZAN, 2022). Na presença de estímulos térmicos, mecânicos e químicos, há uma resposta motora do nervo facial, gerando o reflexo de piscar, e uma resposta autonômica (principalmente simpática) para secreção lacrimal, garantindo a lubrificação e integridade da córnea (LACERDA et al., 2014; LABETOULLE et al., 2019; WU; ZHAO; ZHANG, 2022).

A estrutura histológica da córnea das aves segue a mesma arquitetura dos demais vertebrados, sendo composta mandatoriamente por 4 camadas: mais externamente o epitélio estratificado não queratinizado; após, o estroma, camada que confere espessura à córnea, formado por lamelas de colágeno; a membrana de Descemet, membrana basal acelular da última camada; por fim e mais internamente o endotélio, camada única de células hexagonais. A maioria das aves também apresenta uma quinta camada pertencente ao estroma, a membrana de Bowman, que está logo abaixo da membrana basal do epitélio. As camadas da córnea ainda sofrem variações espécie-específicas, de acordo com o nicho ecológico ocupado pelas aves (KAFARNIK; FRITSCHKE; REESE, 2007; TSUKAHARA et al., 2010;

ABDELFTAH et al., 2021; COLLIN; COLLIN, 2021). Já a espessura da córnea das aves varia não só com a espécie, mas também com o formato do bulbo ocular e de acordo com a região central ou periférica da córnea. Olhos de formato tubular tem córneas marcadamente mais finas no centro do que na periferia (MURPHY; DUBIELZIG, 1993; WERTHER; CANDIOTO; KORBEL, 2017). Diferente de aves com olhos achatados, onde a espessura do centro e da periferia são aproximadas (CHARD; GUNDLACH, 1938; MOORE et al., 2019). A espessura das córneas também não obedece a uma proporção de alometria, já que a mesma não está relacionada ao tamanho e/ou peso da ave (LIU et al., 2016; POPOVA et al., 2022).

Epitélio

O epitélio é a camada superficial da córnea, composta por camadas de células escamosas estratificadas e não queratinizadas. A camada basal consiste em células de formato cuboide ou colunar, sendo coberta por camadas de células que se tornam mais largas e achatadas à medida que se afastam da base. Essas células, que apresentam formas variadas, são chamadas de células poliédricas. As células escamosas mais externas são achatadas, conhecidas como células guarda-chuva ou células alares, devido à sua sobreposição aos ápices de mais de uma célula (COLLIN; COLLIN, 2000; MONÇÃO-SILVA et al., 2016; NAUTSCHER et al., 2016; PINTO et al., 2016; BERGMANSON, 2019; SOKOLENKO et al., 2021). Outra característica das células epiteliais é a presença de microvilos, que são projeções perpendiculares da membrana celular. Os microvilos são responsáveis por aumentar a área de superfície da célula, aumentando o contato com o fluido lacrimal, assim, podendo usufruir melhor de seus benefícios e diminuindo a velocidade de evaporação do mesmo (COLLIN; COLLIN, 2000, 2006). Entre as espécies de aves há variações da espessura do epitélio, da densidade das células epiteliais e o número de camadas epiteliais. Pinguins, aves de rapinas, e aves domésticas entre outros, já foram estudados, e a quantidade de camadas epiteliais varia de 3 a 8 (CHARD; GUNDLACH, 1938; MURPHY; DUBIELZIG, 1993; PINTO et al., 2016; WERTHER; CANDIOTO; KORBEL, 2017; SOKOLENKO et al., 2021; COLLIN; COLLIN, 2021). A espessura do epitélio das aves varia de 5 a 10% da espessura total da córnea (ABDELFTAH et al., 2021; POPOVA et al., 2022). A densidade das células epiteliais demonstra ser maior em aves voadoras do que em aves terrestres, já que essas poderiam sofrer com uma maior velocidade de evaporação da lágrima (COLLIN; COLLIN, 2006).

Membrana de Bowman

A membrana de Bowman é uma camada de fibras colágenas condensadas, também chamada de membrana limitante anterior, devido a sua localização no estroma anterior. É a camada que sofre maior variação morfológica entre as espécies de aves e de outros vertebrados, podendo inclusive, não estar presente na córnea (HAYASHI; OSAWA; TOHYAMA, 2002; KAFARNIK; MERINDANO et al., 2002; FRITSCHÉ; REESE, 2007; POPOVA et al., 2022). A membrana de Bowman é descrita em diversas espécies de aves, como galinhas, codornas, patos, pelicanos, aves de rapina, psitacídeos e passeriformes (MURPHY; DUBIELZIG, 1993; KAFARNIK; FRITSCHÉ; REESE, 2007; GONÇALVES et al., 2016; PINTO et al., 2016; ABDELTAH et al., 2021; POPOVA et al., 2022). Essa tem similaridades com a membrana de humanos, por isso, a córnea de aves é modelo de pesquisa para cirurgias refrativas de humanos (REESE, 2007; GONÇALVES et al., 2016; KAFARNIK; FRITSCHÉ; LIU et al., 2016). Porém, ela é considerada rudimentar por alguns autores, já que comparada aos humanos e outros primatas, a membrana de Bowman das aves não tem a mesma expressão e definição de suas margens na histologia da córnea (MERINDANO et al., 2002; POPOVA et al., 2022).

Estroma

O estroma, ou substância própria, é um tecido conectivo denso, formado por lamelas de colágeno sobrepostas e alinhadas paralelamente a superfície, e com queratócitos dispersos entre as lamelas (MEEK; LEONARD, 1993; TSUKAHARA et al., 2010). Nas aves, as lamelas de colágeno são alinhadas entre si formando um arranjo ortogonal preciso e regular, com grande quantidade de ramificações promovendo anastomose dos feixes, desenhando o formato de uma grade. Esse arranjo é mais evidente na porção anterior e média da substância própria, e é associado à maior rigidez mecânica e melhor transmitância da luz no espectro UV – significa que a luz solar que bate na córnea sofre maior dispersão, diminuindo o ofuscamento (TSUKAHARA et al., 2010; BOOTE et al., 2011; KOUDOUNA et al., 2018). O estroma representa a espessura da córnea, já que corresponde a uma média de 90% da espessura total da córnea (NAUTSCHER et al., 2016; KOUDOUNA et al., 2018; ABDELTAH et al., 2021). Portanto, é o estroma que leva a diferenças de espessuras entre as regiões da córnea (HENRIKSSON; BRON; BERGMANSON, 2012; BERGMANSON; BURNS; WALKER, 2019; BERGMANSON; BURNS; NAROO, 2021).

Membrana de Descemet

A membrana de Descemet é bem desenvolvida nas aves. É a membrana basal do endotélio, e tem a função de auxiliar essa camada. Por ser composta de colágeno concentrado, ela confere resistência mecânica ao endotélio, e também modula a entrada de humor aquoso no estroma anterior. A espessura da membrana de Descemet é variável com a idade da ave, tendo sua espessura aumentada pelo envelhecimento do indivíduo (COLLIN; COLLIN, 2021).

Endotélio

O endotélio é representado como uma monocamada de células principalmente hexagonais de tamanho e forma relativamente uniformes. As células endoteliais têm a capacidade de aumentar de tamanho (polimegatismo) e alterar sua forma (pleomorfismo) para manter o estado de deturgescência da córnea. Esse mecanismo ocorre devido à incapacidade de replicação das células endoteliais e à necessidade de suprir eventuais defeitos. Portanto, é possível visualizar células endoteliais pentagonais, heptagonais, octogonais e até quadradas (COLLIN; COLLIN, 1998; PIGATTO et al., 2004, 2009; DOUGHTY, 2006, 2018; TAMAYO-ARANGO et al., 2009; FRANZEN et al., 2010; ALBUQUERQUE; FREITAS; PIGATTO, 2015; COYO et al., 2019). Em aves jovens, há uma discreta regeneração tecidual, enquanto em adultos e senis, o polimegatismo é evidente. Aves senis podem atingir uma quantidade de 40% ou mais de células endoteliais sem sua forma original (LAING et al., 1976; KAFARNIK; FRITSCHKE; REESE, 2007; ALBUQUERQUE; FREITAS; PIGATTO, 2015; COYO et al., 2015; COLLIN; COLLIN, 2021). As células endoteliais das aves também possuem microvilosidades que emergem de suas margens e superfícies (COLLIN; COLLIN, 1998, 2021; PIGATTO et al., 2018). Por ser uma camada unicelular, as variações interespecíficas do endotélio são avaliadas principalmente de acordo com densidade celular e área celular média. Para avaliar a saúde endotelial, a porcentagem de células hexagonais e o coeficiente de variação da área celular se mostram úteis (DOUGHTY, 1989, 2008). O coeficiente de variação da área celular corresponde ao polimegatismo, a taxa mede a variação do tamanho original das células. E a porcentagem de células hexagonais demonstra o número de células endoteliais que estão em sua forma primária. Portanto, quanto mais próximo de zero estiver o coeficiente de variação, e mais próximo de 100% for a porcentagem de células hexagonais, mais saudável e jovem é esse endotélio (PIGATTO et al., 2005, 2009; ALBUQUERQUE; FREITAS; PIGATTO, 2015; COYO et al., 2019).

CAPÍTULO II

1 Original Article (*Anatomia, Histologia, Embryologia*)

2

3 **Corneal histomorphometry of birds from the Brazilian Midwest**

4

5 Rafaela Alves R. Tozetti¹, Matheus Vilaro L. Moreira ², Rosélia de Lima S. Araújo¹, Liria
6 Queiroz Luz Hirano³, Bret A. Moore⁴ and Paula Diniz Galera¹.

7

8 ¹Post-graduate Program in Animal Sciences, Faculty of Agronomy and Veterinary Medicine,
9 University of Brasília, Distrito Federal, Brazil;

10 ²MVL Patologia Veterinária, Belo Horizonte, Brazil;

11 ³Department of Wild Animals, Faculty of Agronomy and Veterinary Medicine, University of
12 Brasília, Distrito Federal, Brazil

13 ⁴ Department of Small Animal Clinical Sciences, College of Veterinary Medicine, University
14 of Florida, Gainesville, FL, USA.

15

16 Correspondence

17 Paula Diniz Galera, Small Animals Veterinarian Hospital of the University of Brasilia (UnB),
18 L4 Norte, Campus Darcy Ribeiro, UnB – Asa Norte, DF. 70636-200.

19 Phone number: +55 (61) 99266-0799

20 Email: dra.paulagalera@gmail.com

21

22

23

24 **Acknowledgment**

25 This study was funded by *Coordenação de Aperfeiçoamento de Pessoal de Nível*
26 *Superior (CAPES), Brazil – Funding code 001, and by Fundação de Apoio à Pesquisa*
27 *do Distrito Federal (FAPDF), Brazil – proc.n. 00193.00001303/2019-10).*

28

29

30 **Abstract**

31 The visual structures of birds vary according to their environment, habits, needs of
32 breeding, feeding and predators presence. The cornea is one of the structures in which it is
33 possible to observe clear variations, it is responsible for protecting the inside of the eye,
34 assisting in focusing and refracting the image. Based on the need to know the visual and
35 structural differences between bird species, this work aimed to describe the corneal
36 histomorphometry structures of the following birds: *Asio stygius*, *Crotophaga ani*, *Pitangus*
37 *sulphuratus*, *Turdus rufiventris*, *Ramphastos toco*, *Rhea americana*, *Ara macao* and *Nyctibius*
38 *griseus*. These are present in the Brazilian Midwest, an area in which the Cerrado is the
39 predominant vegetation. Through the results it was possible to observe that the gross corneal
40 composition is the same in all birds. Although, they differ from each other in the thickness of
41 the central and peripheral regions, even in the total cornea and in its layers, and in number of
42 epithelial lines.

43

44 **Keywords:** avian; eye; histology; morphometry; ophthalmology; vision.

45

46 **Introduction**

47 The visual system of birds varies as much as the broad variety of species within these
48 taxa, where the morphology and physiology of vision meets the needs for success in the
49 specific ecological niche they occupy. The cornea is a specialized component of the vertebrate
50 eye with essential functions for avian life, providing protection, refractive power,
51 transparency for image formation, and mechanical support (Abdeltah et al., 2021;
52 Bergmanson, 2019; Jones, Pierce, & Ward, 2007; Meek & Fullwood, 2001). It is one such
53 structure of the eye where interspecific variation can clearly be observed, despite its similarity
54 in histological composition to that of other vertebrates (Collin & Collin, 2006; Meyer, 1977).
55 Even sharing the same habitat, it is possible to observe birds with different visual behaviors,
56 which can be reflected in the morphology of their corneas.

57 The cornea of birds is composed of five histological layers: epithelium, Bowman's
58 layer, stroma, Descemet's membrane and endothelium. However, in some birds, the
59 Bowman's layer has not been identified (Abdeltah et al., 2021; Kafarnik et al., 2007; Popova
60 et al., 2022; Sokolenko et al., 2021). Although the gross structure does not differ among most
61 birds, a distinction can be seen in the diameter, thickness and in number of layers of epithelial
62 cells (Collin & Collin, 2021; Moore, Fernandez-Juricic, Hawkins, Montiani-Ferreira, &
63 Lange, 2022; Tamayo-Arango et al., 2009). Due to the plurality of avian species, seeking
64 knowledge of interspecific differences is important to understanding their visual demands,
65 behaviors, and ecology. This study aimed to describe the histomorphometry of the cornea of
66 eight ecologically and phylogenetically diverse avian species from the Midwest region of
67 Brazil bird: *Asio stygius*, *Crotophaga ani*, *Pitangus sulphuratus*, *Turdus rufiventris*,
68 *Ramphastos toco*, *Rhea americana*, *Ara macao* and *Nyctibius griseus*.

69 In the Brazilian cerrado, Scarlet Macaws *Ara macao* and Toco Toucans *Ramphastos*
70 *toco* mainly inhabit forests and feed on fruits, seeds and insects (BirdLife International,
71 2016a, 2017; Massari et al., 2020). The Rufous-bellied Thrush *Turdus rufiventris* and the
72 Great Kiskadee *Pitangus sulphuratus* are two examples of passerines; while belonging to
73 different families, both have an excellent adaptation to urban life (BirdLife International,
74 2016c, 2018; Calegario-Marques & Amato, 2014; Gasperin & Aurélio Pizo, 2009; Lago-
75 Paiva, 1996). The Greater Rheas *Rhea americana* are omnivorous birds that do not have the
76 ability to fly and differ from most other birds in that they have proportionally smaller eyes
77 when compared to the skull (BirdLife International, 2016b; Pérez Orrico & Sabater González,
78 2022). The Smooth-billed Ani *Crotophaga ani* is a cuculiform, a diurnal bird that feeds on

79 insects, arthropods and can catch small fish, usually grabbing prey in mid-flight (Burger &
80 Gochfeld, 2001; Cooke, Haskell, van Rees, & Fessl, 2019; Reavill & Dorrestein, 2018).
81 Stygian Owls *Asio stygius* and Common Potoos *Nyctibius griseus* are nocturnal birds, which
82 have large adapted eyes, providing them high visual sensitivity in dim-light environments
83 (BirdLife International, 2020; Mitkus, Potier, Martin, Duriez, & Kelber, 2018; Potier, Mitkus,
84 & Kelber, 2020).

85

86

87 **Materials and methods**

88 *Animals*

89 Eight adult birds of different species were included in this study. Only the healthy
90 eyes were evaluated, totaling 11 eyes. Two eyes of Stygian Owl (*Asio stygius*), two eyes of
91 Smooth-Billed Ani (*Crotophaga ani*), one eye of Great Kiskadee (*Pitangus sulphuratus*), one
92 eye of Toco Toucan (*Ramphastos toco*), one eye of a Rufous-bellied Thrush (*Turdus*
93 *rufiventris*), one eye of a Greater Rhea (*Rhea americana*), one eye of a Scarlet Macaw (*Ara*
94 *macao*) and finally, two eyes of a Common Potoo (*Nyctibius griseus*) (order, family and
95 popular names described in Table 1). The birds studied were from the Department of Wild
96 Animals (Faculty of Agronomy and Veterinary Medicine of the University of Brasília), where
97 they arrived after being rescued by the Wild Animal Screening Center (Centro de Triagem de
98 Animais Silvestres do Distrito Federal – CETAS), all found in unhealthy conditions. The
99 birds which died naturally from their injuries were evaluated for the integrity of their eyes on
100 presentation. Only eyes that did not show evidence of ophthalmic disease were selected and
101 collected. The collection of biological material from wild native species, for scientific
102 purposes, was authorized by Biodiversity Authorization and Information System (Sistema de
103 Autorização e Informação em Biodiversidade - SISBIO), with protocol number SISBIO
104 n.79141-2.

105 *Sample collection and processing*

106 The eyes were removed within a maximum of 30 minutes after death, with the use of
107 transconjunctival enucleation technique. This technique consisted of a 360° perilimbal
108 incision, dissection of the ocular attachments to isolate the globe, and transection of the optic
109 nerve. The eyes were placed in 10% formaldehyde solution and sent to the Veterinary
110 Pathology Laboratory (MVL Patologia Veterinária, Belo Horizonte, Brazil), where the
111 samples were processed and analyzed by light microscopy.

112 *Light microscopy (LM)*

113 All 11 eyes were processed after fixation. They were embedded in paraffin blocks,
114 then were subjected to serial cuts with a thickness of 4 μm , sections placed on slides, and
115 stained with Hematoxylin and Eosin (HE) (Luna, 1968).

116

117 *Histological analysis and description*

118 The slides were analyzed using light microscopy for a description of the corneal
119 layers. For birds that had both eyes evaluated, the average value of both corneas was
120 calculated. The structures were measured in the central region and periphery of the cornea,
121 and identified as follows: Central Cornea Full Thickness (CCFT), Peripheral Corneal Full
122 Thickness (PCFT), Central Epithelium (CEp), Peripheral Epithelium (PEp), Central
123 Bowman's Layer (CBL), Peripheral Bowman's Layer (PBL), Central Stroma (CS), Peripheral
124 Stroma (PS), Central Descemet's Layer (CDL) and Peripheral Descemet's Layer (PDL).
125 Values given in micrometers (μm). Endothelial thickness was not measured, as it was lost
126 during histological processing.

127

128 **Results**

129 The evaluated corneas revealed an avascular tissue composed of four layers as
130 previous described in other species, from anterior to posterior: the epithelium, Bowman's
131 layer, stroma, Descemet's membrane. The internal endothelium was absent due to histological
132 processing. Total corneal thickness varied between bird species, and between the corneal
133 regions. The central region of the cornea was thinner than the peripheral region in *Asio*
134 *stygius*, *Crotophaga ani*, *Turdus rufiventris*, *Ramphastos toco*, *Rhea americana* and *Nyctibius*
135 *griseus*; and thicker in *Pitangus sulphuratus* and *Ara macao*. Table 2 summarizes the values
136 found in the measurements of the corneal layers.

137 The epithelium is formed by nonkeratinizing stratified squamous cells. The number of
138 epithelial layers is species-specific and corneal region specific, and in this study ranged from
139 three to six cell layers, being composed of one layer of posterior basal cells, 1 to 3 layers of
140 middle polyhedral squamous cells, and 1 to 3 layers of anterior flattened squamous cells. The
141 number of layers and the thickness of the epithelium varied in the central and peripheral
142 regions of the cornea. Table 3 shows the number of epithelial layers in each corneal region of
143 the studied species.

144 The Bowman's layer was possible to be observed in all 8 birds studied. It also showed
 145 variation in its thickness in the center and periphery, and was thinner in the central cornea in
 146 *Turdus rufiventris*, *Ramphastos toco*, *Rhea americana*, *Ara macao*, *Pitangus sulphuratu* and
 147 *Nyctibius griseus* (Table 2).

148 The stroma represents the thickest portion of the cornea in the birds studied. With the
 149 exception of *Pitangus sulphuratu* and *Ara macao*, all birds had a central stroma thinner than
 150 the peripheral one (Table 2).

151 Attached to the innermost part of the stroma, the Descemet's membrane is found. The
 152 thickness of Descemet's membrane varied slightly between the regions of the cornea, and
 153 between the evaluated species (Table 2).

154

155 **Discussion**

156

157 Compared to intraspecific studies of retinal morphology, corneal morphometry has
 158 been much less studied, with the total thickness of the cornea being the most common
 159 measurement among researchers and clinicians. Through different microscopy models,
 160 thicknesses can be obtained, and the scientific purposes include veterinary medicine, human
 161 medicine, and biological sciences (Chard & Gundlach, 1938; Gonzalez-Alonso-Alegre,
 162 Martinez-Nevaldo, Caro-Vadillo, & Rodriguez-Alvaro, 2015; Liu et al., 2016; Moraes, 2018).
 163 Table 4 summarizes the results of studies carried out previously and the findings in this study,
 164 and shows that the cornea varies widely among birds. There is likely a correlation between the
 165 habitat and such morphological differences in the cornea (Abdeltah et al., 2021; Hall, 2008;
 166 Potier et al., 2020). The total thickness of the cornea can also vary significantly between
 167 animals of the same species, in relation to age, breed and regions of the cornea (Coyo et al.,
 168 2015; Montiani-Ferreira, Cardoso, & Petersen-Jones, 2004). Slight variation can be seen
 169 between left and right eyes, and males and females (Werther, Candioto, & Korbel, 2017). The
 170 curvature of the cornea also influences the thickness (Figure 1); birds with a flatter cornea
 171 have little difference between the center and the periphery (Collin & Collin, 2021). On the
 172 other hand, in birds with a large corneal curvature, such as the Golden Eagle *Aquila*
 173 *chrysaetos* (Murphy & Dubielzig, 1993), the Stygian Owl *Asio stygius* and Common Potoo
 174 *Nyctibius griseus* in this study, the periphery is substantially thicker than the center (Brooke,
 175 Hanley, & Laughlin, 1999; Murphy & Howland, 1983).

176 Not only does the total thickness of the cornea have variation, but the individual
 177 corneal layers vary in thickness as well. The epithelium is the corneal anterior surface is

178 composed by layers of stratified squamous and non-keratinized cells. The basal cell layer has
179 a cuboidal or columnar shape, covered by multiple layers of cells that become wider and
180 flatter as they move away from the base, which are polyhedral. The most superficial
181 squamous cells are almost completely flattened. They are called umbrella or wing cells, as
182 their extent overlaps the apices of more than one cell. This epithelial pattern is found in
183 previously studied mammals and birds, including the birds in this study (Figure 2)
184 (Bergmanson, 2019; Collin & Collin, 2000, 2006, 2021; Mayakkannan, Ramesh, Kumaravel,
185 Venkatesan, & Kannan, 2018; Monção-Silva et al., 2016; Nautscher et al., 2016; Pinto, Cruz,
186 Teixeira, Couto, & Carvalho, 2016; Sokolenko et al., 2021). The number of epithelial cell
187 layers varies between species, and among the birds studied here, a variation from 3 to 6 layers
188 was observed (Table 3). In the Little Penguin *Eudyptula minor*, 5 to 6 layers were found in
189 the epithelium (Collin & Collin, 2021). The African Penguin *Spheniscus demersus* was found
190 to have 4 layers of epithelial cells and an epithelial thickness 15 μm (Sokolenko et al., 2021).
191 Raptor epithelium ranges from 2 to 5 layers thick (Pinto et al., 2016), except in the Golden
192 Eagle where an epithelium of 8 layers and 50 μm of thickness was found (Murphy &
193 Dubielzig, 1993). In this study, the thickest epithelium was observed in the Greater Rhea
194 *Rhea americana* (strictly terrestrial and diurnal bird), with up to 6 epithelial layers, and the
195 thinnest being the Stygian Owl and Common Potoo (nocturnal birds), having a maximum of 4
196 lines. The Greater Rhea's cornea also had a high epithelial proportion with respect to the total
197 thickness of the cornea, being 10.3% (Figure 3). In a study by Popova *et al.* (2022), the ratio
198 of the epithelium thickness to the total corneal thickness was similarly defined, where the
199 Hyacinth Macaw *Anodorhynchus hyacinthinus* demonstrated the highest epithelial proportion
200 in the group of birds at 9.9% of the corneal thickness (Popova et al., 2022). In the present
201 study, the Scarlet Macaw *Ara macao* demonstrated that 8.09% of the total thickness of the
202 cornea corresponds to the epithelium (Figure 3). The Smooth-billed Ani *Crotophaga ani* was
203 the bird that showed the highest epithelium vs. total cornea ratio at 16% (Figure 3). The
204 Passeriformes Rufous-bellied Thrush *Turdus rufiventris* and Great Kiskadee *Pitangus*
205 *sulphuratus*, studied here, presented 10.78% and 8.88% of epithelium vs. total cornea ratio, as
206 observed in the Java Sparrow *Lonchura oryzivora*, also passerine, described by Popova *et al.*
207 (2022), with 8.9% of epithelium. Past hypotheses for differential epithelial thicknesses relate
208 to the habitat of different species, where those with greater risk of trauma (diving birds, birds
209 in arid environments, or those living in dense fauna) may have greater epithelial thickness,
210 particularly in proportion to total epithelial thickness (Almubrad & Akhtar, 2012; Collin &
211 Collin, 2006; Nautscher et al., 2016; Popova et al., 2022; Swamynathan, Crawford, Robison,

212 Kanungo, & Piatigorsky, 2003). The total size of the bird also likely plays a role in total
213 epithelial thickness.

214 The Bowman's layer (BL), also referred to as the Anterior Limiting Lamina, is a
215 continuous meshwork of condensed collagen fibers located in the anterior stroma, beneath the
216 epithelium (Bergmanson, 2019; Hayashi, Osawa, & Tohyama, 2002; Meek & Fullwood,
217 2001). This layer is the corneal structure that has the greatest morphological variation
218 between species, with a chance of not even being present (Abdelftah et al., 2021; Hayashi et
219 al., 2002; Kafarnik et al., 2007; Merindano, Costa, Canals, Potau, & Ruano, 2002; Moore et
220 al., 2022; Popova et al., 2022). More developed mammals have a well-defined BL, as
221 observed in deers, giraffes, humans and other primates (Hayashi et al., 2002; Merindano et al.,
222 2002; Popova et al., 2022; Wilson, 2020). This layer is also described in several species of
223 birds, such as chickens, quails, ducks, pelicans, birds of prey, penguins, parrots and
224 Passeriformes (Abdelftah et al., 2021; Carvalho, Rodarte-Almeida, Santana, & Galera, 2018;
225 Collin & Collin, 2021; Gonçalves, Pérez-Merino, Martínez-García, Barcía, & Merayo-Loves,
226 2016; Kafarnik et al., 2007; Mayakkannan et al., 2018; Moore et al., 2022; Murphy &
227 Dubielzig, 1993; Pinto et al., 2016; Popova et al., 2022; Willis & Wilkie, 1999). However,
228 there is no consensus on the definition of BL in animals. Popova *et al.* (2022) and Merindano
229 *et al.* (2002), consider that BL in birds is rudimentary, since when compared to humans and
230 other primates, it is not clearly defined. Alternatively, Kafarnik *et al.* (2007), described the BL
231 of birds as similar to that of primates, being acellular and with homogeneous reflectivity,
232 observed through *in vivo* confocal microscopy. This is in corroboration with Gonçalves *et al.*
233 (2016), who suggested that the chicken cornea is an excellent research model for refractive
234 surgeries in humans, due to the similarity of corneal structures, with an emphasis on the
235 Bowman's layer.

236 In this study, it was possible to observe that the outermost margin of the BL is distinct,
237 as it borders the basement membrane of the epithelium. However, its innermost limit is not as
238 distinct, as the margin is progressively incorporated into the stroma, making it challenging to
239 measure the thickness of this layer. Collin & Collin (2021) describe not having clear enough
240 definition to measure the extent of the BL in the Little Penguin, but stated that it is located
241 5µm deep in the stroma. In another study, by Sokolenko et al. (2021), the African Penguin's
242 BL was not described. Among the birds studied here, we found that the Great Kiskadee, the
243 Stygian Owl, the Greater Rhea and the Rufous-bellied Thrush, have a BL with visible anterior
244 and posterior delimitation, but with low contrast in relation to the stroma (Figure 4). It was
245 observed in many histological samples of this study that the stroma suffers from the presence

246 of artifacts in its interior caused by the penetration of the processing substances (Figure 5).
247 These artifacts are randomly present in the substantia propria, but do not extend into the BL.
248 The same pattern was observed in histological images from other studies (Bastola, Song,
249 Gilger, & Hirsch, 2020; Feizi, 2018; Merindano et al., 2002; Pinto et al., 2016; Popova et al.,
250 2022). It is possible to suggest that this happens due to the high condensation of collagen
251 fibers in the BL, making it more difficult for them to break.

252 The stroma, or substantia propria, is a dense connective tissue meshwork formed by
253 overlapping collagen fibril lamellae aligned parallel to the corneal surface, with scattered
254 keratocytes between them. The density, orientation of the lamellae, and the concentration of
255 keratocytes vary between the regions and the stroma depth, as well as between the species
256 (Abdeltah et al., 2021; Bergmanson, 2019; Crespo-Moral, García-Posadas, López-García, &
257 Diebold, 2020; Kafarnik et al., 2007; Meek & Fullwood, 2001; Meek & Knupp, 2015;
258 Nautscher et al., 2016; Tsukahara et al., 2010). In birds, the collagen lamellae are aligned with
259 each other, forming a precise and regular orthogonal arrangement, with a large number of
260 branches promoting anastomosis of the bundles. This arrangement is most evident in the
261 anterior and middle portion of the substantia propria, and is associated with greater
262 mechanical rigidity and better light transmittance in the UV spectrum – meaning that the
263 sunlight in contact with the cornea is more scattered, decreasing the amount of light entering
264 the eyes (Boote et al., 2011; Collin & Collin, 2021; Gonçalves et al., 2016; Koudouna et al.,
265 2018; Tsukahara et al., 2010). Tsukahara *et al.* (2010) compared the corneas of birds with
266 mammals, demonstrating that birds have a lower density of keratocytes distributed in the
267 stroma, which are more concentrated in the anterior portion. In histological images from this
268 study, it is also possible to identify that Smooth-billed Ani and Rufous-bellied Thrush have
269 more keratocytes in the anterior stroma (Figure 5). Birds also have thicker collagen lamellae
270 than mammals, with greater lamella thickness indicating better light refraction power (Boote
271 et al., 2011; Tsukahara et al., 2010). Another characteristic of the stroma is that it represents
272 the thickest portion of the cornea, measuring greater than 90% of the total corneal thickness
273 (Abdeltah et al., 2021; Boote et al., 2011; Crespo-Moral et al., 2020; Gonçalves et al., 2016;
274 Koudouna et al., 2018; Nautscher et al., 2016). According to the present study, five birds
275 demonstrated a stromal thickness between 91 and 95% of the total thickness of the cornea,
276 while three, Rufous-bellied Thrush, Scarlet Macaw and Smooth-billed Ani, demonstrated 76,
277 78 and 79%, respectively (Figure 3).

278 In most animals, the stroma is thinner at the center than at the periphery of the cornea,
279 thus making the central cornea thinner than the peripheral cornea (Bergmanson, Burns, &

280 Walker, 2019; Meek & Leonard, 1993; Werther et al., 2017). However, some species
281 demonstrate a thinner peripheral cornea than the center, while others do not demonstrate
282 significant differences between the thicknesses of the regions (Collin & Collin, 1998, 2021;
283 Coyo et al., 2015; Henriksson, Bron, & Bergmanson, 2012; Moore et al., 2019). In the present
284 study, the Scarlet Macaw and the Great Kiskadee showed a slightly thinner periphery than the
285 center, with a mean variation of 14 μm . The Rufous-bellied Thrush's cornea also varied
286 slightly, but in an opposite manner, being 13 μm thicker at the periphery. The Stygian Owl,
287 the Toco Toucan, the Greater Rhea and the Common Potoo, have a more pronounced
288 variation between the regions, being between 128 and 387 μm thicker in the periphery,
289 respectively. Reasons why the stroma undergoes size changes between corneal regions have
290 not yet been well explained, but it is known that collagen lamellae undergo variations in size,
291 thickness and quantity according to the stromal region and depth (Bergmanson, Burns, &
292 Naroo, 2021; Boote et al., 2011; Henriksson et al., 2012; Meek & Fullwood, 2001).

293

294 **Conclusion**

295 The histomorphometric description of the cornea, through light microscopy, proved to
296 be efficient for the study of different birds' species from Brazil, being an accessible method.
297 Similarities were found between the cornea of birds and other vertebrates, but with specific
298 differences in the metrics of each species. A better understanding of the structures can help to
299 explain the form of visual interaction of birds with their environment, as well as improve
300 knowledge on how to interpret pathological changes in the birds' cornea.

301

302 **Acknowledgment**

303 This study was funded by *Coordenação de Aperfeiçoamento de Pessoal de Nível*
304 *Superior (CAPES), Brazil – Funding code 001, and by Fundação de Apoio à Pesquisa*
305 *do Distrito Federal (FAPDF), Brazil – proc.n. 00193.00001303/2019-10).*

306

307 **Conflict of Interest**

308 The authors report no conflicts of interest. The authors alone are responsible for the
309 content and writing of this paper.

310

311

312

313 **References**

- 314 Abdelftah, Z., Gaber, A. R., Abo-Eleneen, R. E., & EL-Bakry, A. M. (2021). Microstructure
315 characteristics of cornea of some birds: a comparative study. *Beni-Suef University Journal of*
316 *Basic and Applied Sciences*, 10(1), 66. <https://doi.org/10.1186/s43088-021-00155-2>
- 317 Almubrad, T., & Akhtar, S. (2012). Ultrastructure features of camel cornea - collagen fibril
318 and proteoglycans. *Veterinary Ophthalmology*, 15(1), 36–41. [https://doi.org/10.1111/j.1463-](https://doi.org/10.1111/j.1463-5224.2011.00918.x)
319 [5224.2011.00918.x](https://doi.org/10.1111/j.1463-5224.2011.00918.x)
- 320 Bastola, P., Song, L., Gilger, B. C., & Hirsch, M. L. (2020). Adeno-Associated Virus
321 Mediated Gene Therapy for Corneal Diseases. *Pharmaceutics*, 12(8), 767.
322 <https://doi.org/10.3390/pharmaceutics12080767>
- 323 Bergmanson, J. P. G. (2019). Anatomy and Physiology of the Cornea and Related Structures.
324 In *Contact Lenses* (Sixth Edit, pp. 33–64). Elsevier. [https://doi.org/10.1016/B978-0-7020-](https://doi.org/10.1016/B978-0-7020-7168-3.00003-9)
325 [7168-3.00003-9](https://doi.org/10.1016/B978-0-7020-7168-3.00003-9)
- 326 Bergmanson, J. P. G., Burns, A. R., & Naroo, S. A. (2021). Central versus peripheral corneal
327 thickness – A White spot on the corneal (anatomy) map. *Contact Lens and Anterior Eye*,
328 44(4), 101473. <https://doi.org/10.1016/j.clae.2021.101473>
- 329 Bergmanson, J. P. G., Burns, A., & Walker, M. (2019). Anatomical explanation for the
330 central-peripheral thickness difference in human corneas. In *Investigative Ophthalmology &*
331 *Visual Science* (Vol. 60).
- 332 BirdLife International. (2016a). Ara macao, Scarlet Macaw. *The IUCN Red List of Threatened*
333 *Species*, 8235, 1–9. [https://doi.org/http://dx.doi.org/10.2305/IUCN.UK.2016-](https://doi.org/http://dx.doi.org/10.2305/IUCN.UK.2016-3.RLTS.T22685563A93079992.en)
334 [3.RLTS.T22685563A93079992.en](https://doi.org/http://dx.doi.org/10.2305/IUCN.UK.2016-3.RLTS.T22685563A93079992.en)
- 335 BirdLife International. (2016b). Rhea americana, Greater Rhea. *The IUCN Red List of*
336 *Threatened Species*, 8235, 1–10. [https://doi.org/http://dx.doi.org/10.2305/IUCN.UK.2016-](https://doi.org/http://dx.doi.org/10.2305/IUCN.UK.2016-3.RLTS.T22678073A92754472.en)
337 [3.RLTS.T22678073A92754472.en](https://doi.org/http://dx.doi.org/10.2305/IUCN.UK.2016-3.RLTS.T22678073A92754472.en)
- 338 BirdLife International. (2016c). Turdus rufiventris, Rufous-bellied Thrush. *The IUCN Red*
339 *List of Threatened Species*, 8235, 1–10.
340 [https://doi.org/http://dx.doi.org/10.2305/IUCN.UK.2016- 3.RLTS.T22708882A94182217.en](https://doi.org/http://dx.doi.org/10.2305/IUCN.UK.2016-3.RLTS.T22708882A94182217.en)
- 341 BirdLife International. (2017). Ramphastos toco. *IUCN Red List of Threatened Species 2017*,
342 *e.T2268216*. Retrieved from [http://dx.doi.org/10.2305/IUCN.UK.2017-](http://dx.doi.org/10.2305/IUCN.UK.2017-1.RLTS.T22682164A113557535.en)
343 [1.RLTS.T22682164A113557535.en](http://dx.doi.org/10.2305/IUCN.UK.2017-1.RLTS.T22682164A113557535.en)
- 344 BirdLife International. (2018). Pitangus sulphuratus, Great Kiskadee. *The IUCN Red List of*
345 *Threatened Species*, 8235, 1–10. [https://doi.org/http://dx.doi.org/10.2305/IUCN.UK.2018-](https://doi.org/http://dx.doi.org/10.2305/IUCN.UK.2018-2.RLTS.T22700605A132069895.en)
346 [2.RLTS.T22700605A132069895.en](https://doi.org/http://dx.doi.org/10.2305/IUCN.UK.2018-2.RLTS.T22700605A132069895.en)

- 347 BirdLife International. (2020). *Nyctibius griseus*, Common Potoo. *The IUCN Red List of*
 348 *Threatened Species*, 8235, 2–9. [https://doi.org/https://dx.doi.org/10.2305/IUCN.UK.2020-](https://doi.org/https://dx.doi.org/10.2305/IUCN.UK.2020-3.RLTS.T22689646A163600335.en)
 349 [3.RLTS.T22689646A163600335.en](https://doi.org/https://dx.doi.org/10.2305/IUCN.UK.2020-3.RLTS.T22689646A163600335.en)
- 350 Boote, C., Elsheikh, A., Kassem, W., Kamma-Lorger, C. S., Hocking, P. M., White, N., ...
 351 Meek, K. M. (2011). The Influence of Lamellar Orientation on Corneal Material Behavior:
 352 Biomechanical and Structural Changes in an Avian Corneal Disorder. *Investigative*
 353 *Ophthalmology & Visual Science*, 52(3), 1243. <https://doi.org/10.1167/iovs.10-5962>
- 354 Brooke, M. D. L., Hanley, S., & Laughlin, S. B. (1999). The scaling of eye size with body
 355 mass in birds. *Proceedings of the Royal Society B: Biological Sciences*, 266(1417), 405–412.
 356 <https://doi.org/10.1098/rspb.1999.0652>
- 357 Burger, J., & Gochfeld, M. (2001). Smooth-billed ani (*Crotophaga ani*) predation on
 358 butterflies in Mato Grosso, Brazil: risk decreases with increased group size. *Behavioral*
 359 *Ecology and Sociobiology*, 49(6), 482–492. <https://doi.org/10.1007/s002650100327>
- 360 Calegario-Marques, C., & Amato, S. B. (2014). Urbanization breaks up host-parasite
 361 interactions: A case study on parasite community ecology of rufous-bellied thrushes (*Turdus*
 362 *rufiventris*) along a rural-urban gradient. *PLoS ONE*, 9(7).
 363 <https://doi.org/10.1371/journal.pone.0103144>
- 364 Carvalho, C. M. de, Rodarte-Almeida, A. C. da V., Santana, M. I. S., & Galera, P. D. (2018).
 365 Avian ophthalmic peculiarities. *Ciência Rural*, 48(12), 1–10. [https://doi.org/10.1590/0103-](https://doi.org/10.1590/0103-8478cr20170904)
 366 [8478cr20170904](https://doi.org/10.1590/0103-8478cr20170904)
- 367 Chard, R. D., & Gundlach, R. H. (1938). The structure of the eye of the homing pigeon.
 368 *Journal of Comparative Psychology*, 25(2), 249–272. <https://doi.org/10.1037/h0061438>
- 369 Collin, S. P., & Collin, H. B. (1998). A comparative study of the corneal endothelium in
 370 vertebrates. *Clinical and Experimental Optometry*, 81(6), 245–254.
 371 <https://doi.org/10.1111/j.1444-0938.1998.tb06744.x>
- 372 Collin, S. P., & Collin, H. B. (2000). A Comparative SEM Study of the Vertebrate Corneal
 373 Epithelium. *Cornea*, 19(2), 218–230. Retrieved from
 374 [https://journals.lww.com/corneajrnl/Abstract/2000/03000/A_Comparative_SEM_Study_of_th](https://journals.lww.com/corneajrnl/Abstract/2000/03000/A_Comparative_SEM_Study_of_the_Vertebrate_Corneal.17.aspx)
 375 [e_Vertebrate_Corneal.17.aspx](https://journals.lww.com/corneajrnl/Abstract/2000/03000/A_Comparative_SEM_Study_of_the_Vertebrate_Corneal.17.aspx)
- 376 Collin, S. P., & Collin, H. B. (2006). The corneal epithelial surface in the eyes of vertebrates:
 377 Environmental and evolutionary influences on structure and function. *Journal of Morphology*,
 378 267(3), 273–291. <https://doi.org/10.1002/jmor.10400>
- 379 Collin, S. P., & Collin, H. B. (2021). Functional morphology of the cornea of the Little
 380 Penguin *Eudyptula minor* (Aves). *Journal of Anatomy*, 239(3), 732–746.

- 381 <https://doi.org/10.1111/joa.13438>
- 382 Cooke, S. C., Haskell, L. E., van Rees, C. B., & Fessl, B. (2019). A review of the introduced
383 smooth-billed ani *Crotophaga ani* in Galápagos. *Biological Conservation*, 229, 38–49.
384 <https://doi.org/10.1016/j.biocon.2018.11.005>
- 385 Coyo, N., Peña, M. T., Costa, D., Ríos, J., Lacerda, R., & Leiva, M. (2015). Effects of age
386 and breed on corneal thickness, density, and morphology of corneal endothelial cells in
387 enucleated sheep eyes. *Veterinary Ophthalmology*, 19(5), 367–372.
388 <https://doi.org/10.1111/vop.12308>
- 389 Crespo-Moral, M., García-Posadas, L., López-García, A., & Diebold, Y. (2020). Histological
390 and immunohistochemical characterization of the porcine ocular surface. *PLOS ONE*, 15(1).
391 <https://doi.org/10.1371/journal.pone.0227732>
- 392 Feizi, S. (2018). Corneal endothelial cell dysfunction: etiologies and management.
393 *Therapeutic Advances in Ophthalmology*, 10, 251584141881580.
394 <https://doi.org/10.1177/2515841418815802>
- 395 Gasperin, G., & Aurélio Pizo, M. (2009). Frugivory and habitat use by thrushes (*Turdus* spp.)
396 in a suburban area in south Brazil. *Urban Ecosystems*, 12(4), 425–436.
397 <https://doi.org/10.1007/s11252-009-0090-2>
- 398 Gonçalves, G. C., Pérez-Merino, P., Martínez-García, M. C., Barcía, A., & Merayo-Loves, J.
399 (2016). Comparación de las características corneales en gallina y codorniz como modelos
400 experimentales de cirugía refractiva. *Archivos de La Sociedad Española de Oftalmología*,
401 91(7), 310–315. <https://doi.org/10.1016/j.ofal.2016.01.012>
- 402 Gonzalez-Alonso-Alegre, E. M., Martinez-Nevado, E., Caro-Vadillo, A., & Rodriguez-
403 Alvaro, A. (2015). Central corneal thickness and intraocular pressure in captive black-footed
404 penguins (*Spheniscus demersus*). *Veterinary Ophthalmology*, 18(s1), 94–97.
405 <https://doi.org/10.1111/vop.12206>
- 406 Hall, M. I. (2008). The anatomical relationships between the avian eye, orbit and sclerotic
407 ring: implications for inferring activity patterns in extinct birds. *Journal of Anatomy*, 212(6),
408 781–794. <https://doi.org/10.1111/j.1469-7580.2008.00897.x>
- 409 Hayashi, S., Osawa, T., & Tohyama, K. (2002). Comparative observations on corneas, with
410 special reference to Bowman's layer and Descemet's membrane in mammals and amphibians.
411 *Journal of Morphology*, 254(3), 247–258. <https://doi.org/10.1002/jmor.10030>
- 412 Henriksson, J. T., Bron, A. J., & Bergmanson, J. P. G. (2012). An explanation for the central
413 to peripheral thickness variation in the mouse cornea. *Clinical and Experimental*
414 *Ophthalmology*, 40(2), 174–181. <https://doi.org/10.1111/j.1442-9071.2011.02652.x>

- 415 Jones, M. P., Pierce, K. E., & Ward, D. (2007). Avian Vision: A Review of Form and
 416 Function with Special Consideration to Birds of Prey. *Journal of Exotic Pet Medicine*, *16*(2),
 417 69–87. <https://doi.org/10.1053/j.jepm.2007.03.012>
- 418 Kafarnik, C., Fritsche, J., & Reese, S. (2007). In vivo confocal microscopy in the normal
 419 corneas of cats, dogs and birds. *Veterinary Ophthalmology*, *10*(4), 222–230.
 420 <https://doi.org/10.1111/j.1463-5224.2007.00543.x>
- 421 Koudouna, E., Winkler, M., Mikula, E., Juhasz, T., Brown, D. J., & Jester, J. V. (2018).
 422 Evolution of the vertebrate corneal stroma. *Progress in Retinal and Eye Research*,
 423 *64*(November 2017), 65–76. <https://doi.org/10.1016/j.preteyeres.2018.01.002>
- 424 Lago-Paiva, C. (1996). Cavity Nesting by Great Kiskadees (*Pitangus sulphuratus*): Adaptation
 425 or Expression of Ancestral Behavior? *The Auk*, *113*(4), 953–955.
 426 <https://doi.org/10.2307/4088879>
- 427 Liu, X. X., Zhu, X. P., Wu, J., Wu, Z. J., Yin, Y., Xiao, X. H., ... Mi, S. L. (2016). Acellular
 428 ostrich corneal stroma used as scaffold for construction of tissue-engineered cornea.
 429 *International Journal of Ophthalmology*, *9*(3), 325–331.
 430 <https://doi.org/10.18240/ijo.2016.03.01>
- 431 Luna, L. G. (1968). *Manual of histologic staining methods of the Armed Forces Institute of*
 432 *Pathology* (3rd ed.). New York: Blakiston Division, McGraw-Hill.
- 433 Massari, C. H. de A. L., Silva, A. F., Magalhães, H. I. R., Silva, D. R. S., Sasahara, T. H. de
 434 C., & Miglino, M. A. (2020). Using 3D computed tomography in the anatomical description
 435 of the eye and the vestibulocochlear organ of a blue-and-yellow macaw (*Ara ararauna*
 436 Linnaeus, 1758) and of a toucan (*Ramphastos toco* Statius Muller, 1776). *Acta Veterinaria*
 437 *Brasilica*, *14*(4), 279–285. <https://doi.org/10.21708/avb.2020.14.4.9464>
- 438 Mayakkannan, T., Ramesh, G., Kumaravel, A., Venkatesan, S., & Kannan, T. A. (2018).
 439 Gross and Microanatomical Study of the Cornea in Japanese quail (*Coturnix coturnix*
 440 *japonica*). *International Journal of Current Microbiology and Applied Sciences*, *7*(10), 599–
 441 605. <https://doi.org/10.20546/ijcmas.2018.710.067>
- 442 Meek, K. M., & Fullwood, N. J. (2001). Corneal and scleral collagens—a microscopist’s
 443 perspective. *Micron*, *32*(3), 261–272. [https://doi.org/10.1016/S0968-4328\(00\)00041-X](https://doi.org/10.1016/S0968-4328(00)00041-X)
- 444 Meek, K. M., & Knupp, C. (2015). Corneal structure and transparency. *Progress in Retinal*
 445 *and Eye Research*, *49*, 1–16. <https://doi.org/10.1016/j.preteyeres.2015.07.001>
- 446 Meek, K. M., & Leonard, D. W. (1993). Ultrastructure of the corneal stroma: a comparative
 447 study. *Biophysical Journal*, *64*(1), 273–280. [https://doi.org/10.1016/S0006-3495\(93\)81364-X](https://doi.org/10.1016/S0006-3495(93)81364-X)
- 448 Merindano, M. D., Costa, J., Canals, M., Potau, J. M., & Ruano, D. (2002). A comparative

- 449 study of Bowman's layer in some mammals: Relationships with other constituent corneal
 450 structures. *European Journal of Anatomy*, 6(3), 133–139.
- 451 Meyer, D. B. (1977). The Avian Eye and its Adaptations. In *The Visual System in Vertebrates*
 452 (pp. 549–611). https://doi.org/10.1007/978-3-642-66468-7_10
- 453 Mitkus, M., Potier, S., Martin, G. R., Duriez, O., & Kelber, A. (2018). Raptor Vision. *Oxford*
 454 *Research Encyclopedia of Neuroscience*, (July), 1–39.
 455 <https://doi.org/10.1093/acrefore/9780190264086.013.232>
- 456 Monção-Silva, R. M., Ofri, R., Raposo, A. C. S., Libório, F. A., Estrela-Lima, A., & Oriá, A.
 457 P. (2016). Ophthalmic Parameters of Blue-and-yellow Macaws (*Ara Ararauna*) and Lear's
 458 Macaws (*Anodorhynchus Leari*). *Avian Biology Research*, 9(4), 240–249.
 459 <https://doi.org/10.3184/175815516X14725499175746>
- 460 Montiani-Ferreira, F., Cardoso, F., & Petersen-Jones, S. (2004). Postnatal development of
 461 central corneal thickness in chicks of *Gallus gallus domesticus*. *Veterinary Ophthalmology*,
 462 7(1), 37–39. <https://doi.org/10.1111/j.1463-5224.2004.00319.x>
- 463 Moore, B. A., Fernandez-Juricic, E., Hawkins, M. G., Montiani-Ferreira, F., & Lange, R. R.
 464 (2022). Introduction to Ophthalmology of Aves. In *Wild and Exotic Animal Ophthalmology*
 465 (pp. 321–348). Cham: Springer International Publishing. https://doi.org/10.1007/978-3-030-71302-7_16
- 467 Moore, B. A., Maggs, D. J., Kim, S., Motta, M. J., Bandivadekar, R., Tell, L. A., & Murphy,
 468 C. J. (2019). Clinical findings and normative ocular data for free-living Anna's (*Calypte anna*)
 469 and Black-chinned (*Archilochus alexandri*) Hummingbirds. *Veterinary Ophthalmology*, 22(1),
 470 13–23. <https://doi.org/10.1111/vop.12560>
- 471 Moraes, W. (2018). *Ocular morphology, physiology and selectal ophthalmic clinical tests in*
 472 *the harpy eagle (Harpyia harpyja)*. Doctoral dissertation, Universidade Federal do Paraná
- 473 Murphy, C. J., & Dubielzig, R. R. (1993). The gross and microscopic structure of the golden
 474 eagle (*Aquila chrysaetos*) eye. *Progress in Veterinary and Comparative Ophthalmology*, 3,
 475 74–79.
- 476 Murphy, C. J., & Howland, H. C. (1983). Owl eyes: Accommodation, corneal curvature and
 477 refractive state. *Journal of Comparative Physiology ? A*, 151(3), 277–284.
 478 <https://doi.org/10.1007/BF00623904>
- 479 Nautscher, N., Bauer, A., Steffl, M., & Amselgruber, W. M. (2016). Comparative
 480 morphological evaluation of domestic animal cornea. *Veterinary Ophthalmology*, 19(4), 297–
 481 304. <https://doi.org/10.1111/vop.12298>
- 482 Pérez Orrico, M. L., & Sabater González, M. (2022). Ophthalmology of Palaeognathae:

- 483 Ostriches, Rheas, Emu, Cassowaries, Tinamous, and Kiwis. In *Wild and Exotic Animal*
 484 *Ophthalmology* (pp. 627–648). Cham: Springer International Publishing.
 485 https://doi.org/10.1007/978-3-030-71302-7_25
- 486 Pinto, D. G., Cruz, G. D., Teixeira, R. H. F., Couto, E. P., & Carvalho, M. P. N. de. (2016).
 487 Histological analysis of the eyeball of Neotropical birds of prey Caracara plancus, Falco
 488 sparverius, Rupornis magnirostris, Megascops choliba and Athene cunicularia. *Brazilian*
 489 *Journal of Veterinary Research and Animal Science*, 53(3), 280.
 490 <https://doi.org/10.11606/issn.1678-4456.bjvras.2016.109045>
- 491 Popova, P., Malalana, F., Biddolph, S., Ramos, T., Parekh, M., Chantrey, J., & Ahmad, S.
 492 (2022). Interspecies comparative morphological evaluation of the corneal epithelial stem cell
 493 niche: a pilot observational study. *Journal of Veterinary Science*, 23(4), 1–10.
 494 <https://doi.org/10.4142/JVS.22009>
- 495 Potier, S., Mitkus, M., & Kelber, A. (2020). Visual adaptations of diurnal and nocturnal
 496 raptors. *Seminars in Cell and Developmental Biology*, 106(May), 116–126.
 497 <https://doi.org/10.1016/j.semcdb.2020.05.004>
- 498 Reavill, D. R., & Dorrestein, G. (2018). Cuculiformes. In *Pathology of Wildlife and Zoo*
 499 *Animals* (pp. 775–798). Elsevier Inc. <https://doi.org/10.1016/B978-0-12-805306-5/00032-8>
- 500 Sokolenko, E., Hilken, G., Denk, N., Wyss, F., Wenker, C., Hasler, P. W., & Meyer, P.
 501 (2021). The Eyes of an African Penguin (*Spheniscus demersus*): General Morphology and
 502 Ophthalmopathology. *Klin Monatsbl Augenheilkd*, 238(01), 94–98. [https://doi.org/10.1055/a-](https://doi.org/10.1055/a-1388-3960)
 503 1388-3960
- 504 Swamynathan, S. K., Crawford, M. A., Robison, W. G., Kanungo, J., & Piatigorsky, J.
 505 (2003). Adaptive differences in the structure and macromolecular compositions of the air and
 506 water corneas of the “four-eyed” fish (*Anableps anableps*). *The FASEB Journal*, 17(14),
 507 1996–2005. <https://doi.org/10.1096/fj.03-0122com>
- 508 Tamayo-Arango, L. J., Baraldi-Artoni, S. M., Laus, J. L., Mendes-Vicenti, F. A., Pigatto, J.
 509 A. T., & Abib, F. C. (2009). Ultrastructural morphology and morphometry of the normal
 510 corneal endothelium of adult crossbred pig. *Ciencia Rural*, 39(1), 117–122.
 511 <https://doi.org/10.1590/S0103-84782009000100018>
- 512 [dataset]Tozetti, R. A. R. (2023). Corneal histomorphometry of birds from the Brazilian
 513 Midwest. Harvard Dataverse, DRAFT VERSION.
- 514 Tsukahara, N., Tani, Y., Lee, E., Kikuchi, H., Endoh, K., Ichikawa, M., & Sugita, S. (2010).
 515 Microstructure characteristics of the cornea in birds and mammals. *Journal of Veterinary*
 516 *Medical Science*, 72(9), 1137–1143. <https://doi.org/10.1292/jvms.09-0470>

- 517 Werther, K., Candioto, C. G., & Korbel, R. (2017). Ocular Histomorphometry of Free-Living
518 Common Kestrels (*Falco tinnunculus*). *Journal of Avian Medicine and Surgery*, *31*(4), 319–
519 326. <https://doi.org/10.1647/2014-039>
- 520 Willis, A. M., & Wilkie, D. A. (1999). Avian Ophthalmology Part 1 : Anatomy , Examination
521 , and Diagnostic Techniques. *Journal of Avian Medicine and Surgery*, *13*(3), 160–166.
522 Retrieved from <http://www.jstor.org/stable/30130679> .
- 523 Wilson, S. E. (2020). Bowman’s layer in the cornea– structure and function and regeneration.
524 *Experimental Eye Research*, *195*(January), 108033.
525 <https://doi.org/10.1016/j.exer.2020.108033>



Figure 1. Macroscopy of the ocular bulbs demonstrating the variation of the corneal curvature, of *Crotophaga ani* (A) with a low degree of curvature, and of *Nyctibius griseus* (B), with high convexity.

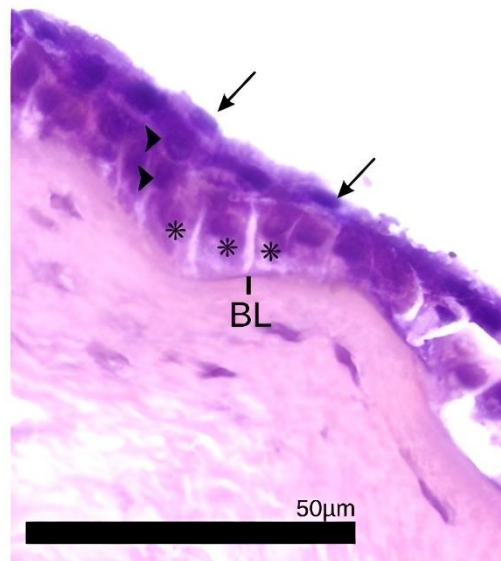


Figure 2. Cornea of the *Turdus rufiventris*. Columnar-shaped basal epithelial squamous cells (asterisk), polyhedral cells (arrowhead), and wing cells (arrows). The Bowman's membrane (BL) can be visualized in the image below. Measurements were carried out using the Opticam O500R microscope, with OPTHD software, 400x magnification.

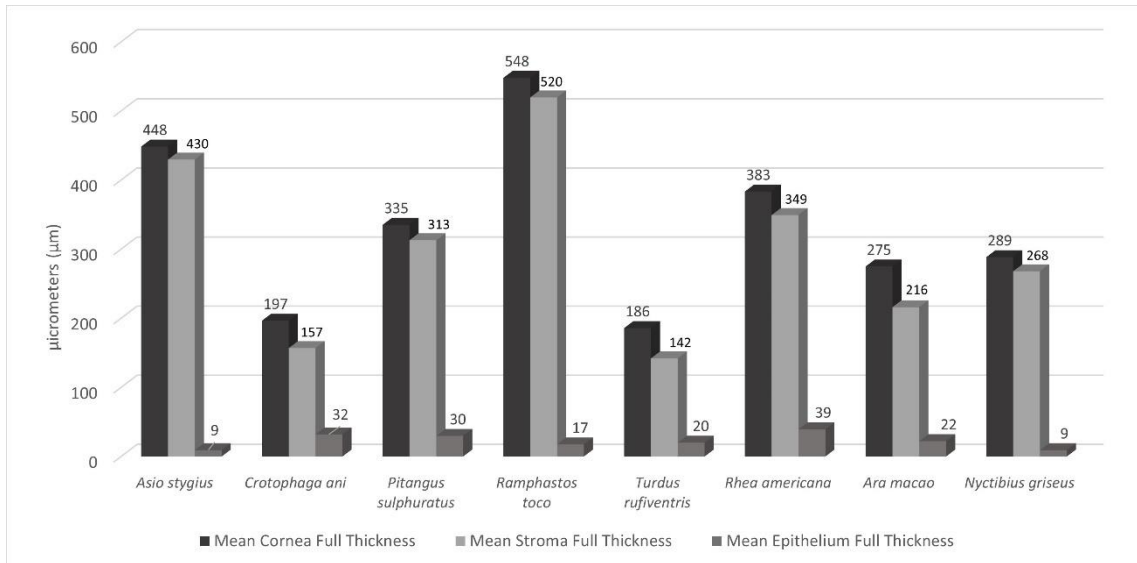


Figure 3. Representation of the percentage of epithelium and stroma in relation to the total corneal thickness of the birds.

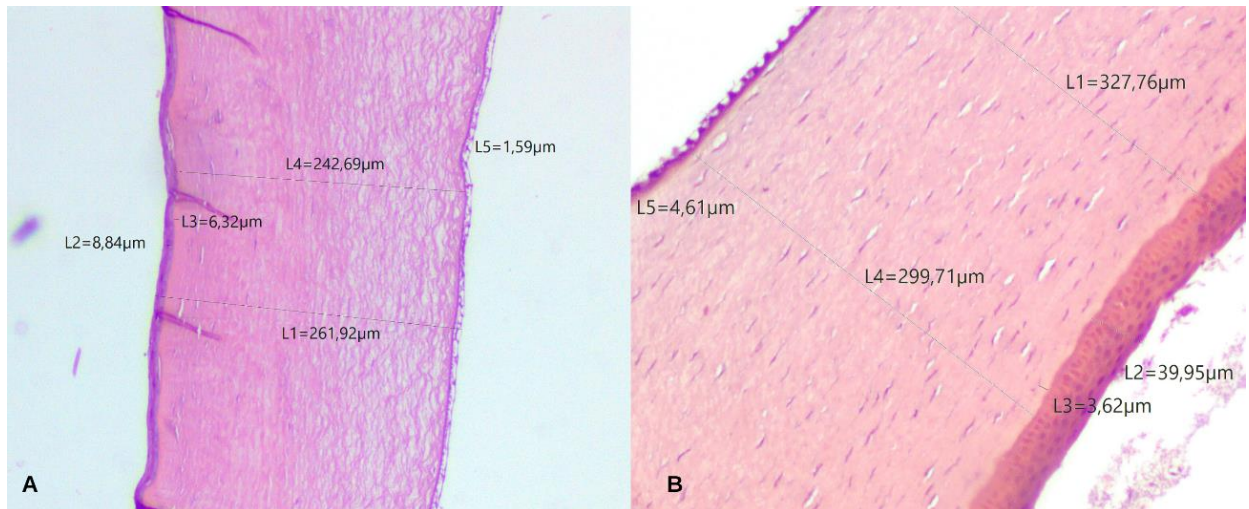


Figure 4. Image of the Image J software interface demonstrating the measurement of total corneal thickness (L1) and its individual layers; Epithelium (L2), Bowman's membrane (L3), stroma (L4), Descemet's membrane (L5). A) Central region of the *Asio stygius* cornea; B) Central corneal region of *Rhea americana*. Measurements were carried out using the Opticam O500R microscope, with OPTHD software, 100x magnification.

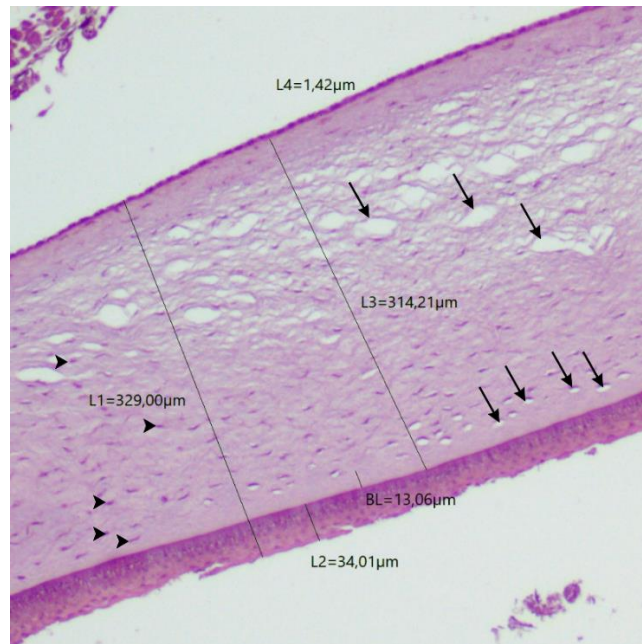


Figure 5. Peripheral region of the *Pitangus sulphuratus* cornea. Eosinophilic keratocyte nuclei (arrowhead) and artifacts (arrows) scattered throughout the stroma. Measurements referring to the thickness of the total cornea (L1), epithelium (L2), Bowman's membrane (BL), stroma (L3) and Descemet's membrane (L4). Measurements were carried out using the Opticam O500R microscope, with OPTHD software, 100x magnification.

Table 1. Order, family, and popular names of bird species.

Species	Order	Family	Brazilian popular names	Popular names in IUCN Red List
<i>Asio stygius</i> (Wagler, 1832)	Strigiformes	Strigidae	Mocho-preto	Stygian Owl
<i>Crotophaga ani</i> (Linnaeus 1758)	Cuculiformes	Cuculidae	Anu-preto	Smooth-billed Ani
<i>Pitangus sulphuratus</i> (Linnaeus, 1766)	Passeriformes	Tyrannidae	Bem-te-vi	Great Kiskadee
<i>Ramphastos toco</i> (Statius Muller, 1776)	Piciformes	Ramphastidae	Tucanuçu	Toco Toucan
<i>Turdus rufiventris</i> (Vieillot, 1818)	Passeriformes	Turdidae	Sabiá-laranjeira	Rufous-bellied Thrush
<i>Rhea americana</i> (Linnaeus, 1758)	Rheiformes	Rheidae	Ema	Greater Rhea
<i>Ara macao</i> (Linnaeus, 1758)	Psittaciformes	Psittacidae	Araracanga	Scarlet Macaw
<i>Nyctibius griseus</i> (Gmelin, 1789)	Nyctibiiformes	Nyctibiidae	Urutau	Common Potoo

Table 2. Measurement of the total cornea and its layers from avian species, in micrometers (μm).

Species	Cornea Full Thickness		Epithelium		Bowman's Layer		Estroma		Descemet's Layer	
	Central	Peripheral	Central	Peripheral	Central	Peripheral	Central	Peripheral	Central	Peripheral
<i>Asio stygius</i>	254.76	642.2	9.53	8.91	4.3	3.02	236.08	623.19	1.92	2.33
<i>Crotophaga ani</i>	172.27	220.75	37.71	26.32	4.24	4.04	131.39	182.40	1.59	1.27
<i>Pitangus sulphuratus</i>	341.45	329	25.58	34	10.16	13.06	311.64	314.21	2.01	1.42
<i>Ramphastos toco</i>	374.36	721.38	18.65	16.31	6.27	9.3	344.2	694.87	3.06	3.27
<i>Turdus rufiventris</i>	179.33	192.25	19	21.09	3	3.34	140.45	143.45	3.14	2.11
<i>Rhea americana</i>	327.76	439	39.95	39.03	3.62	4.32	299.71	399.14	4.61	3.17
<i>Ara macao</i>	282.88	266.97	21.08	23.43	3.52	7.84	232.06	200.07	19.72	13.94
<i>Nyctibius griseus</i>	224.5	352.5	8.5	10	2.81	4.48	206.6	329.44	3.37	1.55

Table 3. Number of layers and characteristics of the corneal epithelium from avian species.

Species	Epithelial layers	
	Central	Peripheral
<i>Asio stygius</i>	3 to 4 layers (1 basal, 1 to 2 polyhedral squamous and 1 flat squamous)	3 to 4 layers (1 basal, 1 to 2 polyhedral squamous and 1 flat squamous)
<i>Crotophaga ani</i>	5 to 6 layers (1 basal, 2 to 3 polyhedral squamous and 2 flat squamous)	4 to 5 layers (1 basal, 1 to 2 polyhedral squamous and 2 flat squamous)
<i>Pitangus sulphuratus</i>	3 to 4 layers (1 basal, 1 to 2 polyhedral squamous and 1 flat squamous)	4 to 5 layers (1 basal, 1 to 2 polyhedral squamous and 2 flat squamous)
<i>Ramphastos toco</i>	3 to 5 layers (1 basal, 1 to 3 polyhedral squamous and 1 flat squamous)	3 to 4 layers (1 basal, 1 to 2 polyhedral squamous and 1 flat squamous)
<i>Turdus rufiventris</i>	3 to 5 layers (1 basal, 1 to 3 polyhedral squamous and 1 flat squamous)	3 to 5 layers (1 basal, 1 to 3 polyhedral squamous and 1 flat squamous)
<i>Rhea americana</i>	3 to 6 layers (1 basal, 1 to 3 polyhedral squamous and 1 to 2 flat squamous)	3 to 6 layers (1 basal, 1 to 3 polyhedral squamous and 1 to 2 flat squamous)
<i>Ara macao</i>	3 to 5 layers (1 basal, 1 to 3 polyhedral squamous and 1 flat squamous)	3 to 5 layers (1 basal, 1 to 3 polyhedral squamous and 1 flat squamous)
<i>Nyctibius griseus</i>	3 to 4 layers (1 basal, 1 to 2 polyhedral squamous and 1 flat squamous)	3 to 4 layers (1 basal, 1 to 2 polyhedral squamous and 1 flat squamous)

Table 4. Total corneal thickness of previously studied bird species and of the birds studied here, including their sizes/weights, habits and feeding.

Species (Popular Name)	Size & Weight ¹	Habits ^{1,2}	Feeding ^{1,2}	Total Corneal Thickness	Source
<i>Eudyptula minor</i> (Little Penguin)	30 cm 1.1 - 1.2 kg	Diurnal, amphibious, flightless	Piscivore	380 ± 54 µm (central region)	(Collin & Collin, 2021)
<i>Spheniscus demersus</i> (African Penguin)	45 cm 3.1 kg	Diurnal, amphibious, flightless	Piscivore	450 µm (region not specified)	(Sokolenko <i>et al.</i> , 2021)
<i>Spheniscus demersus</i> (African Penguin)	45 cm 3.1 kg	Diurnal, amphibious, flightless	Piscivore	384 ± 30 µm (central region)	(Gonzalez-Alonso-Alegre <i>et al.</i> , 2015)
<i>Spheniscus humboldti</i> (Humboldt Penguin)	66 - 70 cm 4 - 5 kg	Diurnal, amphibious, flightless	Piscivore	636 µm† (region not specified)	(Popova <i>et al.</i> , 2022)
<i>Gallus gallus domesticus</i> (Domestic chickens)	40 - 60 cm 2580.2 g	Diurnal, terrestrial, domestic	Granivore and insectivore	242 µm (central region)	(Montiani-Ferreira <i>et al.</i> , 2004)
<i>Gallus gallus domesticus</i> (Domestic chickens)	40 - 60 cm 2.6 - 4.5 kg	Diurnal, terrestrial, domestic	Granivore and insectivore	225.3 ± 30 µm (region not specified)	(Gonçalves <i>et al.</i> , 2016)
<i>Coturnix coturnix</i> (Common Quail)	17.5 cm 70 - 155 g	Diurnal, terrestrial, grassland	Granivore	154 ± 17.7 µm (region not specified)	(Gonçalves <i>et al.</i> , 2016)

<i>Coturnix japonica</i> (Japanese Quail)	16-18 cm 90 - 115 g	Diurnal, terrestrial, grassland	Granivore	138.64 μm (region not specified)	(Mayakkannan <i>et al.</i> , 2018)
Ostrich (species not described by the author)	180 - 270 cm 90 - 130 kg	Diurnal, terrestrial, flightless	Omnivore	550 \pm 35 μm (central region)	(Liu <i>et al.</i> , 2016)
<i>Rhea americana</i> (Greater Rhea)	1.34 - 1.70m 26 - 36 kg	Diurnal, terrestrial, flightless	Omnivore	327.76 μm (central region) 439 μm (peripheral region)	This study
<i>Harpia harpyja</i> (Harpy Eagle)	89 - 102 cm 6 - 9 kg	Diurnal, raptor, rainforests	Carnivore	563 μm (central region)	(Moraes, 2018)
<i>Aquila chrysaetos</i> (Golden Eagle)	70 - 84 cm 3 - 6.125 kg	Diurnal, raptor, open or semi-open areas	Carnivore	640 μm (central region) 1200 μm (peripheral region)	(Murphy & Dubielzig, 1993)
<i>Falcon tinnunculus</i> (Common Kestrel)	36 - 58 cm 907 g	Diurnal, raptor, open or semi-open areas	Carnivore	129 μm (central region) Varies from 197 to 210.8 μm (peripheral region)	(Werther <i>et al.</i> , 2017)
<i>Asio stygius</i> (Stygian Owl)	38 - 46 cm 400 - 675 g	Nocturnal, raptor, open or semi-open areas	Carnivore	254.76 μm (central region) 642.2 μm (peripheral region)	This study
<i>Nyctibius griseus</i> (Common Potoo)	34 - 38 cm 160 - 190 g	Nocturnal, open or semi- open areas	Insectivore	224.5 μm (central region) 352.5 μm (peripheral region)	This study
<i>Columba livia</i> (Domestic pigeon)	29 - 35 cm 315 - 410 g	Diurnal, domestic, urban areas	Granivore	157 μm (central region) 188 μm and 169 μm (peripheral nasal and temporal regions)	(Chard & Gundlach, 1938)
<i>Calypte anna</i> (Anna's Hummingbird)	10 cm 4 - 4.5 g	Diurnal, scrub forest	Nectarivore	59 μm (central region) 48 μm (peripheral region)	(Moore <i>et al.</i> , 2019)

<i>Pitangus sulphuratus</i> (Great Kiskadee)	21 - 26 cm 52 - 68 g	Diurnal, rainforests, urban areas	Omnivore	341.45 μm (central region) 329 μm (peripheral region)	This study
<i>Turdus rufiventris</i> (Rufous-bellied Thrush)	25 cm 68 g	Diurnal, rainforests, urban areas	Omnivore	179.33 μm (central region) 192.25 μm (peripheral region)	This study
<i>Lonchura oryzivora</i> (Java Sparrow)	15 - 17 cm 24.5 g	Diurnal, open grassland	Granivore	166 \pm 5 μm (region not specified)	(Popova <i>et al.</i> , 2022)
<i>Crotophaga ani</i> (Smooth-billed Ani)	35 cm 115 g	Diurnal, rainforests, urban areas	Omnivore	172.27 μm (central region) 220.75 μm (peripheral region)	This study
<i>Ramphastos toco</i> (Toco Toucan)	61 cm 592 - 760 g	Diurnal, scrub forests	Omnivore	374.36 μm (central region) 721.38 μm (peripheral region)	This study
<i>Ara macao</i> (Scarlet Macaw)	89 cm 1.2 kg	Diurnal, rainforests	Frugivore	282.88 μm (central region) 266.97 μm (peripheral region)	This study
<i>Anodorhynchus hyacinthinus</i> (Hyacinth Macaw)	1 m 1.2 - 1.7 kg	Diurnal, rainforests	Frugivore	472 μm † (region not specified)	(Popova <i>et al.</i> , 2022)
<i>Platalea leucorodia</i> (Eurasian Spoonbill)	80 - 90 cm 1.7 - 2 kg	Diurnal, wetlands	Piscivore	436 μm † (region not specified)	(Popova <i>et al.</i> , 2022)

†Approximate mean total corneal thickness.

¹<https://animaldiversity.org/>

²<https://www.iucnredlist.org/>

13/06/2023, 13:24

Gmail - Anatomia, Histologia, Embryologia - Manuscript ID AHE-06-23-OA-154 [email ref: SE-6-a]



Rafaela Tozetti <rafaelartozetti@gmail.com>

Anatomia, Histologia, Embryologia - Manuscript ID AHE-06-23-OA-154 [email ref: SE-6-a]

Vigneshwari Loganathan <onbehalf@manuscriptcentral.com>

8 de junho de 2023 às 08:13

Responder a: aheoffice@wiley.com

Para: dra.paulagalera@gmail.com, rafaelartozetti@gmail.com, mvlpatologiaveterinaria@gmail.com, roseliaraju@hotmail.com, liriahirano@unb.br, bretsximoore@gmail.com

Cc: dra.paulagalera@gmail.com, rafaelartozetti@gmail.com, mvlpatologiaveterinaria@gmail.com, roseliaraju@hotmail.com, liriahirano@unb.br, bretsximoore@gmail.com

08-Jun-2023

Dear Prof. Galera:

Your manuscript entitled "Corneal histomorphometry of birds from the Brazilian Midwest" by Galera, Paula; Tozetti, Rafaela Alves Ribon; Moreira, Matheus Vilar do Loes; Araújo, Rosélia de Lima Sousa; Hirano, Liria Queiroz Luz; Moore, Bret A., has been successfully submitted online and is presently being given full consideration for publication in Anatomia, Histologia, Embryologia.

If you wish your article to be available to non-subscribers on publication, please see the information on Online Open at the bottom of this email.

Co-authors: Please contact the Editorial Office as soon as possible if you disagree with being listed as a co-author for this manuscript.

Your manuscript ID is AHE-06-23-OA-154.

Please mention the above manuscript ID in all future correspondence or when calling the office for questions. If there are any changes in your street address or e-mail address, please log in to Manuscript Central at <https://mc.manuscriptcentral.com/ahe> and edit your user information as appropriate.

*Effective with the 2017 volume, Anatomia, Histologia, Embryologia will be published in an online-only format. No printed edition will be published. All normal author benefits and services remain in place e.g. authors will continue to be able to order print reprints of articles if required. Furthermore, there will be no cost to authors for the publication of colour images in the online-only edition. Please see the journal's Author Guidelines for full details.

You can also view the status of your manuscript at any time by checking your Author Center after logging in to <https://wiley.atyponrex.com/journal/AHE>

OnlineOpen is available to authors of primary research articles who wish to make their article available to non-subscribers on publication, or whose funding agency requires grantees to archive the final version of their article. With OnlineOpen, the author, the author's funding agency, or the author's institution pays a fee to ensure that the article is made available to non-subscribers upon publication via Wiley Online Library, as well as deposited in the funding agency's preferred archive. For the full list of terms and conditions, see http://wileyonlinelibrary.com/onlineopen#OnlineOpen_Terms

Any authors wishing to send their paper OnlineOpen will be required to complete the payment form available from our website at:

<https://onlinelibrary.wiley.com/onlineOpenOrder>

Prior to acceptance there is no requirement to inform an Editorial Office that you intend to publish your paper OnlineOpen if you do not wish to. All OnlineOpen articles are treated in the same way as any other article. They go through the journal's standard peer-review process and will be accepted or rejected based on their own merit.

This journal offers a number of license options for published papers; information about this is available here: <https://authorservices.wiley.com/author-resources/Journal-Authors/licensing/index.html>. The submitting author has confirmed that all co-authors have the necessary rights to grant in the submission, including in light of each co-author's funder policies. If any author's funder has a policy that restricts which kinds of license they can sign, for example if the funder is a member of Coalition S, please make sure the submitting author is aware.

Thank you for submitting your manuscript to Anatomia, Histologia, Embryologia.

CAPÍTULO III

1 Original Article (*Anatomia, Histologia, Embryologia*)

2

3 **Evaluation of the Common Pauraque (*Nyctidromus albicollis*) cornea using light and**
4 **scanning electron microscopy**

5

6 Rafaela Alves Ribon Tozetti¹, Rosélia de Lima Sousa Araújo¹, Matheus Vilardo Loes
7 Moreira², Larissa Cristina de Souza Akiyama¹, José Raimundo Corrêa³, Bret A. Moore⁴ and
8 Paula Diniz Galera¹.

9

10 ¹Comparative Ophthalmology Laboratory, School of Agricultural Sciences and Veterinary
11 Medicine, University of Brasília, Brasília, DF, Brazil.

12 ²Laboratory of Veterinary Pathology, MVL Patologia Veterinária, Belo Horizonte, MG,
13 Brazil

14 ³Laboratory of Microscopy and Microanalyses, Institute of Biology, University of Brasilia,
15 Distrito Federal, Brazil

16 ⁴Department of Small Animal Clinical Sciences, College of Veterinary Medicine, University
17 of Florida, Gainesville, FL, USA

18

19 Correspondence

20 Paula Diniz Galera, University of Brasilia (UnB), Campus Darcy Ribeiro, UnB – Asa Norte,
21 DF, Brazil. 70910-900.

22 Phone number: +55 (61) 99266-0799

23 Email: dra.paulagalera@gmail.com

24

25

26

27

28

29

30

31

32 **Acknowledgments**

33 This study was funded by *Coordenação de Aperfeiçoamento de Pessoal de Nível*
34 *Superior (CAPES), Brazil – Funding code 001, and by Fundação de Apoio à Pesquisa*
35 *do Distrito Federal (FAPDF), Brazil – proc.n. 00193.00001303/2019-10*). The authors
36 thank the team of the Laboratory of Microscopy and Microanalysis IB/UnB and the
37 Department of Wild Animals FAV/UnB in name of DVM, PhD Liria Queiroz Luz Hirano, for
38 providing their facilities to perform this research.

39

40

41

42 **Abstract**

43 The Common Pauraque *Nyctidromus albicollis* (Gmelin, 1789) is a widespread avian
44 species, however due to its nocturnal habits and reclusive behavior, little is known about their
45 vision and ecology. Most avian species are visually dependent with advanced visual systems
46 providing high spatial resolution, temporal resolution, or sensitivity depending on the species
47 needs. Each ocular structure has a specific role in contributing toward high visual function,
48 and the cornea is the first refractive structure in the visual process. No morphological or
49 morphometric evaluation has been described on the Common Pauraque cornea. This study
50 aims to describe the morphology and morphometry of the Common Pauraque cornea by
51 means of light and scanning electron microscopy to evaluate the cross-sectional anatomy as
52 well as the ultrastructure of the endothelial cells. A better understanding of the Common
53 Pauraque cornea can help us better explain the physiology of vision and the visual
54 requirements of this species. In turn, this will help us better understand how this species
55 successfully interacts with its environment, and will improve our knowledge on how to
56 interpret pathological changes in their cornea in a clinical setting.

57

58 **Keywords:** avian eye, bird, cornea, endothelium, histology, morphological.

59

60 **Introduction**

61 The Common Pauraque *Nyctidromus albicollis* (Gmelin, 1789) is a small bird of the
62 caprimulgiform order, weighting 50 to 70g and measuring 20 to 30 cm in length. It can be
63 found throughout Central and South America, largely in tropical regions and barring
64 mountainous regions, and to a lesser degree in the Southern tip of Texas, United States
65 (BirdLife International, 2020; Guilherme & Lima, 2020; Thurber, 2003; Trupkiewicz, Garner,
66 & Juan-Sallés, 2018). This species is insectivorous, hunting along brushwood and forest
67 edges, and has a crepuscular to nocturnal activity pattern (Cadbury, 1981; Pérez-Granados &
68 Schuchmann, 2020). Insectivorous birds generally need high spatial and temporal resolution
69 to successfully capture prey. Caprimulgiformes, however, have the added need for visual
70 specializations that enable successful foraging in scotopic conditions, such as proportionally
71 large eyes positioned to optimize the dorsal visual field, large palpebral openings, and high
72 rod-concentration in the retina (Delaunay, Larsen, Lloyd, Sullivan, & Grant, 2020; Martin,
73 Rojas, Figueroa, & McNeilo, 2004; Moore, Montiani-Ferreira, & Gardner, 2022; Salazar *et*
74 *al.*, 2020). Additionally, high visual resolution may benefit detection of predators in addition
75 to their camouflage brown and gray plumage to help remain conspicuous while nesting on the
76 ground among leaves (Guilherme & Lima, 2020; Pérez-Granados & Schuchmann, 2020;
77 Sandoval & Escalante, 2011; Thurber, 2003).

78 Generally, birds have complex visual systems that provide them with excellent visual
79 acuity, and each ocular structure has its specific role in enabling high acuity (Butler,
80 Templeton, & Fernández-Juricic, 2018; Fernández-Juricic, 2012; Martin, 2022; Salazar *et al.*,
81 2020). However, despite being a common and widespread avian species, there is still much to
82 learn about pauraque vision and ecology (Guilherme & Lima, 2020; Pérez-Granados &
83 Schuchmann, 2020; Thurber, 2003). No morphological and morphometric evaluations have
84 been performed describing the pauraque cornea. The goal of the present study is to describe
85 the normal structure of the Common Pauraque cornea, through light microscopy and scanning
86 electron microscopy, to contribute toward our understanding of their visual biology.
87 Primarily, evaluation of the corneal layers and thickness, the average cell area and cell
88 densities, coefficient of variation of the average cell area, and the morphology of the corneal
89 endothelium are described.

90

91 **Materials and methods**

92 *Animals*

93 Six Common Pauragues *Nyctidromus albicollis* (Caprimulgidae) were included, from
94 which 12 eyes were evaluated. The birds were from the Department of Wild Animals (Faculty
95 of Agronomy and Veterinary Medicine of the University of Brasília). They arrived in
96 unhealthy conditions after being rescued by the Wild Animal Screening Center (Centro de
97 Triagem de Animais Silvestres do Distrito Federal – CETAS). The exact age was not able to
98 be determined since they were free-living animals, although all were adults. The birds died
99 naturally after arrival from their poor condition. The collection of biological material for
100 scientific purposes was authorized by Biodiversity Authorization and Information System
101 (Sistema de Autorização e Informação em Biodiversidade - SISBIO), with protocol number
102 SISBIO n.79141-2. At the time of death, the eyes were evaluated and did not show evidence
103 of ophthalmic disease.

104 *Sample collection and processing*

105 The eyes were removed via transconjunctival enucleation within a maximum of 30
106 minutes after death. The technique consisted of a 360° perilimbal incision, dissection of the
107 ocular attachments to isolate the globe, and transection of the optic nerve. Ten eyes were
108 evaluated via light microscopy, and two eyes by scanning electron microscopy.

109

110 *Light microscopy (LM)*

111 Ten eyes were placed in 10% formaldehyde and were sent to the Veterinary Pathology
112 Laboratory (MVL Patologia Veterinária, Belo Horizonte, Brazil) for light microscopic
113 analysis. After fixation, they were embedded in paraffin. The blocks containing the sample
114 were subjected to serial cuts with a thickness of 4 µm, which were placed on slides and
115 stained with hematoxylin and eosin (HE) (Luna, 1968).

116

117 *Scanning electron microscopy (SEM)*

118 Two eyes were sent to the Microscopy and Microanalyses Laboratory (Institute of
119 Biology at the University of Brasilia) for preparation of scanning electron microscopy (SEM).
120 The cornea was separated from the globe, followed by fixation in 2% paraformaldehyde, 2%
121 glutaraldehyde in 0.1 M sodium cacodylate buffer (pH 7.2), for 24 h at room temperature.

122 After washing in 0.1 M sodium cacodylate buffer (pH 7.2), corneal samples were fixed in 2%
123 osmium tetroxide, 1.6% potassium ferricyanide (1:1 v/v) and 5 mM CaCl₂ in sodium
124 cacodylate buffer for 1 hour at room temperature, followed by washing in 0.1 M sodium
125 cacodylate buffer. The samples were kept for 24 hours in 0.5% aqueous uranyl acetate
126 solution at 4°C, washed in distilled water and dehydrated in an ascending series of acetone
127 (30, 50, 70, 90 and 100%). Subsequently, the corneas were dried at a critical point (Critical
128 Point Drying 0 CPD 0 Balzers) in liquid CO₂ and fixed in metallic *stubs*, with the
129 endothelium facing up, using double-sided carbon tape. Subsequently, they were metallized
130 with a layer of gold at 20 nm, using a high vacuum metallizer (Leica EM SCD500). Sample
131 analysis was performed using a Jeol JSM-7000F Field Emission Scanning Electron
132 Microscope (Jeol Ltd.).

133 Only images of the corneal endothelial cells were segmented and analyzed by SEM.
134 The evaluated parameters were the mean cell area (MCA - μm^2), endothelial cell density (CD
135 - cell/mm²), polymegathism (measured by the coefficient of cell variation - CV) (Doughty,
136 2008) and pleomorphism (measured by the percentage of hexagonal cells) (Coyo et al., 2019,
137 2015; Doughty & Oblak, 2008; Franzen, Pigatto, Abib, Albuquerque, & Laus, 2010). In total,
138 100 endothelial cells were analyzed. The cellular area was determined using Image J
139 Software. Endothelial CD was calculated by dividing the number of cells per 0,033 mm². The
140 results were described by Mean \pm SD (standard deviation). The coefficient of variation (CV)
141 was determined by dividing the standard deviation of the areas by the average of cellular area.
142 Finally, the percentage of pleomorphism was manually counted in the same group of cells.

143

144 **Results**

145 *Histological analysis with light microscopy*

146 The mean thickness of the paraque central cornea ($146.2 \pm 34.5 \mu\text{m}$) was slightly
147 thinner than the peripheral area ($149.2 \pm 35.8 \mu\text{m}$) between the central cornea and the limbus.
148 The paraque cornea was composed of five layers: epithelium, Bowman's layer, stroma,
149 Descemet's membrane and endothelium, from the outermost to innermost. The epithelium was
150 nonkeratinizing stratified squamous cells and formed by 3 to 4 layers measuring 10.2 ± 3.4
151 μm in the center, and 2 to 3 layers in peripheral area measuring $8 \pm 3.9 \mu\text{m}$. Just below it,
152 there was a continuous acellular basement membrane, known as Bowman's layer (center area
153 $3 \pm 1.1 \mu\text{m}$ and peripheral area $3.5 \pm 1.2 \mu\text{m}$). The stroma represents the thickest portion of
154 the cornea and was composed of collagen fibrils arranged approximately parallel to the

155 corneal surface (center thickness $126.7 \pm 30 \mu\text{m}$ and peripheral thickness $135 \pm 37.5 \mu\text{m}$).
 156 Attached to the innermost part of the stroma, Descemet's membrane had a central thickness of
 157 $2.2 \pm 1.2 \mu\text{m}$ and peripheral thickness of $1.9 \pm 0.7 \mu\text{m}$). Posterior to Descemet's membrane
 158 was a single layer of endothelial cells. Figure 1 exemplifies the measurements performed on
 159 the Common Pauraque corneas.

160 *Analysis in Scanning Electron Microscopy*

161 The endothelial cell density, mean cell area, degree of polymegathism and
 162 pleomorphism were obtained by SEM. The Common Pauraque corneal endothelium revealed
 163 a monolayer of polygonal cells with uniform size and shape (Fig. 2). Interdigitations and
 164 microvilli were visualized at the cell borders and in the center (Fig. 3). The mean cell area of
 165 the corneal endothelium was $311.659 \pm 95.86 \mu\text{m}^2$ and the endothelial cell density was
 166 $3,032.70 \text{ cell}/\text{mm}^2$. The coefficient of variation was 0.30. Most endothelial cells were
 167 hexagonal (85%), followed by pentagonal cells (10%), octagonal (2%), heptagonal (2%) and
 168 quadrilateral (1%).

169

170 **Discussion**

171 The present study is the first to describe the characteristics of the Common Pauraque
 172 (*Nyctidromus albicollis*) cornea. Light microscopic evaluation showed similarities to most
 173 avian species previously studied: it is avascular, formed predominantly by collagen tissue, and
 174 composed of five layers from outside to inside: epithelium, Bowman's layer, stroma,
 175 Descemet's membrane, and endothelium (Bayón, Almela, & Talavera, 2008; Carvalho,
 176 Rodarte-Almeida, Santana, & Galera, 2018; Collin & Collin, 2021; Kafarnik, Fritsche, &
 177 Reese, 2007; Pinto, Cruz, Teixeira, Couto, & Carvalho, 2016; Sokolenko *et al.*, 2021;
 178 Werther, Candioto, & Korbel, 2017).

179 The Common Pauraque corneal epithelium consisted of stratified, squamous and non-
 180 keratinized cells, similar to that found in other bird species (Collin & Collin, 2021; Monção-
 181 Silva *et al.*, 2016; Pinto *et al.*, 2016; Sokolenko *et al.*, 2021). Centrally the epithelium
 182 consisted of 3 to 4 layers and measured $10.2 \pm 3.4 \mu\text{m}$ thick, whereas peripherally only 2 to 3
 183 layers were detected measuring $8 \pm 3.9 \mu\text{m}$ thick. Such dimensions are noticeably thinner in
 184 relation to other avian species (Collin & Collin, 2021; Murphy & Dubielzig, 1993; Sokolenko
 185 *et al.*, 2021). For instance, the corneal epithelium of Little Penguins *Eudyptula minor* has a
 186 thickness of $26 \pm 7 \mu\text{m}$ and is composed of 5-6 rows of stratified squamous cells (Collin &

187 Collin, 2021). Yet, the African Penguin *Spheniscus demersus* presented values closer to the
 188 Common Pauraque, demonstrating 4 lines of cells and 15 μm of thickness in the epithelium
 189 (Sokolenko *et al.*, 2021). In the Golden Eagle *Aquila chrysaetos*, Murphy & Dubielzig
 190 (1993), found an epithelium with 8 layers and 50 μm thick. The author suggested that the
 191 distinct number of cell layers is a result of both size differences between species and their
 192 eyes, but also due to the cornea's exposure to adverse environmental conditions depending on
 193 a species ecology (e.g. a diving bird vs. a strictly terrestrial species, as in this study)
 194 (Almubrad & Akhtar, 2012; Collin & Collin, 2006; Nautscher, Bauer, Steffl, & Amselgruber,
 195 2016).

196 The avian cornea has been reported to be thinner than the corneas of similarly sized
 197 mammals (Moore, Fernandez-Juricic, Hawkins, Montiani-Ferreira, & Lange, 2022; Willis &
 198 Wilkie, 1999). Additionally, studies in most species support that the corneal periphery is
 199 thicker than the central cornea (Bergmanson, 2019; Bergmanson, Burns, & Naroo, 2021;
 200 Collin & Collin, 2021; Coyo *et al.*, 2015; Downie *et al.*, 2021; Jones, Pierce, & Ward, 2007;
 201 Pinto *et al.*, 2016). The total corneal thickness of Common Pauraque is $146.2 \pm 34.5 \mu\text{m}$
 202 centrally, and $149.2 \pm 35.8 \mu\text{m}$ in the periphery. In most other avian species, considerably
 203 higher values can be seen (Chard & Gundlach, 1938; Collin & Collin, 2021; Gonçalves,
 204 Pérez-Merino, Martínez-García, Barcía, & Merayo-Loves, 2016; Gonzalez-Alonso-Alegre,
 205 Martinez-Nevado, Caro-Vadillo, & Rodriguez-Alvaro, 2015; Liu *et al.*, 2016; Montiani-
 206 Ferreira, Cardoso, & Petersen-Jones, 2004; Moore & Montiani-Ferreira, 2022; Moraes, 2018;
 207 Murphy & Dubielzig, 1993; Sokolenko *et al.*, 2021; Werther *et al.*, 2017) (Tab. 1). Species
 208 smaller than the Common Pauraque have been shown to have thinner corneas, such as in the
 209 Anna's and Black-Chinned Hummingbirds (Moore *et al.*, 2019), and in the Japanese Quail
 210 (Mayakkannan, Ramesh, Kumaravel, Venkatesan, & Kannan, 2018) (Tab. 1). Similar to
 211 corneal epithelial thickness, the total thickness of the cornea likely is dependent on multiple
 212 factors including body mass and eye size, and the visual ecology of a given species (Hall,
 213 2008; Hall & Ross, 2007; Tyrrell & Fernández-Juricic, 2017).

214 In contrast to the thickness of the epithelium, the central corneal stroma (126.7 ± 30
 215 μm) was thinner than in the periphery ($135 \pm 37.5 \mu\text{m}$) in the Common Pauraque. A same
 216 pattern was observed in Little Penguins *Eudyptula minor* (center 312 μm and periphery 350
 217 μm) (Collin & Collin, 2021), Common Kestrel *Falco tinnunculus* (center ranged from 96 to
 218 112 μm , and periphery 165 to 198 μm) (Werther *et al.*, 2017), and in pigeons *Columba livia*
 219 *domesticus* (center 105 μm , temporal periphery 119 μm and nasal periphery 136 μm) (Chard
 220 & Gundlach, 1938). This differs from that of mice, where an experiment showed a thicker

221 central cornea in both the epithelial and stromal layers (Henriksson, Bron, & Bergmanson,
222 2012). However, Descemet's membrane and the single layer of endothelial cells showed no
223 significant difference in thickness between the cornea regions. Bergmanson *et al.* (2021)
224 suggested that the difference in thickness of the corneal regions still remains unknown,
225 although refraction demands, stem cell development and local environments, cellular aging
226 and nutrition, to name a few, may be contributing reason for differential thickness across the
227 cornea.

228 The cornea plays an important role in the refraction of light onto the retina for focused
229 image formation, and for this to occur, the cornea needs to be completely transparent (Crespo-
230 Moral, García-Posadas, López-García, & Diebold, 2020; Jones *et al.*, 2007; Martin, 2022;
231 Nautscher *et al.*, 2016). Transparency is afforded by the integrity of the epithelial barrier, the
232 parallel arrangement of stromal collagen cells and relative dehydration, the relative
233 acellularity in the stroma, and the efficient active cell membrane fluid pump of the
234 endothelium (Bergmanson, 2019; Collin & Collin, 2021; Jones *et al.*, 2007; Liu *et al.*, 2016;
235 Meek & Fullwood, 2001). A healthy endothelium is represented as a monolayer of polygonal
236 cells of relatively uniform size and shape, in which the cells are mostly hexagonal.
237 Endothelial cells can increase in size (polymegathism) and change their shape
238 (pleomorphism) to maintain the cornea in a state of deturgescence. This mechanism occurs
239 due to the limited ability of endothelial cells to replicate and the need to span deficits in this
240 unicellular layer. Therefore, it is possible to visualize changes in cell shape (from hexagonal
241 to pentagonal, octagonal, quadrilateral and heptagonal) and size (Albuquerque, Freitas, &
242 Pigatto, 2015; Collin & Collin, 1998; Coyo *et al.*, 2019; Doughty, 2006, 2018; Franzen *et al.*,
243 2010; Pigatto *et al.*, 2004, 2009; Tamayo-Arango *et al.*, 2009). In young animals, there is a
244 greater capacity for tissue regeneration, thus with aging, polymegathism and pleomorphism is
245 generally more evident. In fact, senility alone can result in rates of pleomorphism reaching
246 40% or more (Albuquerque *et al.*, 2015; Collin & Collin, 2021; Coyo *et al.*, 2015; Kafarnik *et al.*
247 *et al.*, 2007; Laing, Sandstrom, Berrospi, & Leibowitz, 1976).

248 The viability and health of the endothelium is assessed by visualizing the cellular
249 mosaic of this layer in scanning electron microscopy. Endothelial efficiency can be evaluated
250 from values such as mean cell area, cell density, coefficient of variation and percentage of
251 hexagonal cells. In such manner, it is possible to evaluate endothelial pleomorphism and
252 polymegathism as a marker of past or present endothelial damage or disease (Doughty, 2006,
253 2018; Doughty & Oblak, 2008). Different methods are used, such as specular microscopy,
254 confocal microscopy and scanning electron microscopy. The latter not only provides

255 information on cell morphology, but also is high enough to evaluate the three-dimensional
256 cell organization and the ultrastructure of endothelial cells (Coyo *et al.*, 2019; Doughty, 1989,
257 2018; Meek & Fullwood, 2001; Tamayo-Arango *et al.*, 2009). The downside is that
258 significant cellular contraction occurs with processing by dehydration with glutaraldehyde.
259 The cellular area obtained using other methods in which dehydration is not required can be
260 from 11 to 39% larger than samples prepared for SEM (Doughty, 1989, 2006; Pigatto *et al.*,
261 2004; Tamayo-Arango *et al.*, 2009). Although SEM provides excellent analysis of cellular
262 morphology, interpretation of the results must consider the methods used, including other
263 processing methods during SEM (Doughty, 1989).

264 In the present study, endothelial cellular microvilli were visualized as described in
265 other animals (Collin & Collin, 1998, 2021; Pigatto *et al.*, 2018; Tamayo-Arango *et al.*,
266 2009). The endothelium of Common Pauraque had microvilli located mostly at the cell
267 borders, with less emerging to the cell surface (Fig. 3). Quantitative analyses included: 1) the
268 mean cellular area; 2) the cellular density; 3) the coefficient of variation in size
269 (polymegathism); and 4) the percentage of hexagonal cells (Doughty, 1989).

270 The corneal endothelial mean cell area ($311.659 \pm 95.86 \mu\text{m}^2$) and density ($3,032.70$
271 cell/mm^2) varied from those reported in other birds, also analyzed by SEM, whereas the
272 percentage of hexagonal cells (85%) and the coefficient of variation of the area (0.30) was
273 more similar to previous studies (Collin & Collin, 1998, 2021; Doughty, 2006; Pigatto *et al.*,
274 2004, 2009, 2005; Tamayo-Arango *et al.*, 2009). A study with four different bird species all
275 showed greater endothelial density than the Common Pauraque: Barred owl *Bubo strix* with
276 $4,713 \pm 766 \text{ cells}/\text{mm}^2$, South African ostrich *Struthio camelus* $9,250 \pm 1,080 \text{ cells}/\text{mm}^2$,
277 Emu *Dromaius novaehollandiae* $11,734 \pm 1,687 \text{ cells}/\text{mm}^2$, and Australian Galah
278 *Eolophus roseicapillus* $9,905 \pm 873 \text{ cells}/\text{mm}^2$ (Collin & Collin, 1998). The Magellanic
279 Penguin also had a larger CD than the Common Pauraque ($3717 \text{ cells}/\text{mm}^2$ in the central
280 cornea, and $3731 \text{ cells}/\text{mm}^2$ in the peripheral cornea), however the MCA was lower (269 ± 24
281 μm^2) (Pigatto *et al.*, 2005). Additionally, the CV of the Magellanic Penguin (0.08) was less
282 similar to that of the Common Pauraque than that of a non-avian species, the Yacare Caiman
283 (0.22), although the percentage of hexagonal cells was similar across all three species (~80%)
284 (Pigatto *et al.*, 2004, 2005). Considering that the present evaluated healthy corneas and adult
285 animals, similar to other studies cited above, the low rate of pleomorphism is expected.
286 However, why some corneal endothelial values differ between species (e.g. commonly CD
287 and MCA) while others are most often similar (CV and the degree of pleomorphism) is poorly
288 understood.

289

290 Conclusion

291 The use of both light microscopy and scanning electron microscopy allowed for a
292 broad study of the Common Pauraque's cornea. Generally, similarities in gross structure of
293 the corneal organization and cellular morphology with other birds was found. However,
294 specific differences in MCA, CD, and CV leave open the need for greater understanding of
295 why such variation exists even among closely related species. Increased understanding may
296 help explain the physiology of vision and the visual requirements for a given species to
297 successfully interact with their environment, as well as improved knowledge about how to
298 interpret pathologic changes in the avian cornea.

299

300 Acknowledgments

301 This study was funded by *Coordenação de Aperfeiçoamento de Pessoal de Nível*
302 *Superior (CAPES), Brazil – Funding code 001, and by Fundação de Apoio à Pesquisa*
303 *do Distrito Federal (FAPDF), Brazil – proc.n. 00193.00001303/2019-10). The authors*
304 *thank the team of the Laboratory of Microscopy and Microanalysis IB/UnB and the*
305 *Department of Wild Animals FAV/UnB in name of DVM, PhD Liria Queiroz Luz Hirano, for*
306 *providing their facilities to perform this research.*

307

308 Conflict of Interest

309 The authors report no conflicts of interest. The authors alone are responsible for the
310 content and writing of this paper.

311

312 References

- 313 Albuquerque, L., Freitas, L. V. da R. P., & Pigatto, J. A. T. (2015). Analysis of the corneal
314 endothelium in eyes of chickens using contact specular microscopy. *Semina: Ciências*
315 *Agrárias*, 36(6Supl2), 4199–4206. <https://doi.org/10.5433/1679-0359.2015v36n6Supl2p4199>
- 316 Almubrad, T., & Akhtar, S. (2012). Ultrastructure features of camel cornea - collagen fibril
317 and proteoglycans. *Veterinary Ophthalmology*, 15(1), 36–41. [https://doi.org/10.1111/j.1463-](https://doi.org/10.1111/j.1463-5224.2011.00918.x)
318 [5224.2011.00918.x](https://doi.org/10.1111/j.1463-5224.2011.00918.x)
- 319 Bayón, A., Almela, R. M., & Talavera, J. (2008). Avian Ophthalmology. *European Journal of*
320 *Companion Animal Practice*, 17(3), 253–266.
- 321 Bergmanson, J. P. G. (2019). Anatomy and Physiology of the Cornea and Related Structures.

- 322 In *Contact Lenses* (Sixth Edit, pp. 33–64). Elsevier. [https://doi.org/10.1016/B978-0-7020-](https://doi.org/10.1016/B978-0-7020-7168-3.00003-9)
 323 [7168-3.00003-9](https://doi.org/10.1016/B978-0-7020-7168-3.00003-9)
- 324 Bergmanson, J. P. G., Burns, A. R., & Naroo, S. A. (2021). Central versus peripheral corneal
 325 thickness – A White spot on the corneal (anatomy) map. *Contact Lens and Anterior Eye*,
 326 *44*(4), 101473. <https://doi.org/10.1016/j.clae.2021.101473>
- 327 BirdLife International. (2020). *Nyctidromus albicollis*, Pauraque. *The IUCN Red List of*
 328 *Threatened Species*, 8235, 1–9. [https://doi.org/https://dx.doi.org/10.2305/IUCN.UK.2020-](https://doi.org/https://dx.doi.org/10.2305/IUCN.UK.2020-3.RLTS.T22689731A168860360.en)
 329 [3.RLTS.T22689731A168860360.en](https://doi.org/https://dx.doi.org/10.2305/IUCN.UK.2020-3.RLTS.T22689731A168860360.en)
- 330 Butler, S. R., Templeton, J. J., & Fernández-Juricic, E. (2018). How do birds look at their
 331 world? A novel avian visual fixation strategy. *Behavioral Ecology and Sociobiology*, *72*(3),
 332 38. <https://doi.org/10.1007/s00265-018-2455-0>
- 333 Cadbury, C. J. (1981). Nightjar census methods. *Bird Study*, *28*(1), 1–4.
 334 <https://doi.org/10.1080/00063658109476692>
- 335 Carvalho, C. M. de, Rodarte-Almeida, A. C. da V., Santana, M. I. S., & Galera, P. D. (2018).
 336 Avian ophthalmic peculiarities. *Ciência Rural*, *48*(12), 1–10. [https://doi.org/10.1590/0103-](https://doi.org/10.1590/0103-8478cr20170904)
 337 [8478cr20170904](https://doi.org/10.1590/0103-8478cr20170904)
- 338 Chard, R. D., & Gundlach, R. H. (1938). The structure of the eye of the homing pigeon.
 339 *Journal of Comparative Psychology*, *25*(2), 249–272. <https://doi.org/10.1037/h0061438>
- 340 Collin, S. P., & Collin, H. B. (1998). A comparative study of the corneal endothelium in
 341 vertebrates. *Clinical and Experimental Optometry*, *81*(6), 245–254.
 342 <https://doi.org/10.1111/j.1444-0938.1998.tb06744.x>
- 343 Collin, S. P., & Collin, H. B. (2006). The corneal epithelial surface in the eyes of vertebrates:
 344 Environmental and evolutionary influences on structure and function. *Journal of Morphology*,
 345 *267*(3), 273–291. <https://doi.org/10.1002/jmor.10400>
- 346 Collin, S. P., & Collin, H. B. (2021). Functional morphology of the cornea of the Little
 347 Penguin *Eudyptula minor* (Aves). *Journal of Anatomy*, *239*(3), 732–746.
 348 <https://doi.org/10.1111/joa.13438>
- 349 Coyo, N., Leiva, M., Costa, D., Molina, R., Nicolás, O., Ríos, J., & Peña, M. T. (2019).
 350 Endothelial cell density and characterization of corneal endothelial cells in the Tawny Owl (
 351 *Strix aluco*) using specular microscopy. *Veterinary Ophthalmology*, *22*(2), 177–182.
 352 <https://doi.org/10.1111/vop.12578>
- 353 Coyo, N., Peña, M. T., Costa, D., Ríos, J., Lacerda, R., & Leiva, M. (2015). Effects of age
 354 and breed on corneal thickness, density, and morphology of corneal endothelial cells in
 355 enucleated sheep eyes. *Veterinary Ophthalmology*, *19*(5), 367–372.

- 356 <https://doi.org/10.1111/vop.12308>
- 357 Crespo-Moral, M., García-Posadas, L., López-García, A., & Diebold, Y. (2020). Histological
358 and immunohistochemical characterization of the porcine ocular surface. *PLOS ONE*, *15*(1).
359 <https://doi.org/10.1371/journal.pone.0227732>
- 360 Delaunay, M. G., Larsen, C., Lloyd, H., Sullivan, M., & Grant, R. A. (2020). Anatomy of
361 avian rictal bristles in Caprimulgiformes reveals reduced tactile function in open-habitat,
362 partially diurnal foraging species. *Journal of Anatomy*, *237*(2), 355–366.
363 <https://doi.org/10.1111/joa.13188>
- 364 Doughty, M. J. (1989). Toward a quantitative analysis of corneal endothelial cell morphology:
365 a review of techniques and their application. *Optometry and Vision Science*, *66*(9), 626–642.
366 <https://doi.org/10.1097/00006324-198909000-00010>
- 367 Doughty, M. J. (2006). Subjective vs. objective analysis of the corneal endothelial cells in the
368 rabbit cornea by scanning electron microscopy - a comparison of two different methods of
369 corneal fixation. *Veterinary Ophthalmology*, *9*(2), 127–135. [https://doi.org/10.1111/j.1463-
370 5224.2006.00449.x](https://doi.org/10.1111/j.1463-5224.2006.00449.x)
- 371 Doughty, M. J. (2008). Could the coefficient of variation (COV) of the corneal endothelium
372 be overestimated when a centre-dot method is used? *Clinical and Experimental Optometry*,
373 *91*(1), 103–110. <https://doi.org/10.1111/j.1444-0938.2007.00203.x>
- 374 Doughty, M. J. (2018). On the regional variability of averaged cell area estimates for the
375 human corneal endothelium in relation to the extent of polymegethism. *International*
376 *Ophthalmology*, *38*(6), 2537–2546. <https://doi.org/10.1007/s10792-017-0765-2>
- 377 Doughty, M. J., & Oblak, E. (2008). A comparison of two methods for estimating
378 polymegethism in cell areas of the human corneal endothelium. *Ophthalmic and*
379 *Physiological Optics*, *28*(1), 47–56. <https://doi.org/10.1111/j.1475-1313.2007.00533.x>
- 380 Downie, L. E., Bandlitz, S., Bergmanson, J. P. G., Craig, J. P., Dutta, D., Maldonado-Codina,
381 C., ... Wolffsohn, J. S. (2021). BCLA CLEAR - Anatomy and physiology of the anterior eye.
382 *Contact Lens and Anterior Eye*, *44*(2), 132–156. <https://doi.org/10.1016/j.clae.2021.02.009>
- 383 Fernández-Juricic, E. (2012). Sensory basis of vigilance behavior in birds: Synthesis and
384 future prospects. *Behavioural Processes*, *89*(2), 143–152.
385 <https://doi.org/10.1016/j.beproc.2011.10.006>
- 386 Franzen, A. A., Pigatto, J. A. T., Abib, F. C., Albuquerque, L., & Laus, J. L. (2010). Use of
387 specular microscopy to determine corneal endothelial cell morphology and morphometry in
388 enucleated cat eyes. *Veterinary Ophthalmology*, *13*(4), 222–226.
389 <https://doi.org/10.1111/j.1463-5224.2010.00787.x>

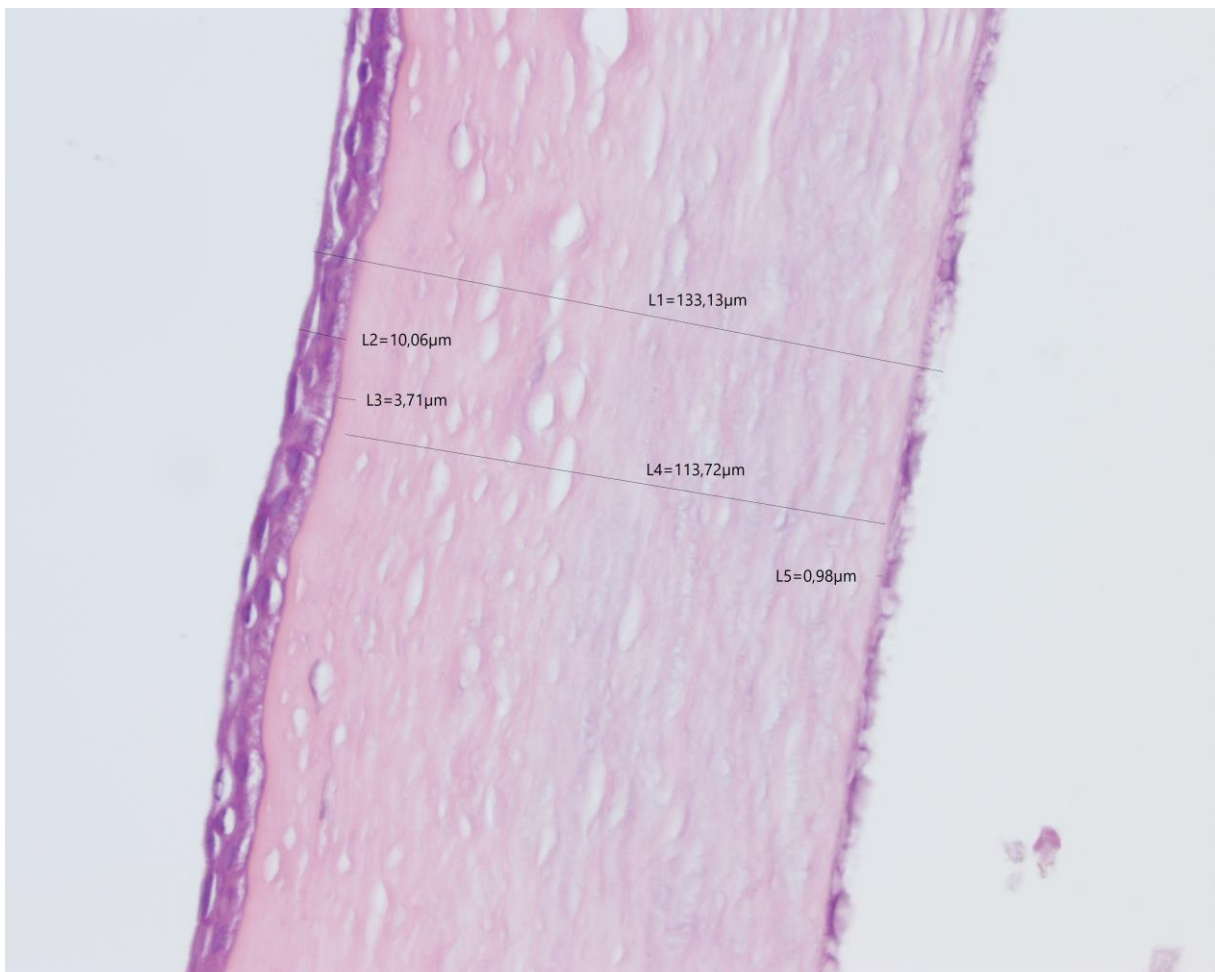
- 390 Gonçalves, G. C., Pérez-Merino, P., Martínez-García, M. C., Barcía, A., & Merayo-Loves, J.
 391 (2016). Comparación de las características corneales en gallina y codorniz como modelos
 392 experimentales de cirugía refractiva. *Archivos de La Sociedad Española de Oftalmología*,
 393 *91*(7), 310–315. <https://doi.org/10.1016/j.ofal.2016.01.012>
- 394 Gonzalez-Alonso-Alegre, E. M., Martinez-Nevado, E., Caro-Vadillo, A., & Rodriguez-
 395 Alvaro, A. (2015). Central corneal thickness and intraocular pressure in captive black-footed
 396 penguins (*Spheniscus demersus*). *Veterinary Ophthalmology*, *18*(s1), 94–97.
 397 <https://doi.org/10.1111/vop.12206>
- 398 Guilherme, E., & Lima, J. (2020). Breeding biology and morphometrics of Common
 399 Pauraque *Nyctidromus a. albicollis* in south-west Amazonia , and the species ' breeding
 400 season and clutch size in Brazil. *Bulletin of the British Ornithologists ' Club*, *3*(140), 344–350.
 401 <https://doi.org/https://doi.org/10.25226/bboc.v140i3.2020.a7>
- 402 Hall, M. I. (2008). The anatomical relationships between the avian eye, orbit and sclerotic
 403 ring: implications for inferring activity patterns in extinct birds. *Journal of Anatomy*, *212*(6),
 404 781–794. <https://doi.org/10.1111/j.1469-7580.2008.00897.x>
- 405 Hall, M. I., & Ross, C. F. (2007). Eye shape and activity pattern in birds. *Journal of Zoology*,
 406 *271*(4), 437–444. <https://doi.org/10.1111/j.1469-7998.2006.00227.x>
- 407 Henriksson, J. T., Bron, A. J., & Bergmanson, J. P. G. (2012). An explanation for the central
 408 to peripheral thickness variation in the mouse cornea. *Clinical and Experimental*
 409 *Ophthalmology*, *40*(2), 174–181. <https://doi.org/10.1111/j.1442-9071.2011.02652.x>
- 410 Jones, M. P., Pierce, K. E., & Ward, D. (2007). Avian Vision: A Review of Form and
 411 Function with Special Consideration to Birds of Prey. *Journal of Exotic Pet Medicine*, *16*(2),
 412 69–87. <https://doi.org/10.1053/j.jepm.2007.03.012>
- 413 Kafarnik, C., Fritsche, J., & Reese, S. (2007). In vivo confocal microscopy in the normal
 414 corneas of cats, dogs and birds. *Veterinary Ophthalmology*, *10*(4), 222–230.
 415 <https://doi.org/10.1111/j.1463-5224.2007.00543.x>
- 416 Laing, R. A., Sandstrom, M. M., Berrospi, A. R., & Leibowitz, H. M. (1976). Changes in the
 417 Corneal Endothelium as a Function of Age. *Experimental Eye Research*, *22*, 587–594.
- 418 Liu, X. X., Zhu, X. P., Wu, J., Wu, Z. J., Yin, Y., Xiao, X. H., ... Mi, S. L. (2016). Acellular
 419 ostrich corneal stroma used as scaffold for construction of tissue-engineered cornea.
 420 *International Journal of Ophthalmology*, *9*(3), 325–331.
 421 <https://doi.org/10.18240/ijo.2016.03.01>
- 422 Luna, L. G. (1968). *Manual of histologic staining methods of the Armed Forces Institute of*
 423 *Pathology* (3rd ed.). New York: Blakiston Division, McGraw-Hill.

- 424 Martin, G. R. (2022). Avian vision. In *Sturkie 's Avian Physiology Seventh Edition* (pp. 139–
425 158). <https://doi.org/https://doi.org/10.1016/B978-0-12-819770-7.00023-2>
- 426 Martin, G. R., Rojas, L., Figueroa, Y. R., & McNeilo, R. (2004). Binocular vision and
427 nocturnal activity in Oilbirds (*Steatornis caripensis*) and Pauraques (*Nyctidromus albicollis*):
428 Caprimulgiformes. *Ornitologia Neotropical*, 15(Jan 1), 233–242.
- 429 Mayakkannan, T., Ramesh, G., Kumaravel, A., Venkatesan, S., & Kannan, T. A. (2018).
430 Gross and Microanatomical Study of the Cornea in Japanese quail (*Coturnix coturnix*
431 japonica). *International Journal of Current Microbiology and Applied Sciences*, 7(10), 599–
432 605. <https://doi.org/10.20546/ijcmas.2018.710.067>
- 433 Meek, K. M., & Fullwood, N. J. (2001). Corneal and scleral collagens—a microscopist's
434 perspective. *Micron*, 32(3), 261–272. [https://doi.org/10.1016/S0968-4328\(00\)00041-X](https://doi.org/10.1016/S0968-4328(00)00041-X)
- 435 Monção-Silva, R. M., Ofri, R., Raposo, A. C. S., Libório, F. A., Estrela-Lima, A., & Oriá, A.
436 P. (2016). Ophthalmic Parameters of Blue-and-yellow Macaws (*Ara Ararauna*) and Lear's
437 Macaws (*Anodorhynchus Leari*). *Avian Biology Research*, 9(4), 240–249.
438 <https://doi.org/10.3184/175815516X14725499175746>
- 439 Montiani-Ferreira, F., Cardoso, F., & Petersen-Jones, S. (2004). Postnatal development of
440 central corneal thickness in chicks of *Gallus gallus domesticus*. *Veterinary Ophthalmology*,
441 7(1), 37–39. <https://doi.org/10.1111/j.1463-5224.2004.00319.x>
- 442 Moore, B. A., Fernandez-Juricic, E., Hawkins, M. G., Montiani-Ferreira, F., & Lange, R. R.
443 (2022). Introduction to Ophthalmology of Aves. In *Wild and Exotic Animal Ophthalmology*
444 (pp. 321–348). Cham: Springer International Publishing. https://doi.org/10.1007/978-3-030-71302-7_16
- 445 71302-7_16
- 446 Moore, B. A., Maggs, D. J., Kim, S., Motta, M. J., Bandivadekar, R., Tell, L. A., & Murphy,
447 C. J. (2019). Clinical findings and normative ocular data for free-living Anna's (*Calypte anna*)
448 and Black-chinned (*Archilochus alexandri*) Hummingbirds. *Veterinary Ophthalmology*, 22(1),
449 13–23. <https://doi.org/10.1111/vop.12560>
- 450 Moore, B. A., & Montiani-Ferreira, F. (2022). Ophthalmology of Accipitrimorphae, Strigidae,
451 and Falconidae: Hawks, Eagles, Vultures, Owls, Falcons, and Relatives. In *Wild and Exotic*
452 *Animal Ophthalmology* (pp. 429–504). Cham: Springer International Publishing.
453 https://doi.org/10.1007/978-3-030-71302-7_20
- 454 Moore, B. A., Montiani-Ferreira, F., & Gardner, A. (2022). Ophthalmology of Strisores:
455 Nightjars, Frogmouths, Swifts, Hummingbirds, and Relatives. In *Wild and Exotic Animal*
456 *Ophthalmology* (pp. 551–569). Cham: Springer International Publishing.
457 https://doi.org/10.1007/978-3-030-71302-7_23

- 458 Moraes, W. (2018). *OCULAR MORPHOLOGY, PHYSIOLOGY AND SELECTEAL*
 459 *OPHTHALMIC CLINICAL TESTS IN THE HARPY EAGLE (Harpy harpyja)*.
 460 UNIVERSIDADE FEDERAL DO PARANÁ.
- 461 Murphy, C. J., & Dubielzig, R. R. (1993). The gross and microscopic structure of the golden
 462 eagle (*Aquila chrysaetos*) eye. *Progress in Veterinary and Comparative Ophthalmology*, 3,
 463 74–79.
- 464 Nautscher, N., Bauer, A., Steffl, M., & Amselgruber, W. M. (2016). Comparative
 465 morphological evaluation of domestic animal cornea. *Veterinary Ophthalmology*, 19(4), 297–
 466 304. <https://doi.org/10.1111/vop.12298>
- 467 Pérez-Granados, C., & Schuchmann, K. (2020). Illuminating the nightlife of two Neotropical
 468 nightjars: vocal behavior over a year and monitoring recommendations. *Ethology Ecology &*
 469 *Evolution*, 32(5), 466–480. <https://doi.org/10.1080/03949370.2020.1753117>
- 470 Pigatto, J. A. T., Abib, F. C., Pizzeti, J. C., Laus, J. L., Santos, J. M. dos, & Barros, P. S. D.
 471 M. (2018). Análise morfométrica do endotélio corneano de coelhos à microscopia. *Acta*
 472 *Scientiae Veterinariae*, 33(1), 41. <https://doi.org/10.22456/1679-9216.14441>
- 473 Pigatto, J. A. T., Andrade, M. C., Laus, J. L., Santos, J. M., Brooks, D. E., Guedes, P. M., &
 474 Barros, P. S. M. (2004). Morphometric analysis of the corneal endothelium of Yacare caiman
 475 (*Caiman yacare*) using scanning electron microscopy. *Veterinary Ophthalmology*, 7(3), 205–
 476 208. <https://doi.org/10.1111/j.1463-5224.2004.04025.x>
- 477 Pigatto, J. A. T., Franzen, A. A., Pereira, F. Q., Rodarte-Almeida, A. C. da V., Laus, J. L.,
 478 Santos, J. M. dos, ... Barros, P. S. de M. (2009). Scanning electron microscopy of the corneal
 479 endothelium of ostrich. *Ciência Rural*, 39(3), 926–929.
- 480 Pigatto, J. A. T., Laus, J. L., Santos, J. M., Cerva, C., Cunha, L. S., Ruoppolo, V., & Barros,
 481 P. S. M. (2005). Corneal Endothelium Of The Magellanic Penguin (*Spheniscus Magellanicus*)
 482 By Scanning Electron Microscopy. *Journal of Zoo and Wildlife Medicine*, 36(4), 702–705.
 483 <https://doi.org/10.1638/05017.1>
- 484 Pinto, D. G., Cruz, G. D., Teixeira, R. H. F., Couto, E. P., & Carvalho, M. P. N. de. (2016).
 485 Histological analysis of the eyeball of Neotropical birds of prey *Caracara plancus*, *Falco*
 486 *sparverius*, *Rupornis magnirostris*, *Megascops choliba* and *Athene cunicularia*. *Brazilian*
 487 *Journal of Veterinary Research and Animal Science*, 53(3), 280.
 488 <https://doi.org/10.11606/issn.1678-4456.bjvras.2016.109045>
- 489 Salazar, J. E., Severin, D., Vega-Zuniga, T., Fernández-Aburto, P., Deichler, A., Sallaberry,
 490 M. A., & Mpodozis, J. (2020). Anatomical Specializations Related to Foraging in the Visual
 491 System of a Nocturnal Insectivorous Bird, the Band-Winged Nightjar (Aves:

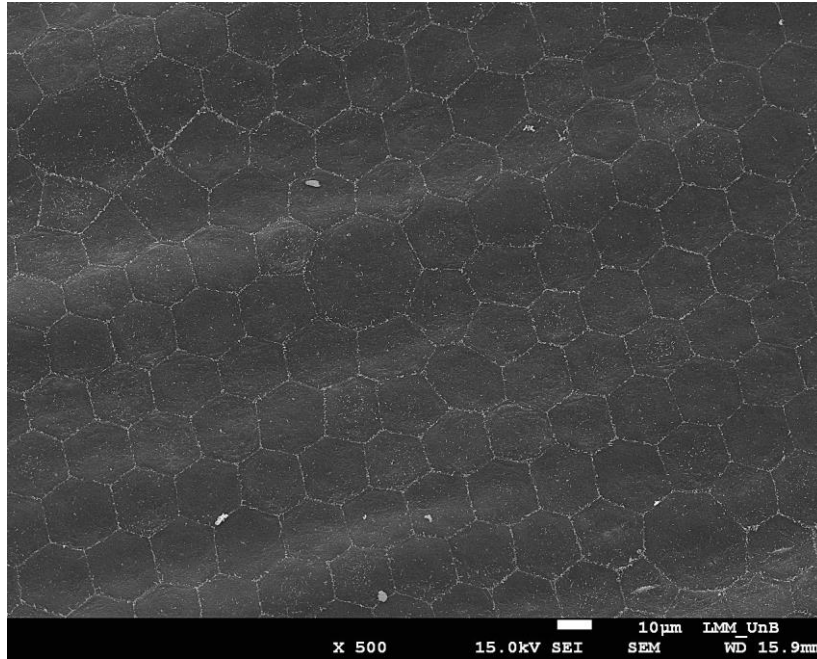
- 492 Caprimulgiformes). *Brain, Behavior and Evolution*, 94(1–4), 27–36.
 493 <https://doi.org/10.1159/000504162>
- 494 Sandoval, L., & Escalante, I. (2011). Song description and individual variation in males of the
 495 common pauraque (*Nyctidromus Albicollis*). *Ornitologia Neotropical*, 22, 173–185.
- 496 Sokolenko, E., Hilken, G., Denk, N., Wyss, F., Wenker, C., Hasler, P. W., & Meyer, P.
 497 (2021). The Eyes of an African Penguin (*Spheniscus demersus*): General Morphology and
 498 Ophthalmopathology. *Klin Monatsbl Augenheilkd*, 238(01), 94–98. [https://doi.org/10.1055/a-](https://doi.org/10.1055/a-1388-3960)
 499 1388-3960
- 500 Tamayo-Arango, L. J., Baraldi-Artoni, S. M., Laus, J. L., Mendes-Vicenti, F. A., Pigatto, J.
 501 A. T., & Abib, F. C. (2009). Ultrastructural morphology and morphometry of the normal
 502 corneal endothelium of adult crossbred pig. *Ciencia Rural*, 39(1), 117–122.
 503 <https://doi.org/10.1590/S0103-84782009000100018>
- 504 Thurber, W. A. (2003). Behavioral notes on the common Pauraque (*Nyctidromus albicollis*).
 505 *Ornitologia Neotropical*, 14, 99–105.
- 506 [dataset]Tozetti, R. A. R. (2023). The cornea of the Common Pauraque (*Nyctidromus*
 507 *albicollis*). *Harvard Dataverse, DRAFT VERSION*.
 508 <https://doi.org/https://doi.org/10.7910/DVN/QJ161G>
- 509 Trupkiewicz, J., Garner, M. M., & Juan-Sallés, C. (2018). Passeriformes, Caprimulgiformes,
 510 Coraciiformes, Piciformes, Bucerotiformes, and Apodiformes. In *Pathology of Wildlife and*
 511 *Zoo Animals: Vol. d* (pp. 799–823). Elsevier. [https://doi.org/10.1016/B978-0-12-805306-](https://doi.org/10.1016/B978-0-12-805306-5.00033-X)
 512 5.00033-X
- 513 Tyrrell, L. P., & Fernández-Juricic, E. (2017). The hawk-eyed songbird: Retinal morphology,
 514 eye shape, and visual fields of an aerial insectivore. *American Naturalist*, 189(6), 709–717.
 515 <https://doi.org/10.1086/691404>
- 516 Werther, K., Candioto, C. G., & Korbelt, R. (2017). Ocular Histomorphometry of Free-Living
 517 Common Kestrels (*Falco tinnunculus*). *Journal of Avian Medicine and Surgery*, 31(4), 319–
 518 326. <https://doi.org/10.1647/2014-039>
- 519 Willis, A. M., & Wilkie, D. A. (1999). Avian Ophthalmology Part 1 : Anatomy , Examination
 520 , and Diagnostic Techniques. *Journal of Avian Medicine and Surgery*, 13(3), 160–166.
 521 Retrieved from <http://www.jstor.org/stable/30130679> .
 522
 523
 524
 525

526
527
528
529
530
531
532



533
534 Figure 1. Histology of Common Pauraque cornea. L1 - total corneal thickness; L2 -
535 epithelium thickness; L3 - Bowman's layer thickness; L4- stroma thickness; L5 – Descemet's
536 layer thickness. HE. Measurements were carried out using the Opticam O500R microscope,
537 with OPTHD software, 400x magnification.

538
539

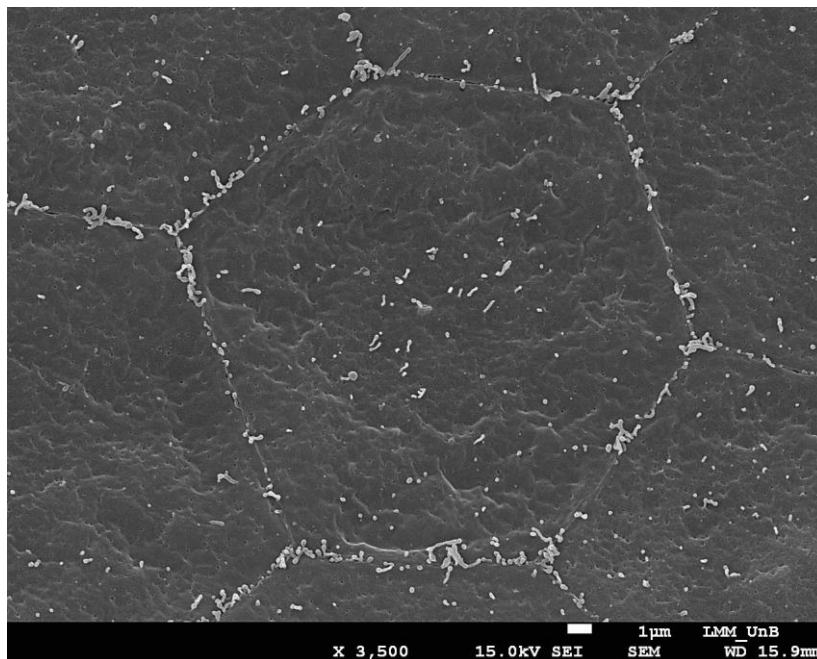


540

541 Figure 2. Scanning electron micrograph showing the corneal endothelium of the Common
542 Pauraque (*Nyctidromus albicollis*). Note majority of cells are healthy, small, and hexagonal,
543 compared to scant larger cells with variable shapes.

544

545



546

547 Figure 3. Scanning electron micrograph of normal corneal endothelial cell of the Common
548 Pauraque (*Nyctidromus albicollis*) showing microvilli (white structures). Note the highest
549 density localized at the intercellular junctions.

1
2 Table 1. Total corneal thickness of birds described in previous studies.

Species (Popular Name)	Total corneal thickness	Source
<i>Eudyptula minor</i> (Little Penguin)	380 ± 54 µm (central region)	(Collin & Collin, 2021)
<i>Spheniscus demersus</i> (African Penguin)	450 µm (region not specified)	(Sokolenko et al., 2021)
<i>Spheniscus demersus</i> (African Penguin)	384 ± 30 µm (central region)	(Gonzalez-Alonso-Alegre et al., 2015)
<i>Gallus gallus domesticus</i> (Chicken)	242 µm (central region)	(Montiani-Ferreira et al., 2004)
<i>Gallus gallus domesticus</i> (Chicken)	225.3 ± 30 µm (region not specified)	(Gonçalves et al., 2016)
<i>Coturnix coturnix</i> (Common Quail)	154 ± 17.7 µm (region not specified)	(Gonçalves et al., 2016)
<i>Coturnix japonica</i> (Japanese Quail)	138.64 µm (region not specified)	(Mayakkannan et al., 2018)
Ostrich (species not specified)	550 ± 35 µm (central region)	(Liu et al., 2016)
<i>Harpia harpyja</i> (Harpy Eagle)	563 µm (central region)	(Moraes, 2018)

<i>Aquila chrysaetos</i> (Golden Eagle)	640 μm (central region) 1200 μm (peripheral region)	(Murphy & Dubielzig, 1993)
<i>Falcon tinnunculus</i> (Common Kestrel)	129 μm (central region) Varies from 197 to 210.8 μm (peripheral regions)	(Werther et al., 2017)
<i>Columba livia</i> (Domestic pigeon)	157 μm (central region) Varies from 188 to 169 μm (peripheral regions)	(Chard & Gundlach, 1938)
<i>Calypte anna</i> (Anna's Hummingbird)	59 μm (central region) 48 μm (peripheral region)	(Moore et al., 2019)

13/06/2023, 13:23

Gmail - Anatomia, Histologia, Embryologia - Manuscript ID AHE-12-22-OA-315 [email ref: SE-6-a]



Rafaela Tozetti <rafaelartozetti@gmail.com>

Anatomia, Histologia, Embryologia - Manuscript ID AHE-12-22-OA-315 [email ref: SE-6-a]

Vigneshwari Loganathan <onbehalf@manuscriptcentral.com>

30 de maio de 2023 às 08:25

Responder a: aheoffice@wiley.com

Para: dra.paulagalera@gmail.com, rafaelartozetti@gmail.com, roseliaraju@hotmail.com,

mvlpatologiaveterinaria@gmail.com, akiyamaps@gmail.com, joseraimundocorrea@gmail.com, bretskimoore@gmail.com

Cc: dra.paulagalera@gmail.com, rafaelartozetti@gmail.com, roseliaraju@hotmail.com,

mvlpatologiaveterinaria@gmail.com, akiyamaps@gmail.com, joseraimundocorrea@gmail.com, bretskimoore@gmail.com

30-May-2023

Dear Prof. Galera:

Your manuscript entitled "Evaluation of the Common Pauraque (*Nyctidromus albicollis*) cornea using light and scanning electron microscopy" by Galera, Paula; Tozetti, Rafaela Alves Ribon; Araújo, Rosélia de Lima Sousa; Moreira, Matheus Vilardo Loes; Akiyama, Larissa Cristina de Souza; Corrêa, José Raimundo; Moore, Bret A., has been successfully submitted online and is presently being given full consideration for publication in Anatomia, Histologia, Embryologia.

If you wish your article to be available to non-subscribers on publication, please see the information on Online Open at the bottom of this email.

Co-authors: Please contact the Editorial Office as soon as possible if you disagree with being listed as a co-author for this manuscript.

Your manuscript ID is AHE-12-22-OA-315.

Please mention the above manuscript ID in all future correspondence or when calling the office for questions. If there are any changes in your street address or e-mail address, please log in to Manuscript Central at <https://mc.manuscriptcentral.com/ahe> and edit your user information as appropriate.

*Effective with the 2017 volume, Anatomia, Histologia, Embryologia will be published in an online-only format. No printed edition will be published. All normal author benefits and services remain in place e.g. authors will continue to be able to order print reprints of articles if required. Furthermore, there will be no cost to authors for the publication of colour images in the online-only edition. Please see the journal's Author Guidelines for full details.

You can also view the status of your manuscript at any time by checking your Author Center after logging in to <https://wiley.atyponrex.com/journal/AHE>

OnlineOpen is available to authors of primary research articles who wish to make their article available to non-subscribers on publication, or whose funding agency requires grantees to archive the final version of their article. With OnlineOpen, the author, the author's funding agency, or the author's institution pays a fee to ensure that the article is made available to non-subscribers upon publication via Wiley Online Library, as well as deposited in the funding agency's preferred archive. For the full list of terms and conditions, see http://wileyonlinelibrary.com/onlineopen#OnlineOpen_Terms

Any authors wishing to send their paper OnlineOpen will be required to complete the payment form available from our website at:

<https://onlinelibrary.wiley.com/onlineOpenOrder>

Prior to acceptance there is no requirement to inform an Editorial Office that you intend to publish your paper OnlineOpen if you do not wish to. All OnlineOpen articles are treated in the same way as any other article. They go through the journal's standard peer-review process and will be accepted or rejected based on their own merit.

This journal offers a number of license options for published papers; information about this is available here: <https://authorservices.wiley.com/author-resources/Journal-Authors/licensing/index.html>. The submitting author has confirmed that all co-authors have the necessary rights to grant in the submission, including in light of each co-author's funder policies. If any author's funder has a policy that restricts which kinds of license they can sign, for example if the funder is a member of Coalition S, please make sure the submitting author is aware.

Thank you for submitting your manuscript to Anatomia, Histologia, Embryologia.

<https://mail.google.com/mail/u/0/?ik=bd1d9d1500&view=pt&search=all&permmsgid=msg-f:1767299259478933424&simpl=msg-f:1767299259478...> 1/2

CAPÍTULO IV

CONSIDERAÇÕES FINAIS

Com base nas análises e resultados apresentados, além da literatura citada, ao longo do presente manuscrito, pode-se afirmar que os dados morfométricos e morfológicos permitem a descrição e comparação das córneas das aves estudadas. Portanto, embora os dados sejam considerados representativos das espécies aviárias, esses não são suficientes para compreender a variabilidade intra ou interespecífica.

As metodologias utilizadas para a coleta das informações, a microscopia de luz e de varredura, foram eficientes para concluir o objetivo do estudo e podem ser reproduzidas na prática.

Finalmente, gostaríamos de referir que a análise das métricas e da histomorfologia corneana foi feita com vista a oferecer uma descrição elementar dos dados, sem pretender uma inferência estatística, já que apenas um indivíduo de cada espécie foi estudado.

REFERÊNCIAS BIBLIOGRÁFICAS

- ABDELFTAH, Z. et al. Microstructure characteristics of cornea of some birds: a comparative study. **Beni-Suef University Journal of Basic and Applied Sciences**, v. 10, n. 1, p. 66, 18 dez. 2021.
- ABUMANDOUR, M. M. A.; BASSUONI, N. F.; HANAFY, B. G. Ultrastructural studies of the pecten oculi of the Garganey (*Anas querquedula*, Linnaeus 1758) and the Eurasian common moorhen (*Gallinula chloropus chloropus*, Linnaeus 1758). **Microscopy Research and Technique**, v. 84, n. 9, p. 1967–1976, 2021.
- ALBINI, T. A.; DAVIS, J. L. Ocular immunity and inflammation. **Developments in Ophthalmology**, v. 55, p. 38–45, 2015.
- ALBUQUERQUE, L.; FREITAS, L. V. DA R. P.; PIGATTO, J. A. T. Analysis of the corneal endothelium in eyes of chickens using contact specular microscopy. **Semina: Ciências Agrárias**, v. 36, n. 6Supl2, p. 4199–4206, 16 dez. 2015.
- AUSPREY, I. J.; NEWELL, F. L.; ROBINSON, S. K. Adaptations to light predict the foraging niche and disassembly of avian communities in tropical countrysides. **Ecology**, v. 102, n. 1, p. 0–2, 2020.
- BAYÓN, A.; ALMELA, R. M.; TALAVERA, J. Avian Ophthalmology. **European Journal of Companion Animal Practice**, v. 17, n. 3, p. 253–266, 2008.
- BEEBE, D. C.; COATS, J. M. The lens organizes the anterior segment: Specification of neural crest cell differentiation in the avian eye. **Developmental Biology**, v. 220, n. 2, p. 424–431, 2000.
- BERGMANSON, J. P. G. Anatomy and Physiology of the Cornea and Related Structures. In: **Contact Lenses**. Sixth Edit ed. [s.l.] Elsevier, 2019. p. 33–64.
- BERGMANSON, J. P. G.; BURNS, A. R.; NAROO, S. A. Central versus peripheral corneal thickness – A White spot on the corneal (anatomy) map. **Contact Lens and Anterior Eye**, v. 44, n. 4, p. 101473, ago. 2021.
- BERGMANSON, J. P. G.; BURNS, A.; WALKER, M. **Anatomical explanation for the central-peripheral thickness difference in human corneas.** *Investigative*

Ophthalmology & Visual Science. [s.l: s.n.].

- BOOTE, C. et al. The Influence of Lamellar Orientation on Corneal Material Behavior: Biomechanical and Structural Changes in an Avian Corneal Disorder. **Investigative Ophthalmology & Visual Science**, v. 52, n. 3, p. 1243, 9 mar. 2011.
- BORGES, R. et al. Avian Binocularity and Adaptation to Nocturnal Environments: Genomic Insights from a Highly Derived Visual Phenotype. **Genome Biology and Evolution**, v. 11, n. 8, p. 2244–2255, 1 ago. 2019.
- BUTLER, S. R.; TEMPLETON, J. J.; FERNÁNDEZ-JURICIC, E. How do birds look at their world? A novel avian visual fixation strategy. **Behavioral Ecology and Sociobiology**, v. 72, n. 3, p. 38, 16 mar. 2018.
- CARVALHO, C. M. DE et al. Avian ophthalmic peculiarities. **Ciência Rural**, v. 48, n. 12, p. 1–10, 6 dez. 2018.
- CHARD, R. D.; GUNDLACH, R. H. The structure of the eye of the homing pigeon. **Journal of Comparative Psychology**, v. 25, n. 2, p. 249–272, 1938.
- CHEN, C. K. et al. Feather evolution from precocial to altricial birds. **Zoological Studies**, v. 58, p. 1–12, 2019a.
- CHEN, X. et al. Comparative study of eggshell antibacterial effectivity in precocial and altricial birds using *Escherichia coli*. **PLOS ONE**, v. 14, n. 7, p. e0220054, 24 jul. 2019b.
- COLLIN, S. P.; COLLIN, H. B. A comparative study of the corneal endothelium in vertebrates. **Clinical and Experimental Optometry**, v. 81, n. 6, p. 245–254, 12 nov. 1998.
- COLLIN, S. P.; COLLIN, H. B. A Comparative SEM Study of the Vertebrate Corneal Epithelium. **Cornea**, v. 19, n. 2, p. 218–230, 2000.
- COLLIN, S. P.; COLLIN, H. B. The corneal epithelial surface in the eyes of vertebrates: Environmental and evolutionary influences on structure and function. **Journal of Morphology**, v. 267, n. 3, p. 273–291, mar. 2006.
- COLLIN, S. P.; COLLIN, H. B. Functional morphology of the cornea of the Little Penguin *Eudyptula minor* (Aves). **Journal of Anatomy**, v. 239, n. 3, p. 732–746, set. 2021.
- COYO, N. et al. Effects of age and breed on corneal thickness, density, and morphology of

- corneal endothelial cells in enucleated sheep eyes. **Veterinary Ophthalmology**, v. 19, n. 5, p. 367–372, set. 2015.
- COYO, N. et al. Endothelial cell density and characterization of corneal endothelial cells in the Tawny Owl (*Strix aluco*) using specular microscopy. **Veterinary Ophthalmology**, v. 22, n. 2, p. 177–182, mar. 2019.
- DAYAN, M. O.; OZAYDN, T. A comparative morphometrical study of the pecten oculi in different avian species. **The Scientific World Journal**, v. 2013, 2013.
- DE STEFANO, M. E.; MUGNAINI, E. Fine structure of the choroidal coat of the avian eye. **Anatomy and Embryology**, v. 195, n. 5, p. 393–418, 1997.
- DELAUNAY, M. G. et al. Anatomy of avian rictal bristles in Caprimulgiformes reveals reduced tactile function in open-habitat, partially diurnal foraging species. **Journal of Anatomy**, v. 237, n. 2, p. 355–366, 23 ago. 2020.
- DOUGHTY, M. J. Toward a quantitative analysis of corneal endothelial cell morphology: a review of techniques and their application. **Optometry and Vision Science**, v. 66, n. 9, p. 626–642, 1989.
- DOUGHTY, M. J. Subjective vs. objective analysis of the corneal endothelial cells in the rabbit cornea by scanning electron microscopy - a comparison of two different methods of corneal fixation. **Veterinary Ophthalmology**, v. 9, n. 2, p. 127–135, mar. 2006.
- DOUGHTY, M. J. Could the coefficient of variation (COV) of the corneal endothelium be overestimated when a centre-dot method is used? **Clinical and Experimental Optometry**, v. 91, n. 1, p. 103–110, 1 jan. 2008.
- DOUGHTY, M. J. On the regional variability of averaged cell area estimates for the human corneal endothelium in relation to the extent of polymegathism. **International Ophthalmology**, v. 38, n. 6, p. 2537–2546, 2018.
- DOWNIE, L. E. et al. BCLA CLEAR - Anatomy and physiology of the anterior eye. **Contact Lens and Anterior Eye**, v. 44, n. 2, p. 132–156, abr. 2021.
- EGBUNIWE, I. C.; AYO, J. O. Physiological roles of avian eyes in light perception and their responses to photoperiodicity. **World's Poultry Science Journal**, v. 72, n. 3, p. 605–614, 1 set. 2016.

- ESPINHEIRA GOMES, F. et al. Spectral-domain optical coherence tomography imaging of normal foveae: A pilot study in 17 diurnal birds of prey. **Veterinary Ophthalmology**, v. 23, n. 2, p. 347–357, 24 mar. 2020.
- FERREIRA, T. A. C. et al. The use of sulfur hexafluoride microbubbles for contrast-enhanced ocular ultrasonography of the pecten oculi in birds. **Veterinary Ophthalmology**, v. 22, n. 4, p. 423–429, 15 jul. 2019.
- FERREIRA, T. A. C.; GIANNICO, A. T.; MONTIANI-FERREIRA, F. Hemodynamics of the pectinis oculi artery in American pekin ducks (*Anas platyrhynchos domestica*). **Veterinary Ophthalmology**, v. 19, n. 5, p. 409–413, 2016.
- FISCHER, O.; SCHOENEMANN, B. Why are bones in vertebrate eyes? Morphology, development and function of scleral ossicles in vertebrate eyes - a comparative study. **Journal of Anatomy and Physiological Studies**, v. 3, n. 2, 2019.
- FRANZEN, A. A. et al. Use of specular microscopy to determine corneal endothelial cell morphology and morphometry in enucleated cat eyes. **Veterinary Ophthalmology**, v. 13, n. 4, p. 222–226, 1 jul. 2010.
- GARAMSZEGI, L. Z.; MØLLER, A. P.; ERRITZØE, J. Coevolving avian eye size and brain size in relation to prey capture and nocturnality. **Proceedings of the Royal Society of London. Series B: Biological Sciences**, v. 269, n. 1494, p. 961–967, 7 maio 2002.
- GLASSER, A.; HOWLAND, H. C. A History of Studies of Visual Accommodation in Birds. **The Quarterly Review of Biology**, v. 71, n. 4, p. 475–509, dez. 1996.
- GONÇALVES, G. C. et al. Comparación de las características corneales en gallina y codorniz como modelos experimentales de cirugía refractiva. **Archivos de la Sociedad Española de Oftalmología**, v. 91, n. 7, p. 310–315, jul. 2016.
- GRIGG, N. P. et al. Anatomical evidence for scent guided foraging in the Turkey vulture. **Scientific Reports**, v. 7, n. 1, p. 1–10, 2017.
- GUNJI, M.; FUJITA, M.; HIGUCHI, H. Function of head-bobbing behavior in diving little grebes. **Journal of Comparative Physiology A: Neuroethology, Sensory, Neural, and Behavioral Physiology**, v. 199, n. 8, p. 703–709, 2013.
- GÜNTHER, A. et al. Double cones and the diverse connectivity of photoreceptors and bipolar cells in an avian retina. **Journal of Neuroscience**, v. 41, n. 23, p. 5015–5028, 2021.

- HALL, M. I.; ROSS, C. F. Eye shape and activity pattern in birds. **Journal of Zoology**, v. 271, n. 4, p. 437–444, 13 abr. 2007.
- HARRIS, M. C. et al. Ophthalmic examination findings in a colony of Screech owls (*Megascops asio*). **Veterinary Ophthalmology**, v. 11, n. 3, p. 186–192, maio 2008.
- HAYASHI, S.; OSAWA, T.; TOHYAMA, K. Comparative observations on corneas, with special reference to Bowman's layer and Descemet's membrane in mammals and amphibians. **Journal of Morphology**, v. 254, n. 3, p. 247–258, 2002.
- HE, J.; PHAM, T. L.; BAZAN, H. E. P. Neuroanatomy of Adult and Aging Chicken Cornea. **Current Eye Research**, v. 47, n. 10, p. 1374–1380, 2022.
- HENRIKSSON, J. T.; BRON, A. J.; BERGMANSON, J. P. G. An explanation for the central to peripheral thickness variation in the mouse cornea. **Clinical and Experimental Ophthalmology**, v. 40, n. 2, p. 174–181, 2012.
- HOSSLER, F. E.; OLSON, K. R. Microvasculature of the avian eye: Studies on the eye of the duckling with microcorrosion casting, scanning electron microscopy, and stereology. **American Journal of Anatomy**, v. 170, n. 2, p. 205–221, 1984.
- IWANIUK, A. N.; WYLIE, D. R. Sensory systems in birds: What we have learned from studying sensory specialists. **Journal of Comparative Neurology**, v. 528, n. 17, p. 2902–2918, 2020.
- JONES, M. P.; PIERCE, K. E.; WARD, D. Avian Vision: A Review of Form and Function with Special Consideration to Birds of Prey. **Journal of Exotic Pet Medicine**, v. 16, n. 2, p. 69–87, 2007.
- KAFARNIK, C.; FRITSCHKE, J.; REESE, S. In vivo confocal microscopy in the normal corneas of cats, dogs and birds. **Veterinary Ophthalmology**, v. 10, n. 4, p. 222–230, 2007.
- KAMMERLING, J. D. et al. Lighting of Poultry Houses to Meet the Needs of Bird Eyes. **LOHMANN Information**, v. 52, n. 1, p. 22–31, 2018.
- KIAMA, S. G. et al. Functional morphology of the pecten oculi in the nocturnal spotted eagle owl (*Bubo bubo africanus*), and the diurnal black kite (*Milvus migrans*) and domestic fowl (*Gallus gallus* var. *domesticus*): A comparative study. **Journal of Zoology**, v. 254, n. 4, p. 521–528, 2001.

- KOUDOUNA, E. et al. Evolution of the vertebrate corneal stroma. **Progress in Retinal and Eye Research**, v. 64, n. November 2017, p. 65–76, 2018.
- LABETOULLE, M. et al. Role of corneal nerves in ocular surface homeostasis and disease. **Acta Ophthalmologica**, v. 97, n. 2, p. 137–145, 2019.
- LACERDA, R. P. et al. A comparative study of corneal sensitivity in birds of prey. **Veterinary Ophthalmology**, v. 17, n. 3, p. 190–194, 2014.
- LAING, R. A. et al. Changes in the Corneal Endothelium as a Function of Age. **Experimental Eye Research**, v. 22, p. 587–594, 1976.
- LI, T.; HOWLAND, H. C. A true neuronal consensual pupillary reflex in chicks. **Vision Research**, v. 39, n. 5, p. 897–900, 1999.
- LIU, X. X. et al. Acellular ostrich corneal stroma used as scaffold for construction of tissue-engineered cornea. **International Journal of Ophthalmology**, v. 9, n. 3, p. 325–331, 2016.
- MACHADO, M.; DOS SANTOS SCHMIDT, E. M.; MONTIANI-FERREIRA, F. Interspecies variation in orbital bone structure of psittaciform birds (with emphasis on Psittacidae). **Veterinary Ophthalmology**, v. 9, n. 3, p. 191–194, maio 2006.
- MARTIN, G. R. et al. Binocular vision and nocturnal activity in Oilbirds (*Steatornis caripensis*) and Pauraques (*Nyctidromus albicollis*): Caprimulgiformes. **Ornitologia Neotropical**, v. 15, n. Jan 1, p. 233–242, 2004.
- MARTIN, G. R. Visual fields and their functions in birds. **Journal of Ornithology**, v. 148, n. SUPPL. 2, 2007.
- MARTIN, G. R. What is binocular vision for? A birds' eye view. **Journal of Vision**, v. 9, n. 11, p. 1–19, 2009.
- MARTIN, G. R. Avian vision. In: **Sturkie 's Avian Physiology Seventh Edition**. [s.l: s.n.]. p. 139–158.
- MARTIN, G. R.; ASHASH, U.; KATZIR, G. Ostrich ocular optics. **Brain, Behavior and Evolution**, v. 58, n. 2, p. 115–120, 2001.
- MATTHYSSEN, S. et al. Corneal regeneration: A review of stromal replacements. **Acta Biomaterialia**, v. 69, p. 31–41, 2018.

- MCLELLAND, J. Skeleton. In: **A Color Atlas of Avian Anatomy**. [s.l: s.n.]. p. 33–35.
- MEEK, K. M.; LEONARD, D. W. Ultrastructure of the corneal stroma: a comparative study. **Biophysical Journal**, v. 64, n. 1, p. 273–280, 1993.
- MERINDANO, M. D. et al. A comparative study of Bowman's layer in some mammals: Relationships with other constituent corneal structures. **European Journal of Anatomy**, v. 6, n. 3, p. 133–139, 2002.
- MEYER, D. B. The Avian Eye and its Adaptations. In: **The Visual System in Vertebrates**. [s.l: s.n.]. p. 549–611.
- MITKUS, M. et al. Raptor Vision. **Oxford Research Encyclopedia of Neuroscience**, n. July, p. 1–39, 26 abr. 2018.
- MONÇÃO-SILVA, R. M. et al. Ophthalmic Parameters of Blue-and-yellow Macaws (*Ara Ararauna*) and Lear's Macaws (*Anodorhynchus Leari*). **Avian Biology Research**, v. 9, n. 4, p. 240–249, 1 nov. 2016.
- MOORE, B. A. et al. Clinical findings and normative ocular data for free-living Anna's (*Calypte anna*) and Black-chinned (*Archilochus alexandri*) Hummingbirds. **Veterinary Ophthalmology**, v. 22, n. 1, p. 13–23, 2019.
- MOORE, B. A. et al. Introduction to Ophthalmology of Aves. In: **Wild and Exotic Animal Ophthalmology**. Cham: Springer International Publishing, 2022a. p. 321–348.
- MOORE, B. A. et al. Ophthalmology of Strisores: Nightjars, Frogmouths, Swifts, Hummingbirds, and Relatives. In: **Wild and Exotic Animal Ophthalmology**. Cham: Springer International Publishing, 2022. p. 551-569b.
- MURPHY, C. J.; DUBIELZIG, R. R. The gross and microscopic structure of the golden eagle (*Aquila chrysaetos*) eye. **Progress in Veterinary and Comparative Ophthalmology**, v. 3, p. 74–79, 1993.
- MURPHY, C. J.; HOWLAND, H. C. Owl eyes: Accommodation, corneal curvature and refractive state. **Journal of Comparative Physiology ? A**, v. 151, n. 3, p. 277–284, 1983.
- NAUTSCHER, N. et al. Comparative morphological evaluation of domestic animal cornea. **Veterinary Ophthalmology**, v. 19, n. 4, p. 297–304, 20 jul. 2016.
- OROSZ, S. E.; BRADSHAW, G. A. Avian Neuroanatomy Revisited: From Clinical

- Principles to Avian Cognition. **Veterinary Clinics of North America - Exotic Animal Practice**, v. 10, n. 3, p. 775–802, 2007.
- PIGATTO, J. A. T. et al. Morphometric analysis of the corneal endothelium of Yacare caiman (Caiman yacare) using scanning electron microscopy. **Veterinary Ophthalmology**, v. 7, n. 3, p. 205–208, maio 2004.
- PIGATTO, J. A. T. et al. Corneal Endothelium Of The Magellanic Penguin (Spheniscus Magellanicus) By Scanning Electron Microscopy. **Journal of Zoo and Wildlife Medicine**, v. 36, n. 4, p. 702–705, dez. 2005.
- PIGATTO, J. A. T. et al. Scanning electron microscopy of the corneal endothelium of ostrich. **Ciência Rural**, v. 39, n. 3, p. 926–929, 2009.
- PIGATTO, J. A. T. et al. Análise morfométrica do endotélio corneano de coelhos à microscopia. **Acta Scientiae Veterinariae**, v. 33, n. 1, p. 41, 27 jun. 2018.
- PINTO, D. G. et al. Histological analysis of the eyeball of Neotropical birds of prey Caracara plancus, Falco sparverius, Rupornis magnirostris, Megascops choliba and Athene cunicularia. **Brazilian Journal of Veterinary Research and Animal Science**, v. 53, n. 3, p. 280, 4 out. 2016.
- PLATZL, C. et al. The choroid-sclera interface: An ultrastructural study. **Heliyon**, v. 8, n. 5, p. e09408, 2022.
- POPOVA, P. et al. Interspecies comparative morphological evaluation of the corneal epithelial stem cell niche: a pilot observational study. **Journal of Veterinary Science**, v. 23, n. 4, p. 1–10, 2022.
- PORTER, W. R.; WITMER, L. M. Avian Cephalic Vascular Anatomy, Sites of Thermal Exchange, and the Rete Ophthalmicum. **Anatomical Record**, v. 299, n. 11, p. 1461–1486, 2016.
- POTIER, S. et al. How fast can raptors see? **Journal of Experimental Biology**, v. 223, n. 1, 2020a.
- POTIER, S. et al. Inter-individual differences in foveal shape in a scavenging raptor, the black kite *Milvus migrans*. **Scientific Reports**, v. 10, n. 1, p. 6133, 9 dez. 2020b.
- POTIER, S.; MITKUS, M.; KELBER, A. Visual adaptations of diurnal and nocturnal raptors.

- Seminars in Cell & Developmental Biology**, v. 106, n. May, p. 116–126, out. 2020.
- PUSCH, R. et al. Visual categories and concepts in the avian brain. **Animal Cognition**, v. 26, n. 1, p. 153–173, 10 jan. 2023.
- REESE, S.; HORST, C.; LIEBICH, H.-G. Vascularization of the Ciliary Body and Iridocorneal Angle in the Avian Eye. **Anatomia, Histologia, Embryologia: Journal of Veterinary Medicine Series C**, v. 34, n. s1, p. 41–41, dez. 2005.
- RODARTE-ALMEIDA, A. C. V. et al. O olho da coruja-orelhuda: observações morfológicas, biométricas e valores de referência para testes de diagnóstico oftálmico. **Pesquisa Veterinária Brasileira**, v. 33, n. 10, p. 1275–1289, out. 2013.
- ROJAS, L. M. et al. Capacidad visual en caprimulgiformes. **Ornitologia Neotropical**, v. 15, p. 251–260, 2004a.
- ROJAS, L. M. et al. Retinal Morphology and Electrophysiology of Two Caprimulgiformes Birds: The Cave-Living and Nocturnal Oilbird (*Steatornis caripensis*), and the Crepuscularly and Nocturnally Foraging Common Pauraque (*Nyctidromus albicollis*). **Brain, Behavior and Evolution**, v. 64, n. 1, p. 19–33, 2004b.
- RUGGERI, M. et al. Retinal Structure of Birds of Prey Revealed by Ultra-High Resolution Spectral-Domain Optical Coherence Tomography. **Investigative Ophthalmology & Visual Science**, v. 51, n. 11, p. 5789, 1 nov. 2010.
- SALAZAR, J. E. et al. Anatomical Specializations Related to Foraging in the Visual System of a Nocturnal Insectivorous Bird, the Band-Winged Nightjar (Aves: Caprimulgiformes). **Brain, Behavior and Evolution**, v. 94, n. 1–4, p. 27–36, 2020.
- SCHAEFFEL, F.; HOWLAND, H. C. Corneal accommodation in chick and pigeon. **Journal of Comparative Physiology A**, v. 160, n. 3, p. 375–384, 1987.
- SCHEIBER, I. B. R. et al. The importance of the altricial – precocial spectrum for social complexity in mammals and birds – a review. **Frontiers in Zoology**, v. 14, n. 1, p. 3, 18 dez. 2017.
- SIVAK, J. G. Through the Lens Clearly: Phylogeny and Development. **Investigative Ophthalmology & Visual Science**, v. 45, n. 3, p. 740, 1 mar. 2004.
- SIVAK, J. G.; BOBIER, W. R.; LEVY, B. The refractive significance of the nictitating

- membrane of the bird eye. **Journal of Comparative Physiology** □ **A**, v. 125, n. 4, p. 335–339, 1978.
- SOKOLENKO, E. et al. The Eyes of an African Penguin (*Spheniscus demersus*): General Morphology and Ophthalmopathology. **Klin Monatsbl Augenheilkd**, v. 238, n. 01, p. 94–98, 14 jan. 2021.
- TAMAYO-ARANGO, L. J. et al. Ultrastructural morphology and morphometry of the normal corneal endothelium of adult crossbred pig. **Ciencia Rural**, v. 39, n. 1, p. 117–122, 2009.
- TSUKAHARA, N. et al. Microstructure characteristics of the cornea in birds and mammals. **Journal of Veterinary Medical Science**, v. 72, n. 9, p. 1137–1143, 2010.
- TYRRELL, L. P.; FERNÁNDEZ-JURICIC, E. The hawk-eyed songbird: Retinal morphology, eye shape, and visual fields of an aerial insectivore. **American Naturalist**, v. 189, n. 6, p. 709–717, 2017a.
- TYRRELL, L. P.; FERNÁNDEZ-JURICIC, E. Avian binocular vision: It's not just about what birds can see, it's also about what they can't. **PLOS ONE**, v. 12, n. 3, p. e0173235, 29 mar. 2017b.
- VELADIANO, I. A. et al. Computed tomographic anatomy of the heads of blue-and-gold macaws (*Ara ararauna*), African grey parrots (*Psittacus erithacus*), and monk parakeets (*Myiopsitta monachus*). **American Journal of Veterinary Research**, v. 77, n. 12, p. 1346–1356, dez. 2016.
- VOSS, J.; BISCHOF, H. J. Eye movements of laterally eyed birds are not independent. **Journal of Experimental Biology**, v. 212, n. 10, p. 1568–1575, 2009.
- WAGENER, L.; NIEDER, A. Categorical Auditory Working Memory in Crows. **iScience**, v. 23, n. 11, p. 101737, 2020.
- WERTHER, K.; CANDIOTO, C. G.; KORBEL, R. Ocular Histomorphometry of Free-Living Common Kestrels (*Falco tinnunculus*). **Journal of Avian Medicine and Surgery**, v. 31, n. 4, p. 319–326, dez. 2017.
- WILLIAMS, D. L. The avian eye. In: **Ophthalmology of Exotic Pets**. 1. ed. [s.l: s.n.]. p. 119–158.
- WILLIS, A. M.; WILKIE, D. A. Avian Ophthalmology Part 1 : Anatomy , Examination , and

Diagnostic Techniques. **Journal of Avian Medicine and Surgery**, v. 13, n. 3, p. 160–166, 1999.

WU, F.; ZHAO, Y.; ZHANG, H. Ocular Autonomic Nervous System: An Update from Anatomy to Physiological Functions. **Vision**, v. 6, n. 1, p. 6, 14 jan. 2022.

YILMAZ, B. et al. Macroanatomic, light and scanning electron microscopic structure of the pecten oculi in northern bald ibis (*Geronticus eremita*). **Anatomia, Histologia, Embryologia**, v. 50, n. 2, p. 373–378, 4 mar. 2021.

YORZINSKI, J. L. Conjugate eye movements guide jumping locomotion in an avian species. **Journal of Experimental Biology**, v. 222, n. 20, 15 out. 2019.

ZEHTABVAR, O. et al. Anatomical study of the scleral ring and eyeball of the long-eared owl (*Asio otus*) with anatomical methods and diagnostic imaging techniques. **Veterinary Medicine and Science**, v. 8, n. 4, p. 1735–1749, 4 jul. 2022.

ZUEVA, L. et al. Quantum mechanism of light energy propagation through an avian retina. **Journal of Photochemistry and Photobiology B: Biology**, v. 197, p. 111543, ago. 2019.